Gondwana Research 88 (2020) 220–249

Contents lists available at ScienceDirect

Gondwana Research

journal homepage: www.elsevier.com/locate/gr

GR Focus Review

The role of subduction erosion in the generation of Andean and other convergent plate boundary arc magmas, the continental crust and mantle

Charles R. Stern

Department of Geological Sciences, University of Colorado, Boulder, CO 80309-0399, USA

ARTICLE INFO

Article history:
Received 2 March 2020
Received in revised form 2 August 2020
Accepted 4 August 2020
Available online 17 September 2020

Handing Editor: M. Santosh

Keywords:
Subduction erosion
Convergent plate boundary arc magmatism
Mantle source region contamination
Andean volcanism
Andesite genesis
Crustal evolution
Mantle evolution

ABSTRACT

Subduction erosion, which occurs at all convergent plate boundaries associated with magmatic arcs formed on crystalline forearc basement, is an important process for chemical recycling, responsible globally for the transport of ~1.7 Armstrong Units (1 AU = 1 km^3/yr) of continental crust back into the mantle. Along the central Andean convergent plate margin, where there is very little terrigenous sediment being supplied to the trench as a result of the arid conditions, the occurrence of mantle-derived olivine basalts with distinctive crustal isotopic characteristics ($^{87}Sr/^{86}Sr \geq 0.7050$; $\varepsilon_{Nd} \leq -2$; $\varepsilon_{Hf} \leq +2$) correlates spatially and/or temporally with regions and/or episodes of high rates of subduction erosion, and a strong case can be made for the formation of these basalts to be due to incorporation into the subarc mantle wedge of tectonically eroded and subducted forearc continental crust. In other convergent plate boundary magmatic arcs, such as the South Sandwich and Aleutian Islands intra-oceanic arcs and the Central American and Trans-Mexican continental margin volcanic arcs, similar correlations have been demonstrated between regions and/or episodes of relatively rapid subduction erosion and the genesis of mafic arc magmas containing enhanced proportions of tectonically eroded and subducted crustal components that are chemically distinct from pelagic and/or terrigenous trench sediments. It has also been suggested that larger amounts of melts derived from tectonically eroded and subducted continental crust, rising as diapirs of buoyant low density subduction mélanges, react with mantle peridotite to form pyroxenite metasomatites that than melt to form andesites. The process of subduction erosion and mantle source region contamination with crustal components, which is supported by both isotopic and U-Pb zircon age data implying a fast and efficient connectivity between subduction inputs and magmatic outputs, is a powerful alternative to intra-crustal assimilation in the generation of andesites, and it negates the need for large amounts of mafic cumulates to form within and then be delaminated from the lower crust, as required by the basalt-input model of continental crustal growth. However, overall, some significant amount of subducted crust and sediment is neither underplated below the forearc wedge nor incorporated into convergent plate boundary arc magmas, but instead transported deeper into the mantle where it plays a role in the formation of isotopically enriched mantle reservoirs. To ignore or underestimate the significance of the recycling of tectonically eroded and subducted continental crust in the genesis of convergent plate boundary arc magmas, including andesites, and for the evolution of both the continental crust and mantle, is to be on the wrong side of history in the understanding of these topics.

Contents

E-mail address: Charles.Stern@colorado.edu.

https://doi.org/10.1016/j.gr.2020.08.006
1342-937X/

1. Introduction

Subduction (or tectonic) erosion removes crystalline crustal basement from the forearc wedge above the lower subducting plate (Fig. 1; von Huene et al., 2004; Clift and Vannucchi, 2004; Stern, 2011; Straub et al., 2020). Frontal subduction erosion results from the structural collapse of the forearc wedge into the subduction channel, and basal subduction erosion is caused by abrasion and hydro-fracturing above this channel. Subduction of both marine and terrigenous trench sediments also occurs in subduction zones (Figs. 1 and 2), but in this paper trench sediment subduction is considered an independent process from subduction erosion. Trench sediment subduction may transport continental components into the mantle source of convergent plate boundary arc magmas, but this contribution can in some cases, as reviewed in detail in this paper, be distinguished from the contribution made by subduction erosion of the crystalline basement of the forearc wedge.

It has been suggested that subduction erosion of the crystalline forearc wedge occurs at all convergent plate boundaries even if they are accretionary margins (Scholl and von Huene, 2007, 2009). Subduction erosion is responsible globally for the transport of at least ~1.7 Armstrong Units (1 AU = 1 km^3/yr; Armstrong, 1981, 1991) of continental crust into the mantle (Fig. 2; Stern, 2011). Global scale mass balance estimates suggest that subduction erosion accounts for greater than half of all the crust recycled along with trench sediments into subduction zones (Clift et al., 2009; Scholl and von Huene, 2009; Stern and Scholl, 2010; Straub et al., 2020). Thus subduction erosion is probably the most important process involved in recycling continental crust back into the mantle, and regionally, such as in the central Andes of northern Chile (Lamb and Davis, 2003), tectonically eroded crust may greatly exceed the mass of subducted trench sediment (Vannucchi et al., 2003, 2016; Stern, 2011; Straub et al., 2015, 2020).

Subducted crustal materials may be underplated below the forearc wedge, or returned to the crust by being incorporated in the source of arc magmas (Stern, 1989, 1990, 1991a, 1991b, 2011; Kay et al., 2005, 2013; Hacker et al., 2011, 2015; Stern et al., 2011a, 2019; Castro et al., 2013; Kelemen et al., 2014; Straub et al., 2015, 2020; Gómez-Tuena et al., 2018; Parolari et al., 2018). Some subducted continental crust may be transported deeper into the mantle (Ye et al., 2000; Willbold and Stracke, 2006, 2010), perhaps as deep as the mantle transition zone (Maruyama and Safonova, 2019), or even the core–mantle boundary, where the D″ layer may be derived from subducted former continental and oceanic crust (Komabayashi et al., 2009; Senshu et al., 2009; Yamamoto et al., 2009).

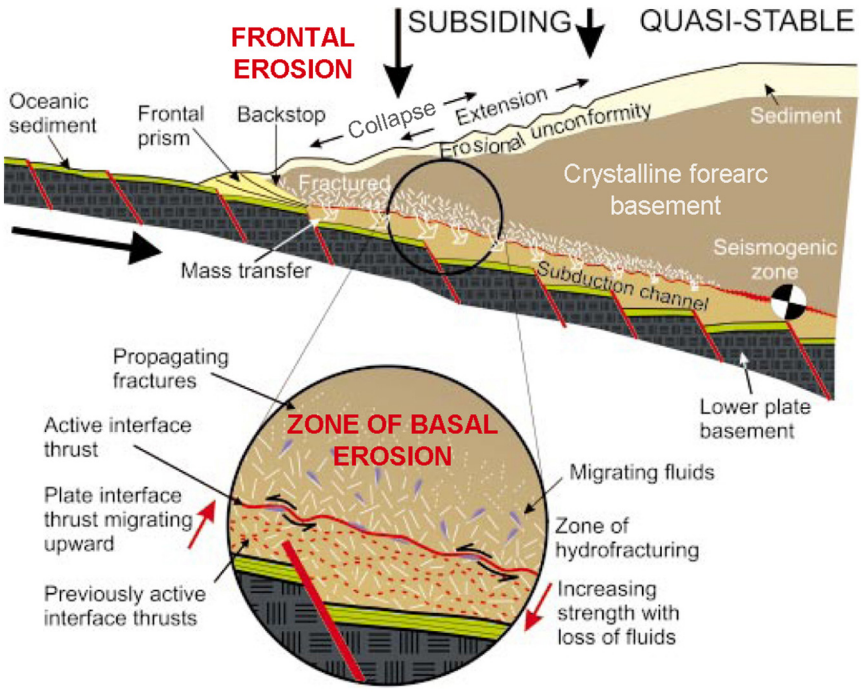

Fig. 1. Cross-section, modified from von Huene et al. (2004), illustrating the components of the forearc wedge and different processes involved in subduction erosion. The subduction channel is filled initially with both oceanic sediment and debris eroded off the forearc wedge surface that accumulates in the frontal prism. Both frontal and basal subduction erosion results in mass transfer from the bottom of the forearc wedge to the lower plate as dislodged fragments of crystalline basement are dragged into the subduction channel along with trench sediments. As pore fluid is lost from the sediments in the channel, the strength of coupling between the two plates increases and the seismogenic zone begins.

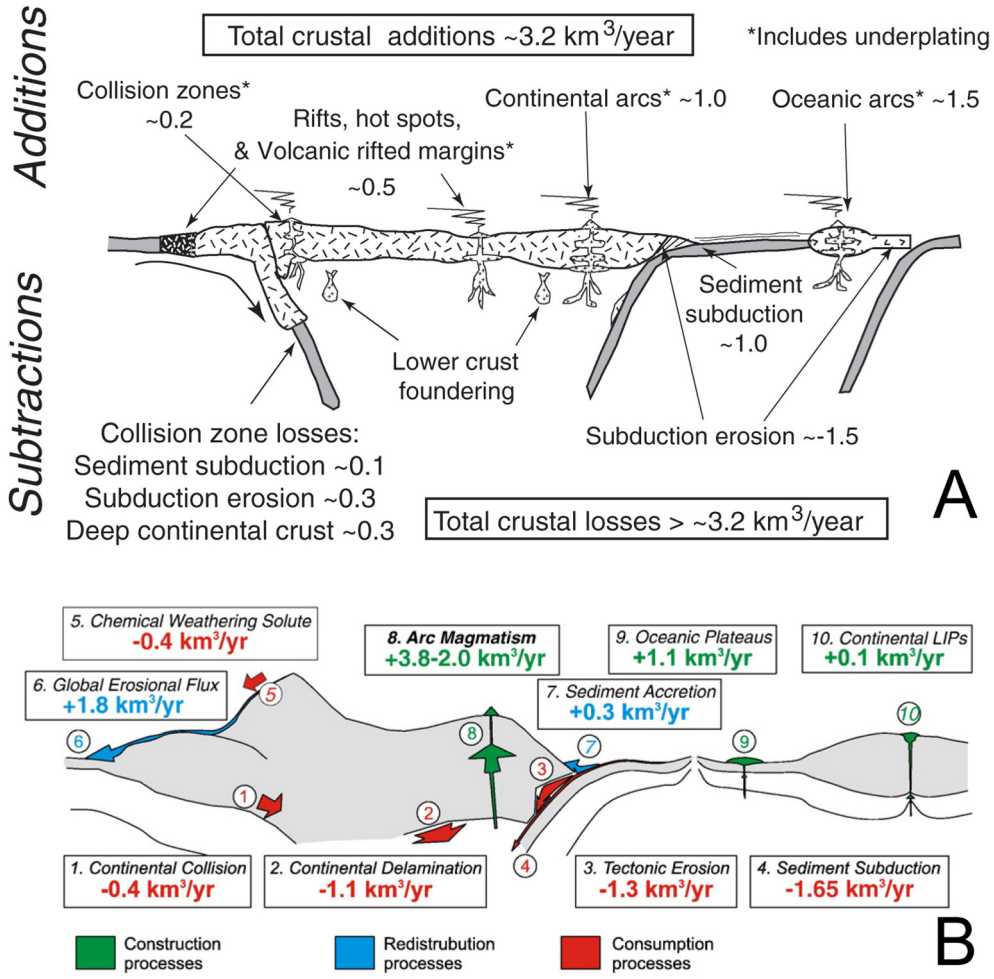

Fig. 2. Two recent compilations by (A) Stern and Scholl (2010) and (B) Clift et al. (2009) of different estimates of global rates of crustal losses and additions. Revised estimates made by Stern (2011) for both global long-term rates of subduction erosion of ~1.7 AU and total crustal losses of ~5.25 AU are higher than in either of their models, and also higher than estimates of total global crustal additions.

Since convergent plate boundary arc magmatism plays a significant role in the formation of new continental crust (Taylor, 1967; Rudnick, 1995; Plank, 2004; Hacker et al., 2011, 2015; Castro et al., 2013), it is important to evaluate the role of tectonically eroded continental crust in the formation of convergent plate boundary arc magmas. This evaluation is complicated by a number of issues. The first is that it is often not easy to determine the composition of the tectonically eroded crust being subducted. Furthermore, along with tectonically eroded crust, continental components are also being subducted in the form of both terrigenous and pelagic sediments, as well as incorporated in hydrothermally altered oceanic crust (Fig. 1). Large values for times sensitive subduction tracers such as $^{10}Be/^{9}Be$ and $^{238}U/^{230}Th$, as well as Pb isotopic data from many convergent plate boundary arc volcanic rocks, imply the incorporation of subducted pelagic marine sediments into their mantle source (Kay et al., 1978; Barreiro, 1984; Tera et al., 1986; Morris and Tera, 1989, 2000; Morris et al., 1990, 2002a; Sigmarsson et al., 1990; Plank and Langmuir, 1998; Macfarlane, 1999; Hickey-Vargas et al., 2002, 2016; Jacques et al., 2013, 2014). If components from pelagic sediments are incorporated into arc magmas, it is hard to argue that aqueous fluid soluable and/or low temperature melting components from subducted terrigenous sediment and tectonically eroded continental crust would not also be incorporated in these magmas. However, because the isotopic compositions of pelagic and terrigenous sediment and tectonically eroded continental crust often overlap, and also may overlap with continental arc crustal basement, distinguishing the specific source or proportion of these different materials in arc magmas is a difficult, but is in some cases a solvable problem.

Another complication is that the various subducted crustal materials may be transferred into the mantle source of arc magmas by a variety of different processes. The enrichment of elements soluble in aqueous fluids (B, K, Rb, Ba, Sr, U, etc) relative to less fluid-mobile elements (Ti, Zr Hf, Th, REE, etc) in many arc magmas suggests that they were transferred from the subducted slab into the mantle source of these magmas in association with the dehydration of the slab (Hickey et al., 1986; Hickey-Vargas et al., 1989, 2002, 2016; Stern et al., 1990; Morris et al., 1990, 2002a, 2002b; Sigmarsson et al., 1990, 2002; Tonarini et al., 2011). Trace-element and radiogenic isotope data (Kay, 1978, 1980; Stern et al., 1984; Defant and Drummond, 1990; Stern and Kilian, 1996; Goss and Kay, 2006; Jacques et al., 2013, 2014; Turner et al., 2017; Jicha and Kay, 2018; Wieser et al., 2019), as well as oxygen isotopes (Bindeman et al., 2005) and U-Th disequilibrium data (Sigmarsson et al., 1998), indicate that in some other cases the subducted oceanic crust, including subducted crustal materials, melts, and such slab melts transfer crustal components into the subarc mantle wedge. Reaction of these melts with the ultramafic peridotites in the mantle wedge may generate pyroxenite metasomatites capable of generating basaltic andesites and andesites, as well as basalts, by partial melting (Kelemen, 1995; Straub et al., 2011, 2015; Vogt et al., 2013; Kelemen et al., 2014; Chen et al., 2014, 2016; Chen and Zhao, 2017). Low density subducted crustal materials may also separate from the down-going slab and form subduction mélanges constituted by a mixture of oceanic sediments, tectonically eroded forearc debris, subducted

altered oceanic crust and hydrous mantle peridotite (Gómez-Tuena et al., 2018; Parolari et al., 2018). This mélange may melt, generating andesites, which erupt without significant interaction with the overlying mantle wedge (Blatter and Carmichael, 1998), or be relaminated and partially melted below the arc crust (Hacker et al., 2011, 2015; Behn et al., 2011; Castro et al., 2013; Kelemen and Behn, 2016).

One convergent plate boundary at which subduction erosion plays a significant role in the generation of arc magmas is the Andean continental margin volcanic arc along the west coast of South America. Soon after the advent and widespread acceptance of the theory of plate tectonics in the late 1960's, Rutland (1971), followed by Kulm et al. (1977), Schweller and Kulm (1978) and Ziegler et al. (1981), all suggested that in order to explain the lack of Mesozoic or Cenozoic accretionary complexes, the occurrence of pre-Andean Paleozoic crystalline basement and the Jurassic magmatic arc along the coast, and the eastward migration of the Andean Jurassic to Cenozoic magmatic belts, subduction erosion was removing crust from along the western margin South America. It wasn't until ~20 years later that Stern (1989, 1990, 1991a, 1991b), and subsequently Stern and Skewes (1995), suggested that tectonically eroded continental crust was being incorporated into the mantle source of Andean arc magmas (Fig. 3), and that variations in the amount of tectonically eroded crust incorporated in the mantle source of these magmas could explain both spatial along-arc differences and temporal changes in the isotopic composition of Andean arc basalts. Previous explanations for these isotopic variations involved either intra-crustal assimilation in deep crustal MASH zones of Mixing, Assimilation, Storage and Homogenization (Fig. 3; Hildreth and Moorbath, 1988), or differences in the isotopic compositions of lithospheric mantle source rocks of different ages below the Andean arc (Rogers and Hawkesworth, 1989). These three proposals continue to be debated, but in the last 20 years Kay and Mpodozis (2002), Kay et al. (2005, 2013), Stern et al. (2011a, 2019), Goss et al. (2013), Risse et al. (2013), Holm et al. (2014, 2016), Søager and Holm, 2013) and Søager et al. (2013, 2015a 2015b) have all provided new data to support the role of the incorporation of tectonically eroded continental crust into the mantle source of Andean magmas, and others have provided evidence for this process playing a significant role in the generation of magmas in other convergent plate boundary arcs, including the intra-oceanic Aleutian (Jicha and Kay, 2018) and South Sandwich island arcs (Tonarini et al., 2011), and the Central American (Goss and Kay, 2006) and Trans-Mexican continental margin volcanic belts (Straub et al., 2015; Gómez-Tuena et al., 2018; Parolari et al., 2018).

Stern (2011) summarized the geologic, geophysical and detrital zircon chronologic evidence used to explain the mechanisms and estimate rates of subduction erosion in different arcs. This paper reviews petrochemical evidence for the participation of tectonically eroded continental crust in the generation of magmas associated with subduction zones along convergent plate boundaries, and the implications for crustal and mantle evolution. It focuses first on the Andean continental margin arc, followed by the growing body of evidence from the other convergent plate boundaries mentioned above. In each of these arcs there are certainly counter-proposals to the crustal recycling processes associated with subduction erosion, some of which are referenced and discussed. However, in each of these arcs there is good a correlation between episodes of relatively high rates of subduction erosion and the genesis of magmas with distinctive geochemical characteristics that are suggested to reflect the recycling of tectonically eroded crustal components, not

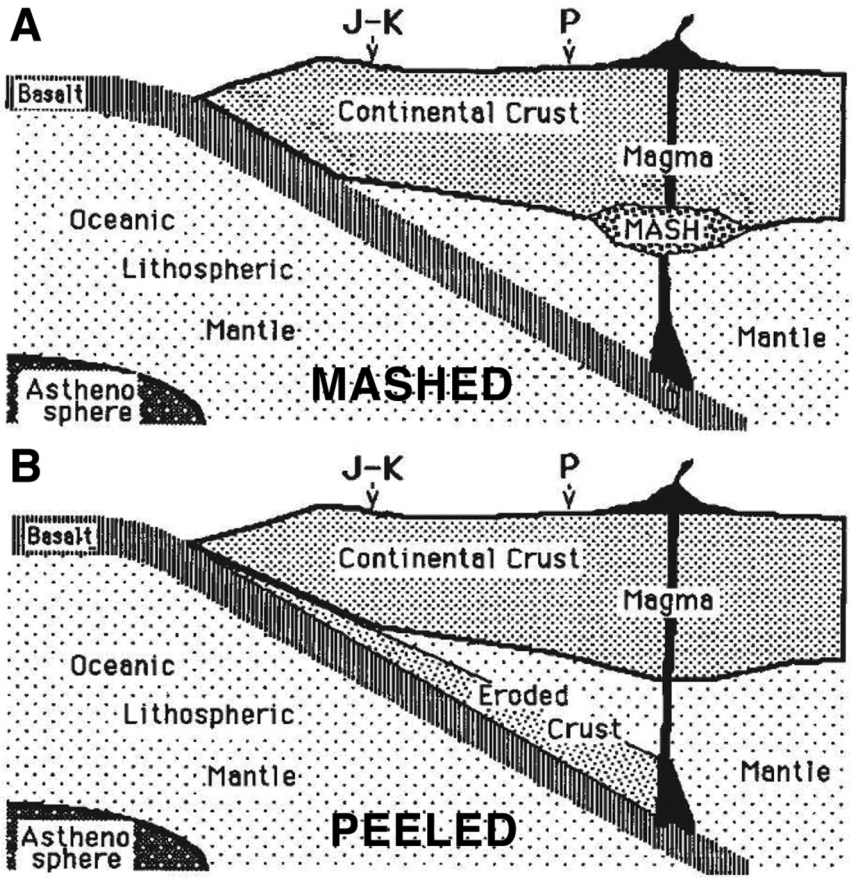

Fig. 3. Two alternative explanations, as originally illustrated by Hickey-Vargas (1991), for the incorporation of continental crust into Andean magmas. (A) MASHED involves Mixing, Assimilation, Storage and Homogenization in a zone located at either the lower crust/mantle boundary or within the crust as suggested by Hildreth and Moorbath (1988). (B) PEELED involves recycling of subduction eroded crust into the mantle wedge source as suggested by Stern (1989, 1990, 1991a, 1991b). J–K and P indicate the position of the Jurassic-Cretaceous and Pliocene plutonic belts, respectively, in the Andes of northern Chile. The recently active volcanic arc is ~250 km east of the Jurassic arc as a result in part of subduction erosion (Rutland, 1971).

trench sediments. Just to be clear, this review paper focuses more on the pros than the cons of those recent petrochemical studies, which, when taken as a whole, provide strong support for an important role for subduction erosion in the formation of convergent plate boundary arc magmas in some arcs, as well as the evolution of the continental crust and the mantle.

2. The Andean volcanic arc

2.1. Brief tectonic background

The Andean volcanic arc is divided into four separate volcanically active arc segments separate by gaps without volcanoes (Fig. 4; Stern, 2004). The Northern (NVZ), Central (CVZ) and Southern (SVZ) Volcanic Zones result from the subduction of the Nazca plate at ~7 to 9 cm/yr, while the Austral Volcanic Zone (AVZ) results from the subduction of the Antarctic plate at only ~2 cm/yr. The three volcanically active NVZ, CVZ and SVZ arc segments occur above regions below which the subducted slab dips down into the asthenospheric mantle at angles of ~25° (Barazangi and Isacks, 1976). In contrast, subduction angle flattens and the subducted slab is occluded to the base of the lithosphere below the two volcanically inactive gaps that separate these three active arc segments (Fig. 4). This implies a direct relation between subduction, the asthenospheric mantle wedge above the subducted slab, and Andean arc volcanism. This genetic connection is further supported by the nearly uniform 200 to 300 km arc-trench gap distance and the 70 to 120 km depth to the subducted slab below the entire Andean volcanic front. The volumes of magma erupted from the large stratovolcanoes along the volcanic front are greater than from the smaller volcanic centers to the east of the front above deeper portions of the subducted slab (Völker et al., 2011), and the proportion of subducted crustal components progressively decreases in the magmas erupted in the back-arc region east of the volcanic front (Stern et al., 1990; Jacques et al., 2014).

Other important geologic and tectonic factors that have been suggested to influence the composition of Andean magmas include the thickness and age of the crust through which mafic magmas, generated in the subducted slab or in the mantle wedge above the slab, pass and assimilate crust as they rise to the surface (Fig. 3), and the rates of subduction erosion that transports continental crust into the mantle below the arc. Below the southern Andes, in the central and southern parts of the SVZ (CSVZ and SSVZ), crustal thickness is only ~35 km thick (Tassara and Echaurren, 2012), while below the northern part of the SVZ (NSVZ) the crust thickens to ~50 km and further north below the CVZ in the central Andes it reaches ~70 km in thickness (McGlashan et al., 2008). The exposed crystalline basement below the CVZ includes Neoproterozoic crust, while below the SVZ exposed basement consists only of Paleozoic and Mesozoic igneous and metamorphic rocks, although older Proterozoic terranes may underlie the region (Ramos, 2010).

Estimates of subduction erosion rates are lowest west of the CSVZ and SSVZ (~35 km^3/km/my; Fig. 4; Stern, 2011), in the southern Andes of south-central Chile south of 39°S, where due to the humid and cold conditions the trench is filled with fined-grained, clay-rich fluvial-glacial sediments. West of the CVZ, in the central Andes of northern Chile, subduction erosion rates are higher (~70 km^3/km/my; Fig. 4) due to the hyper-arid conditions, first established in the Miocene (Rech et al., 2006), and much lower sediment supply to the trench, which is devoid of terrigenous sediment. Lamb and Davis (2003) suggested that in convergent plate boundary margins with high sediment supply to the trench, such as the southern Andes, layered turbidite sequences smooth out the top of the subducting plate and provide an abundant source of weak water-rich lubricating material along the plate interface. In contrast, the chaotic debris cannibalized from the plate toe in the sediment starved erosive margin west of the central Andes does not have the same lubricating effect, and the resultant higher shear stress along the plate interface in the subduction zone may support the higher elevation of the central compared to the southern Andean mountain chain.

Subduction erosion rates are also significantly higher where buoyant, topographically high features such as seamount chains and spreading ridges are being subducted, such as south of the southernmost end of the SVZ where the Chile spreading rise enters the trench (Fig. 4; Stern, 2011). They are also higher west of the NSVZ, where the Juan Fernández Ridge seamount chain is being subducted (>100 km^3/km/my; Fig. 4; Stern, 1989, 2004, 2011). What is important for evaluating the role of subduction erosion in the genesis of Andean arc magmas through time in SVZ, the focus of the next section of this paper, is that the locus of subduction of the Juan Fernández Ridge has migrated southward over the last ~22 m.y. (Fig. 5; Yáñez et al., 2001, 2002), so that the current high rate of subduction erosion west of the NSVZ was established only relatively recently, in the last <7 m.y. (Laursen et al., 2002; Kay et al., 2005; Kukowski and Oncken, 2006). Kay et al. (2005) estimate that while only ~35 km of crust was removed from the coast at 34°S between 19 and 7 Ma, ~50 km was removed after 7 Ma (Fig. 6) as the locus of subduction of the Juan Fernández Ridge migrated south towards its current position.

Subduction of the Juan Fernández Ridge also caused the angle of subduction to decrease (Stern, 1989, 2004, 2011; Stern and Skewes, 1995; Kay and Coira, 2009; Goss and Kay, 2009; Stern et al., 2011a, 2019; Goss et al., 2013; Kay et al., 2013) and the volcanic arc front of the NSVZ to migrate ~50 km eastward after 2 Ma. Although Giambiagi et al. (2015) suggest that the volcanic front at 34°S may have migrated eastward due to crustal shortening without either subduction erosion or changing subduction angle, the angle of subduction clearly does in fact flatten significantly east of the locus of subduction of the Juan Fernández Ridge, as demonstrated by Bevis and Isacks (1984). They conclude that the marked decrease in subduction angle from below the NSVZ to below the flat-slab segment north of 33°S is not an abrupt tear in the subducting plate, but rather a smooth transition achieved by flexure of a coherent slab. Since lower subduction angle enhances rates of subduction erosion (Stern, 2011), the flattening of the subduction angle below the NSVZ as the locus of subduction of the Juan Fernández Ridge migrated south to 33°S is another one of the factors that causes the estimate of this rate to be higher than further south in the SSVZ (Fig. 4).

2.2. Temporal variations at 34°S

Isotopic data for the volcanic rocks recently erupted from the active volcanoes in the NSVZ indicate that they have higher $^{87}Sr/^{86}Sr \geq 0.7050$ and lower $\varepsilon_{Nd} \leq -1$ (Figs. 6 and 7) compared to further south in the CSVZ ($^{87}Sr/^{86}Sr \leq 0.704$; $\varepsilon_{Nd} \geq 5$). Hildreth and Moorbath (1988) argued that this was due to the thicker crust in the region below the NSVZ and greater intra-crustal contamination as mantle derived magmas rose to the surface (Fig. 3). In contrast, Stern (1989, 1990, 1991a, 1991b) suggested that this was due to increased rates of subduction erosion (Fig. 4) and mantle source region contamination by subducted crustal components (Fig. 3). More recently, Turner et al. (2017) and Wieser et al. (2019) have suggested that substantial, but nearly uniform contribution of melts from subducted sediment and altered oceanic crust are required at all latitudes of the SVZ, and that the distinctive isotopic characteristics of magmas erupted from recently active NSVZ volcanoes are derived from an enriched ambient mantle component, similar to EM1-type ocean island basalts, superimposed on a northward decline in melt extent.

These different suggestions are best evaluated in the context of the temporal evolution of the isotopic compositions of magmas, in particular olivine-bearing mafic magmas erupted through time at the latitude of the NSVZ. This is one of the best studied segments of the Andean arc because of its proximity to the giant El Teniente Cu-Mo deposit (Fig. 6; Cuadra, 1986; Stern and Skewes, 1995; Skewes et al., 2002; Kay et al., 2005; Stern et al., 2011b, 2019; Muñoz et al., 2012, 2013). At this latitude, detailed studies of the chronology, petrochemistry and isotopic compositions of volcanic and plutonic rocks emplaced between the early Miocene and Quaternary allow an evaluation of the possible

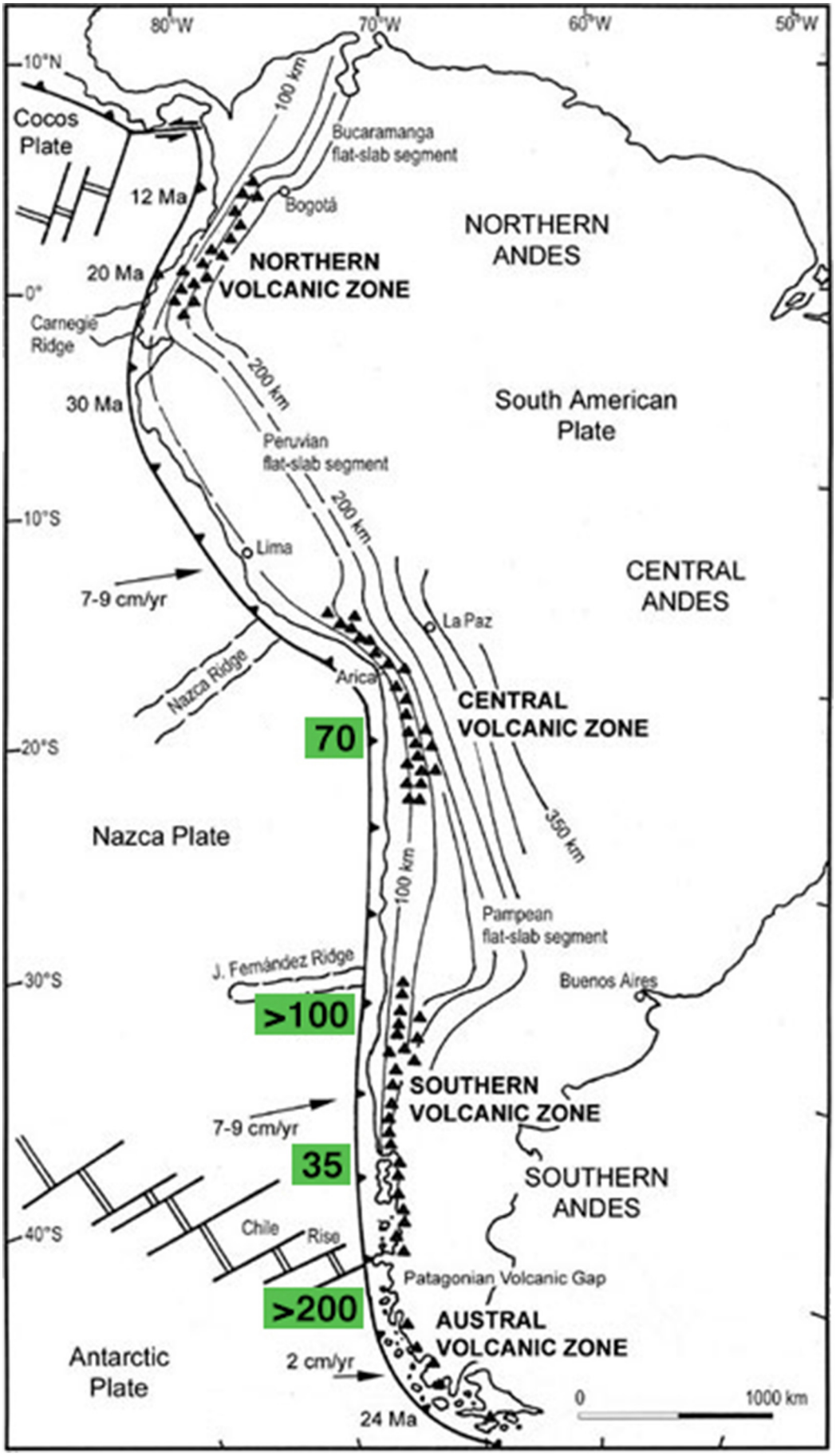
80°W
70°W
60°W
50°W
10°N
0°
10°S
20°S
30°S
40°S
Cocos Plate
12 Ma
20 Ma
30 Ma
Carnegie Ridge
Nazca Ridge
Chile Rise
Antarctic Plate
Nazca Plate
South American Plate
100 km
200 km
350 km
Bucaramanga flat-slab segment
Peruvian flat-slab segment
Pampean flat-slab segment
Patagonian Volcanic Gap
Bogotá
Lima
La Paz
Arica
Buenos Aires
J. Fernández Ridge
NORTHERN VOLCANIC ZONE
CENTRAL VOLCANIC ZONE
SOUTHERN VOLCANIC ZONE
AUSTRAL VOLCANIC ZONE
NORTHERN ANDES
CENTRAL ANDES
SOUTHERN ANDES
7-9 cm/yr
7-9 cm/yr
2 cm/yr
70
>100
35
>200
24 Ma
0
1000 km

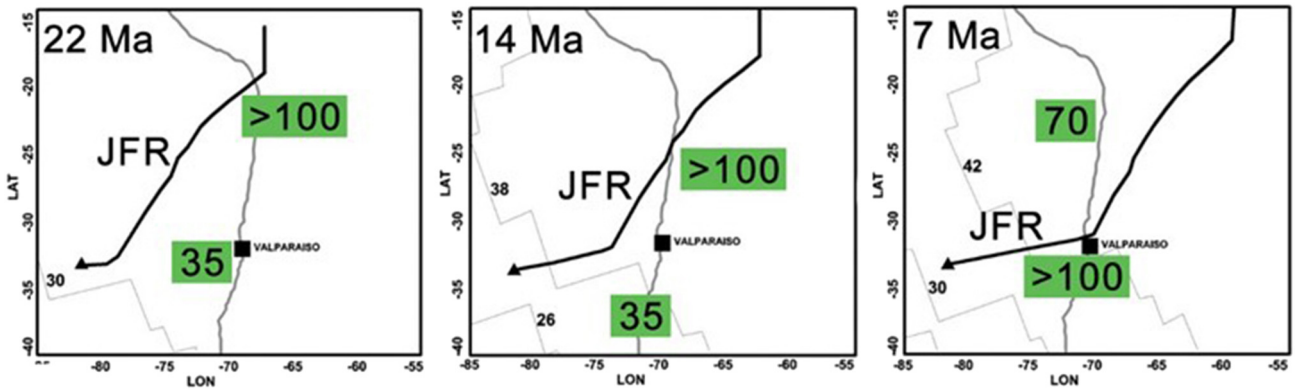

Fig. 5. Predicted path for the southward migration of the Juan Fernández Ridge (JFR, dark solid line) during the Miocene, modified from Yáñez et al. (2001, 2002). The location of the hot-spot generating the ridge is indicated by the triangle. The margin of South America (light solid line) moves westward, while the hot-spot location remains stationary. Sea-floor magnetic lineations are indicated with their magnetic number. The location of Valparaíso along the coast of Chile (33°S) west of the northern end of the Andean SVZ (Fig. 4) is indicated as a reference. Estimated rates of subduction erosion within the pale green boxes (in km^3/km/my; Stern, 2011) are highest just south of the locus of subduction of the ridge, and these high rates of subduction erosion only began to affect the northern end of the SVZ during the last 7 m.y. (Laursen et al., 2002; Kay et al., 2005; Kukowski and Oncken, 2006), ultimately resulting in the ~50 km eastward migration of the northern SVZ volcanic arc after 2 Ma (Fig. 6; Stern, 1989).

processes involved in magma genesis as the Juan Fernández Ridge migrated southward to its current locus of subduction just west of this region (Figs. 4, 5 and 6). As this occurred the crust thickened (Fig. 8), the angle of subduction of the Nazca plate flattened (Stern, 1989), the volume of the igneous rocks decreased though time, the arc front migrated eastward after ~16 Ma and again at ~2 Ma as subduction erosion rates increased (Fig. 6; Stern and Skewes, 1995; Charrier et al., 2002; Nyström et al., 2003; Kay et al., 2005; Muñoz et al., 2006, 2012, 2013; Stern et al., 2011a, 2011b, 2019), and the isotopic compositions of the late Tertiary volcanic and plutonic rocks changed significantly (Figs. 7 and 9-11).

The sequence of progressively younger igneous rocks at the latitude of El Teniente (34°S) include first the continental volcanic rocks, up to 3300 m thick, of the late Oligocene to early Miocene (≥15 Ma) Coya-Machali or Abanico Formations (pale pink in Fig. 6; Charrier et al., 2002; Nyström et al., 2003; Kay et al., 2005; Muñoz et al., 2006), erupted above thin (<30 km) crust in a transtensional intra-arc basin. Olivine-bearing tholeiites of this age formed by relatively high degrees of partial melting of nearly anhydrous subarc mantle (Grove et al., 2012), as indicated by their low La/Yb ratios (2–6), modified to only a small degree by the influx from below of slab-derived components as implied by their low initial $^{87}Sr/^{86}Sr$ (0.7033–0.7039) and high ε_{Nd} (+6.5 to +4; Figs. 7 and 11).

Subsequently, after an early Miocene (19–16 Ma) episode of crustal deformation, thickening and uplift, extrusive rocks of the middle to late Miocene Farellones Formation, locally referred to as the Teniente Volcanic Complex at 34°S, were erupted (dark red in Fig. 6). The Teniente Volcanic Complex consists of tholeiitic to calc-alkaline lavas, which plot in the medium to high-K group of convergent plate boundary arc magmas (Kay et al., 2005). Olivine-bearing basalts of the Teniente Volcanic Complex generally have higher La/Yb (4–9) compared with mafic rocks of the older Coya-Machali Formation, and the mafic, intermediate and silicic rocks of the Teniente Volcanic Complex also have higher initial $^{87}Sr/^{86}Sr$ (0.7039–0.7041) and lower initial ε_{Nd} (+2.7 to +3.6; Fig. 7). These isotopic values may reflect increased rates of subduction erosion associated with the approximately 35 km eastward migration of the volcanic front at this time (Fig. 6; Stern and Skewes, 1995; Kay et al., 2005). The higher La/Yb suggest a somewhat lower percentage of mantle partial melting, and the volume of the middle and late Miocene Teniente Volcanic Complex is less than the previously erupted Coya-Machali Formation. Volcanism in this belt decreased through time and no extrusive rocks with ages <6.5 Ma have been found within the vicinity of the El Teniente deposit.

The extrusive rocks of the Teniente Volcanic Complex were intruded between ~8.9 and 4.6 Ma, during an episode of further crustal deformation, thickening and uplift (Fig. 8), by gabbro, diabase, diorite, tonalite, latite, and dacite porphyry plutons of the Teniente Plutonic Complex (Cuadra, 1986; Stern and Skewes, 1995; Kurtz et al., 1997; Skewes et al., 2002; Maksaev et al., 2004; Kay et al., 2005; Stern et al., 2011b, 2019). These include 1) the >50 km^3 Teniente Mafic Complex (8.9 ± 2.4 Ma) of mafic intrusives with the form of a laccolith 2000 m thick in the center of the deposit; 2) the equigranular holocrystalline Sewell Tonalite complex (7.05 ± 0.14 Ma), with an estimated volume of ~30 km^3; and 3) a series of much smaller volume (<1 km each) dacite and diorite porphyries (6.09 ± 0.18 Ma), the unusual Cu- and S-rich anhydrite-bearing Porphyry A stock (5.67 ± 0.19 Ma), the Teniente Dacite Porphyry dike (5.28 ± 0.10 Ma), a few latite dikes (4.82 ± 0.09 Ma), and finally a small dacite porphyry (4.58 ± 0.10 Ma). These progressively smaller in volume intrusive rocks all have isotopic compositions similar to Teniente Volcanic Complex extrusives (Figs. 7, 9-11), suggesting that they formed in a large long-lived well-mixed magma chamber below the El Teniente deposit (Fig. 8; Skewes et al., 2002; Stern et al., 2011b, 2019).

Multiple Cu-mineralized magmatic-hydrothermal breccia pipes were emplaced into these plutonic rocks during the same time period as the felsic porphyry intrusions, between 6.3 and 4.4 Ma (Skewes et al., 2002). Pliocene post-mineralization igneous phases include small volume, high-MgO (≥7.50 wt%) olivine (Fo88) and hornblende lamprophyre dikes (3.8 to 2.9 Ma; Cuadra, 1986; Stern and Skewes, 1995; Kay et al., 2005; Stern et al., 2011a, 2011b, 2019), with higher La/Yb (10−13), as well as higher initial $^{87}Sr/^{86}Sr$ (0.7040–0.7045) and lower initial ε_{Nd} (+1.2 to +0.2; Fig. 7) compared to the older Miocene volcanic and plutonic rocks at this latitude. Their small volume and higher La/Yb suggest a smaller percentage of mantle partial melting compared to the older Miocene basalts (Stern et al., 2011a). Moore and Carmichael (1998), Blatter and Carmichael (1998, 2001) and Barcley and Carmichael (2004) have all suggested that the genesis of high-MgO olivine and hornblende bearing lamprophyres involves partial melting of a more hydrated mantle compared to plagioclase-rich hornblende-free basalts.

The youngest igneous rocks in the area are primitive olivine-bearing (Fo72–64) basaltic andesite (MgO ≥ 4.5 wt%) Pliocene lavas in the valley

Fig. 4. Schematic map, modified from Stern (2004), of the four volcanically active zones in the Andes, the three volcanically inactive gaps that separate these four zones, subduction geometry as indicated by depth in kilometers to the Benioff zone, oceanic ridges, ages of oceanic plates close to the trench, convergence rates and directions along the length of the Andes, and the estimated rates of subduction erosion in km^3/km/my from Stern (2011) within the pale green boxes.

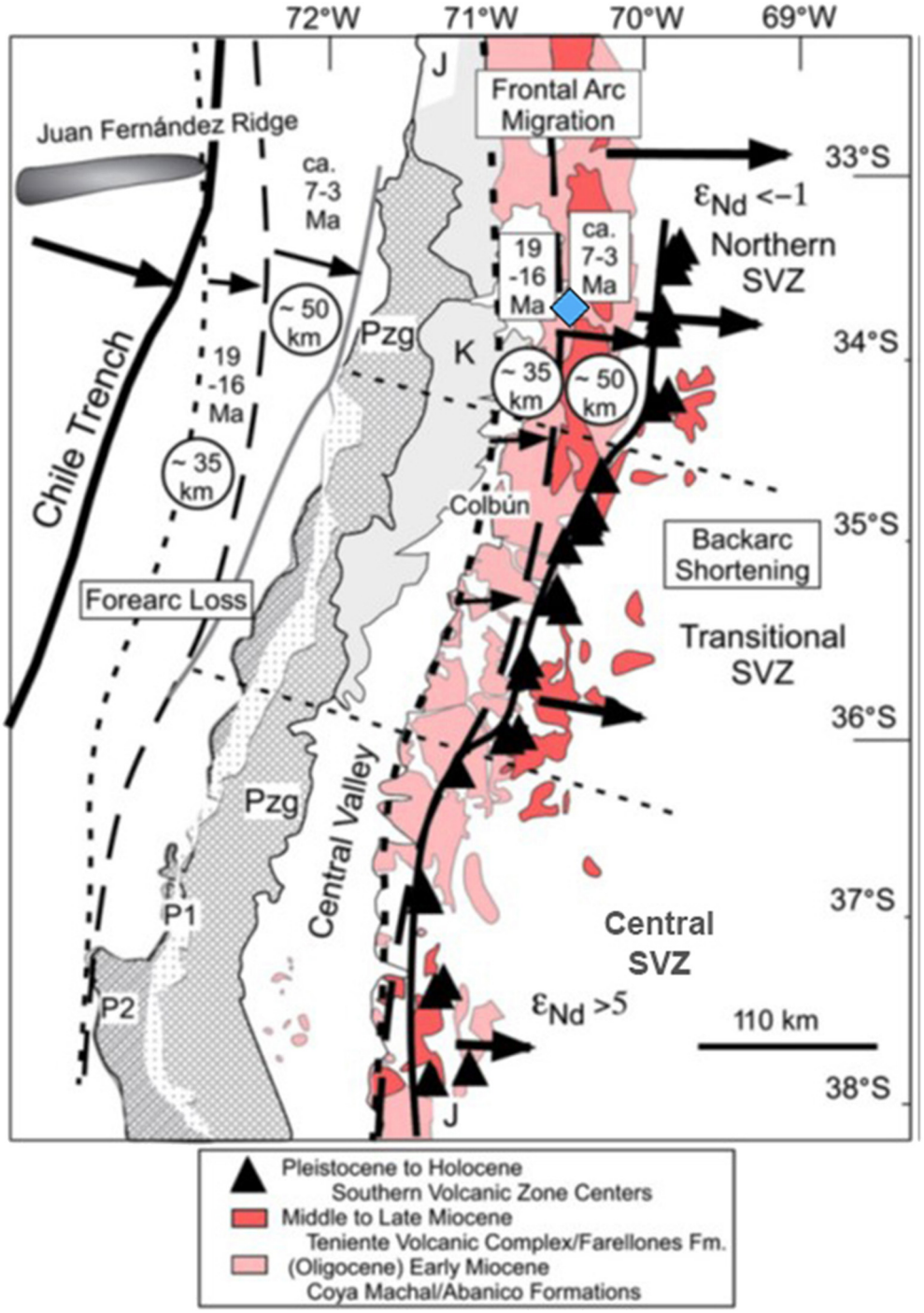

Fig. 6. Regional map of central Chile between ~32°S and 38°S, modified from Kay et al. (2005), with lines showing correlations of early Miocene to Holocene arc fronts on land and inferred position of corresponding coastlines offshore. Arrows show relative amounts of frontal-arc migration, forearc loss, and backarc shortening. Northwest–southeast trending dashed lines show offsets in the modern volcanic front that separate the Southern Volcanic Zone (SVZ) into the northern, transitional, and central segments (Stern, 2004). In the active arc region, lines connect outcrop patterns marking early Miocene (pink), middle to late Miocene (red), and the Pleistocene to Holocene volcanic centers of the SVZ (triangles) magmatic fronts. Arrows between the lines indicate inferred distance (given in circles) of frontal-arc migration from 19 to 16 Ma and from 7 to 3 Ma. In the forearc, lines between the trench and the coast show inferred early Miocene (short dashed) and middle to late Miocene (long dashed) coastlines under the assumption that the distance of frontal-arc migration equals the width of missing coast. Arrows between the lines in this region indicate distance (shown in circles) of inferred loss by subduction erosion from ca. 19 to 16 Ma and 7 to 3 Ma. In the back-arc, the length and position of arrows show the location and proportional amounts of crustal shortening over the past 20 my inferred from structural profiles. Also shown are other outcrop patterns that have long been used as evidence for forearc subduction erosion along this margin (Rutland, 1971). The first is the northward narrowing and disappearance of the Paleozoic high pressure (P1) and low pressure (P2) paired metamorphic and granitoid (Pzg) belts along the coast. The second is the presence of Jurassic arc rocks (marked by J) along the coast north of 33°S, but inland near the SVZ at ~38°S. K indicates Cretaceous magmatic rocks. ε_{Nd} is +5 for active central SVZ volcanoes south of 37°S, and ≤−1 for those in the NSVZ north of 34°S, as a result of increased mantle source region contamination by subducted crust due to the northward increase in the rate of subduction erosion associated with the subduction of the Juan Fernández Ridge at 33°S (Stern, 1989, 1990, 1991a, 1991b; Stern and Skewes, 1995; Stern et al., 2011a, 2019). The El Teniente Cu-Mo deposit occurs at the blue diamond (Skewes et al., 2002; Stern et al., 2011b).

of the Cachapoal river just west of the El Teniente deposit (2.3 Ma; Charrier and Munizaga, 1979; Stern and Skewes, 1995), with still higher initial $^{87}Sr/^{86}Sr$ (0.7049) and lower initial ε_{Nd} (−1.1; Fig. 7). The generation of primitive olivine-bearing basaltic andesites, as with the somewhat older olivine lamprophyres, also requires relatively high H_2O contents in the mantle (3 to 6 wt%; Grove et al., 2012) or

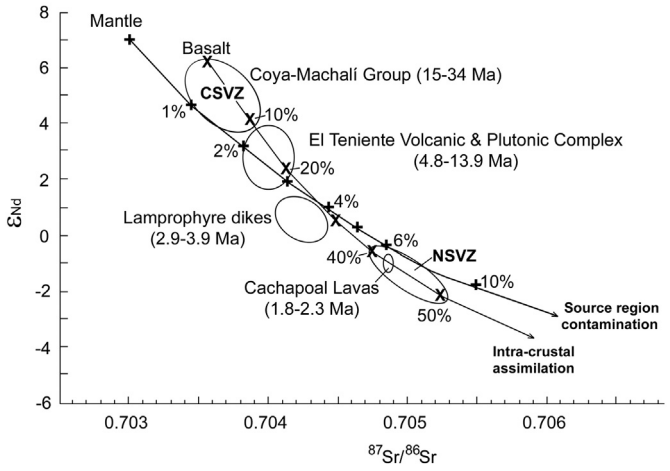

Fig. 7. Sr versus Nd isotopic values of the various groups of igneous rocks of different ages in a transect across the Andes at the latitude of El Teniente (34°S; Stern and Skewes, 1995; Kay et al., 2005; Stern et al., 2011a, 2011b, 2019). The figure illustrates both a source region contamination model of primitive mantle (+'s, Sr = 36 ppm with $^{87}Sr/^{86}Sr = 0.703$ and Nd = 1.8 ppm with $\varepsilon_{Nd} = +7$) mixed with various proportion of subducted sediment and Paleozoic Coastal Cordillera granitoids (Sr = 340 ppm with $^{87}Sr/^{86}Sr = 0.7074$ and Nd = 40 ppm with $\varepsilon_{Nd} = -6$; Parada et al., 1999; Macfarlane, 1999), and also a MASH intra-crustal assimilation model for a Coya-Machali basalt (x's, Sr = 450 ppm with $^{87}Sr/^{86}Sr = 0.7035$ and Nd = 9 ppm with $\varepsilon_{Nd} = +6$) assimilating various proportion of Paleozoic-Triassic Choiyoi granite Andean basement (Sr = 340 ppm with $^{87}Sr/^{86}Sr = 0.7074$ and Nd = 20 ppm with $\varepsilon_{Nd} = -6$). Both models reproduce the isotopic compositions of the progressively younger rocks in the transect, but the latter MASH model requires assimilation of unacceptably high proportions of granite crust and is inconsistent with generation of primitive low SiO_2 olivine-bearing mafic rocks in each age group (see Fig. 11), as well as the progressively higher Sr content of the sequentially younger rocks, which is due instead to decreasing degrees of partial mantle melting (Stern, 1989, 1991a; Stern and Skewes, 1995; Kay et al., 2005) associated with decreasing volume of magmas erupted through time at this latitude in the Andes. Basalts from the active central Southern Volcanic Zone (CSVZ) are isotopically similar to early Miocene Coya-Machali basalts, and those from the northern SVZ (NSVZ) are isotopically similar to the Pliocene Cachapoal mafic lavas, so that the spatial isotopic variations between the active CSVZ and NSVZ mirror the temporal isotopic variations between the early Miocene and Pliocene mafic rocks at the 34°S, and are due to the same process of increased subduction erosion rates and mantle source region contamination northwards from the CSVZ towards the NSVZ.

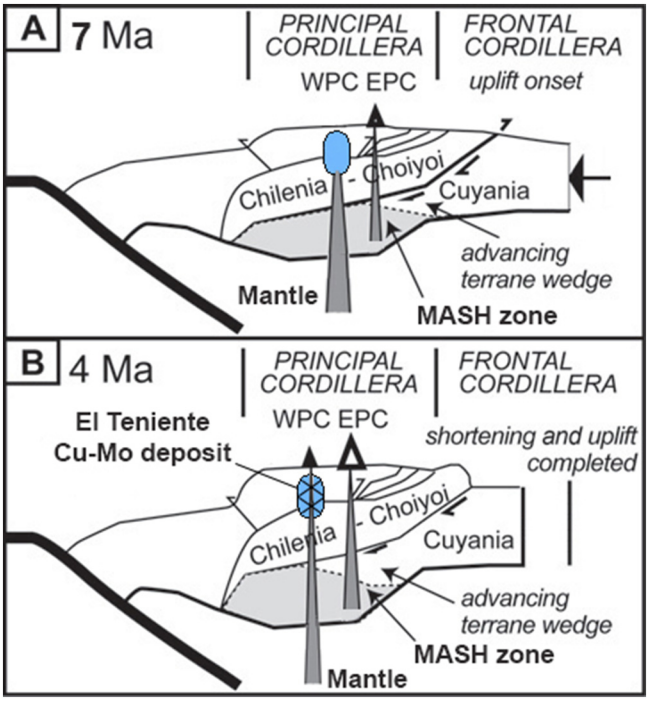

Fig. 8. Schematic profiles, modified after Muñoz et al. (2013), of crustal evolution of the Andes of central Chile and Argentina at 7 Ma (**A**) and 4 Ma (**B**). Evolution is characterized by increased shortening rates along the eastern flank of the orogenic belt after 7 Ma, where the Chilenia-Choiyoi block overrides the Cuyania terrane, producing uplift of the Frontal Cordillera. This produced increasing crustal thickness, which led to uplift of the entire belt. Deformation amounts suggest that the Cuyania block descended immediately below the eastern part of the magmatic arc, changing composition of the base of the crust and thus changing the crustal magmatic source (MASH zone) below the Eastern Principle Cordillera (EPC). However, below the Western Principle Cordillera (WPC), mafic olivine-bearing magmas continued to rise from the mantle without intra-crustal assimilation in a MASH zone. Between 7 and 4 Ma, these mantle-derived mafic magmas did not reach the surface, but were mixed, stored and homogenized in a large magma chamber (blue) below the El Teniente Cu-Mo deposit (Skewes et al., 2002; Stern et al., 2011b, 2019). Within this chamber, the felsic plutons of the deposit developed without crustal assimilation and above it the mineralized breccias in the deposit were emplaced. As subduction angle flattened and magma supply from the mantle decreased this chamber solidified. After 4 Ma, high-MgO olivine lamprophyres and olivine-bearing basaltic andesites, derived from a mantle hydrated and isotopically modified by increased proportions of subducted crust (Fig. 7), rose through the now crystallized magma chamber, without any intra-crustal assimilation, to form dikes and lavas.

modification of the subarc mantle composition by subducted silicic components. After 2 Ma the locus of Andean arc magmatism migrated eastwards ~50 km (Fig. 6). However, the mafic olivine-bearing basaltic andesites and andesites erupted from both small monogenetic cones and stratovolcanoes along the recently active volcanic front in the NSVZ have isotopic compositions similar to the Pliocene basaltic andesite in the valley of the Cachapoal river (Fig. 7; Futa and Stern, 1988; Wieser et al., 2019). This suggests that the processes that produced the temporal isotopic variation at 34°S are also responsible for the isotopic compositions of the recently erupted magmas in the NSVZ and also therefore for their isotopic differences with basalts erupted further south in the active CSVZ (Figs. 7 and 11).

The Pb (Fig. 9; Stern et al., 2011a) and Hf (Fig. 10; Stern et al., 2019) isotopic compositions of these igneous rocks also change through time from the early Miocene to the Pliocene, with $^{206}Pb/^{204}Pb$ increasing from an average of 18.50 to 18.67 and $^{176}Hf/^{177}Hf$ decreasing ten $\varepsilon_{Hf(t)}$ units, from +11.6 down to +1.6, in the 12.7 million years between 15 and 2.3 Ma (Stern et al., 2019). What is of most significance is that all these temporal isotopic changes occur specifically in olivine-bearing mafic rocks derived from the mantle directly below the general area of the El Teniente Cu-Mo deposit, and that there is no spatial change in the location of the subarc mantle source of these mafic phases. Also, although the early Miocene Abanico Formation volcanic rocks and the middle to late Miocene El Teniente Volcanic and Plutonic Complex rocks include a wide range of compositions, from mafic olivine-bearing basalts and gabbros through silicic rhyolites and granites (Fig. 11), the isotopic compositions of these rocks vary systematically with age (Figs. 9 and 10), but at each stage the isotopic compositions are relatively independent of SiO_2 content.

In the Andean Central Volcanic Zone (CVZ; Fig. 4) of Chile at latitude 22°S, temporal isotopic changes between the Mesozoic and Quaternary are similar to those observed between the early Miocene and Pliocene igneous rocks at 34°S. In the CVZ the magmatic arc migrated progressively eastward through time, and the observed temporal isotopic changes occurred in association with arc migration. Rogers and Hawkesworth (1989) suggested that these changes were caused by increased mobilization of old, Neoproterozoic subcontinental mantle lithosphere as the locus of volcanism in the central Andes migrated eastward. Neoproterozoic terranes are not exposed, but may also occur below the NSVZ in the area of El Teniente at 34°S (Fig. 8), although the oldest inherited zircons in any of the igneous rocks in the region are only 250 to 300 Ma (Muñoz et al., 2013). However, unlike in the CVZ of northern Chile, the isotopic changes observed in mafic mantle-derived rocks through time at the latitude of the NSVZ occur in rocks sourced sequentially from the same section of subcontinental mantle and are not associated with the eastward arc migration which occurred after 2 Ma (Fig. 8; Stern, 1989; Stern and Skewes, 1995). Therefore, these temporal isotopic changes are not due to any progressive changes in the age of the subcontinental mantle lithosphere within which these mafic magmas were generated.

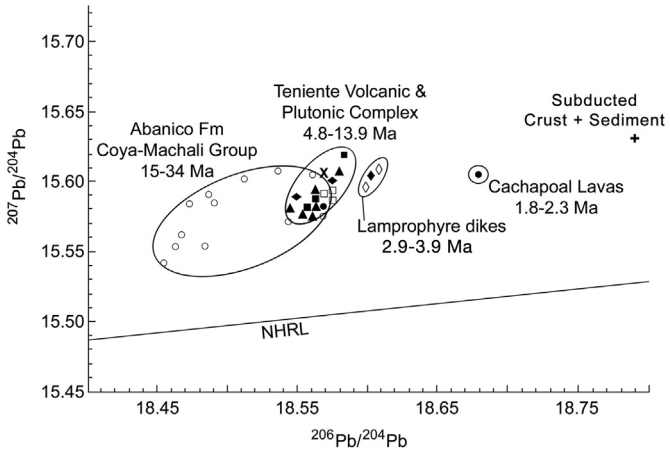

Fig. 9. $^{206}Pb/^{204}Pb$ versus $^{207}Pb/^{204}Pb$ for lamprophyre dikes (solid and open diamonds) from the vicinity of El Teniente deposit and basaltic andesite flows (solid circle) in the valley of the Cachapoal River (Stern et al., 2011a), compared to older Coya-Machali and Abanico Formation volcanics (circles; Nyström et al., 2003; Kay et al., 2005; Muñoz et al., 2006), El Teniente Volcanic and Plutonic Complex samples (open squares; Stern and Skewes, 1995; Kay et al., 2005), the host plutons of El Teniente deposit (solid squares, circles and triangles; Skewes et al., 2002; Stern et al., 2011b), the regionally defined Young Plutonic Complex (open triangles; Kay et al., 2005). Also shown is the Pb isotopic composition of El Teniente ores (X from Puig, 1988) and that of a model composition of subducted sediment and continental crust (+) as calculated by Macfarlane (1999). The data show a temporal trend of $^{206}Pb/^{204}Pb$ towards this value.

The temporal isotopic changes observed in the igneous rocks emplaced sequentially through time in the vicinity of El Teniente at 34°S are also similar to those differences observed spatially in magmas erupted from active volcanoes in the CSVZ compared to the NSVZ (Figs. 6 and 7). Hildreth and Moorbath (1988) attributed these differences to a greater amount of crustal assimilation due to the thicker crust (≥50 km) below the NSVZ compared to the CSVZ (≤35 km) through which mantle-derived magmas passed as they rose to the surface. The crust thickened through time below the Andes at latitude 34°S (Fig. 8) and Muñoz et al. (2012, 2013) proposed that the temporal changes in the isotopic compositions of the magmas generated through time along the Miocene to Pliocene volcanic front at this latitude also reflect increased crustal assimilation as the crust thickened. However, three facts argue against this suggestion. The first is that the temporal isotopic changes are observed in mafic, olivine-bearing mantle-derived rocks for which any significant amount of crustal assimilation is unlikely. The second is that crustal assimilation should result in a correlation of increasing SiO_2 content with changing isotopic compositions (Curve 2 in Fig. 11). The data indicate that for each age group of igneous rocks, intermediate and silicic compositions have isotopic compositions essentially similar to the associated mafic rocks of the same age (Curve 1 in Fig. 11), implying that the genesis of these intermediate and silicic compositions did not involve significant assimilation of isotopically evolved crustal rocks. Instead the observed isotopic changes occurred through time, and they occurred in mafic as well as more silicic rocks, so that these changes are not correlated with SiO_2 content. The third, noted by Kay et al. (2005), is that the increasing crustal isotopic character through time of the igneous rocks at 34°S would require increasing amount of crustal assimilation, but because the volume of these rocks progressively decreases though time, the available heat for crustal melting and thus the potential for assimilation also decreases, opposite to what is required to explain the isotopic changes by increased intra-crustal assimilation.

Muñoz et al. (2013) do demonstrate that for late Miocene (8 to 3 Ma) igneous rocks emplaced east of the volcanic front, in the Eastern Principle Cordillera (EPC; Fig. 8) in Argentina, crustal contamination processes are evidently involved in the genesis of at least some of the more silicic igneous rocks formed as the crust thickened below this area. However, compared to rocks erupted in the Western Principle Cordillera (WPC), along the volcanic front in the vicinity of El Teniente, these EPC volcanics have both a wider range in $\varepsilon_{Hf(i)}$ values, between −4 to +4, and contain zircon crystals which show abundant inherited cores of 250 to 300 Ma, documenting the assimilation of mainly Paleozoic basement. This is not the case for any of the mantle-derived mafic rocks (Fig. 10), or the intermediate and silicic rocks of any age emplaced along the Miocene to Pliocene volcanic front in the vicinity of El Teniente, and there is no isotopic or petrologic evidence that the genesis of any of these rocks involved extensive intra-crustal assimilation as the crust thickened below this area.

Alternatively, Stern (1989, 1990, 1991a, 1991b), Stern and Skewes (1995), Kay et al. (2005) and Stern et al. (2011a, 2019) have modeled the amount of mantle source region contamination by subducted continental crust (Figs. 7 and 11) required to produce the temporal isotopic

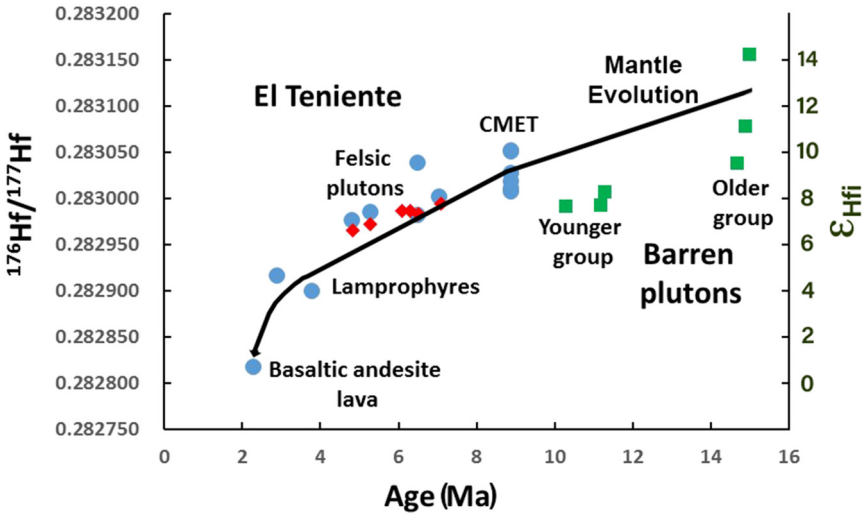

Fig. 10. $^{176}Hf/^{177}Hf$ versus age (Ma) for samples from within the El Teniente deposit (blue circles from Stern et al. (2019) and red diamonds from Muñoz et al. (2012)) and Middle Miocene barren plutons in the same general area (green squares from Deckart et al. (2010)). The size of the symbols is greater than the error in the $^{176}Hf/^{177}Hf$ values. The mantle isotopic evolution line is drawn from the average of the older group of middle Miocene barren plutons through the late Miocene Teniente Mafic Complex (CMET) olivine basalts and gabbros, and then to the Pliocene olivine lamprophyres and olivine-bearing basaltic andesites, ignoring the younger group of barren plutons because these have macroscopic evidence for intra-crustal assimilation (Deckart et al., 2010). The amount of subducted crust added to the mantle to generate this line varies from 1 wt% for the middle Miocene older group of barren plutons, to 2 wt% for the late Miocene Teniente Mafic Complex rocks, to 4 wt% for the Pliocene olivine lamprophyres and 6 wt% for olivine-bearing basaltic andesites (Stern et al., 2019), consistent with the amount of crust required to produce the Sr- and Nd-isotopic variations in these same rocks (Figs. 7 and 11).

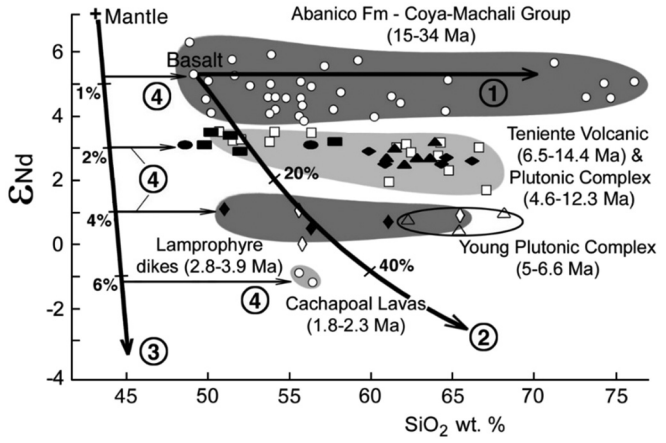

Fig. 11. Published values of ε_{Nd} vs SiO_2 (wt%) for igneous rocks of different ages from the transect across the Andes at the latitude of El Teniente (34°S; open symbols including the Abanico Formation (o), Teniente Volcanic and Plutonic Complexes (□), Young Plutonic Complex (Δ) and lamprophyres (◊); Stern and Skewes, 1995; Kay et al., 2005; Stern et al., 2011a, 2011b, 2019), compared with values for samples of the host-rocks in the deposit (filled symbols including the Teniente Mafic Complex (■), Sewell Tonalite (▲), felsic porphyries(♦), and Porphyry A granitoid (●)). Three curves (Stern et al., 2019) illustrate the progressive changes in SiO_2 and ε_{Nd} for crystal-liquid fractionation without assimilation (curve #1), intra-crustal assimilation of Choiyoi granite Andean basement by a Coya-Machali basalt, combined with crystal-liquid fractionation (MASH; curve #2), and mantle source region contamination by subducted Andean Coastal Cordillera granite plus marine sediment (curve #3). Parameters for these models are the same as in Fig. 7, and the tic marks along each curve indicate the same amount of crustal contamination as in the MASH and source region contamination models illustrated in Fig. 7. Crystal-liquid fractionation increases SiO_2 without changing isotopic composition. MASH increases SiO_2 as ε_{Nd} decreases. Source region contamination decreases ε_{Nd} in the mantle, but mantle partial melting (curves #4) for the modified mantle still produces mafic olivine-bearing basalts and lamprophyres.

variations observed in the igneous rocks at 34°S between the Miocene to the Pliocene. These models suggest that, because of the low Sr, Nd and Hf contents of the subarc mantle, only a small (1 to 6 wt%) but increasing amount of tectonically eroded late Paleozoic to early Jurassic granites exposed in the Andean Coastal Cordillera range (Parada et al., 1999; Kay et al., 2005; Stern et al., 2011a, 2019) must be added to depleted subarc mantle to produce these temporal isotopic changes. The subduction of terrigenous sediments can be ruled out because the terrigenous sediment in the trench west of the NSVZ are derived from erosion of the Mesozoic and Cenozoic rocks of the High Andes (Thornburg and Kulm, 1987a, 1987b) and do not have the same isotopic leverage as the Paleozoic granites of the Coastal Cordillera.

Based on these geochemical models, Stern (1989, 1990, 1991a, 1991b), Stern and Skewes (1995), and Stern et al. (2011a, 2019) have proposed that the isotopic changes observed between the Miocene and Pliocene in the area of the NSVZ are due to increased rates of subduction erosion and mantle source region contamination as the locus of subduction of the Juan Fernández Ridge migrated southwards from the early Miocene to the present (Fig. 5). Current estimated rates of subduction erosion west of the NSVZ are >100 km^3/km/my, approximately three time the rate of subduction erosion west of the CSVZ to the south (~35 km^3/km/my; Fig. 4). This latter lower rate was the likely rate of subduction erosion at 34°S prior to the late Miocene approach of the locus of subduction of the Juan Fernández Ridge (Fig. 5).

Although the amount of subducted crust required to generate the observed isotopic changes in the mantle source of these rocks increased through time, it nevertheless remained relatively small (Figs. 7 and 11) compared to that required by models of intra-crustal assimilation. The decreasing volume of magmas erupted through time, leading ultimately to the eastward migration of the volcanic front after 2 Ma, and the increasing La/Yb rations of the magmas generated between the early Miocene and Pliocene, suggests a progressive reduction in the partial melting percentage of a cooler mantle wedge over a shallower subducting slab (Stern, 1989, 2004, 1991; Kay et al., 2005; Stern et al., 2011a, 2011b, 2019). The high La/Ta ratios of the Andean igneous rocks of all ages at 34°S (Kay et al., 2005) provide evidence for the relative light REE (rare-earth-element) and LILE (large-ion-lithophile-element) enrichment by fluid interaction, consistent with the small proportions of crust required to produce the observed temporal isotopic changes.

What is unambiguous is that the amount of tectonically eroded forearc Paleozoic crust being subducted west of the NSVZ progressively increased through time because of the increase in the rate of subduction erosion as the locus of subduction of the Juan Fernández Ridge migrated southwards (Fig. 5). The positive correlation between increased subduction erosion rates and the progressive increase in the crustal isotopic character of the igneous rocks, in particular of the olivine-bearing mantle-derived mafic rocks emplaced between the early Miocene and Pliocene at 34°S, provides strong support for the suggestion that these temporal isotopic changes resulted from the addition into their mantle source through time of greater amounts of tectonically eroded Paleozoic crust. In an analogous situation, Kay and Mpodozis (2002), Goss et al. (2013) and Kay et al. (2013) have shown that further north in the CVZ, at 27–28.5°S, the distinctive petrochemical features of the 7.2 Ma Pircas Negras andesites, specifically the higher $^{87}Sr/^{86}Sr$ and lower $^{143}Nd/^{144}Nd$ ratios at the same wt% SiO_2 than in older Maricunga Belt lavas erupted at the same latitude, are compatible with forearc crust, removed by subduction erosion, being incorporated into their mantle source (Fig. 12). This occurred during an episode of high subduction erosion rates, when the Andean arc front was displaced ~40–50 km to the east as the Juan Fernández Ridge was entering the trench at this latitude. They exclude a major role for subducted terrigenous sediments in the generation of the Pircas Negras lavas, as due to the development of hyper-arid conditions in the central Andes by ~16 Ma (Rech et al., 2006) such sediments generally ceased to enter the trench well before 9 Ma, and also for a pelagic sediment contribution, which was constant from the west through time. Risse et al. (2013) also suggest a mantle source geochemically enriched by continental material introduced through subducted erosion processes for the late Miocene and younger primitive olivine-bearing (Fo88) mantle-derived mafic back-arc basalts east of the southern end of the CVZ (25–27°S).

2.3. Along-strike spatial variations in the SVZ

Futa and Stern (1988) and Hildreth and Moorbath (1988) showed that, compared to the magmas erupted from active volcanoes in the southern and central CSVZ and SSVZ south of 39°S, the $^{87}Sr/^{86}Sr$ and $^{143}Nd/^{144}Nd$ isotopic ratios increase and decrease, respectively, in the magmas erupted in the NSVZ (Figs. 6 and 7), below which the crust is thicker and west of which subduction erosion rates are higher (Fig. 4). Hildreth and Moorbath (1988) attributed this south-to-north along-strike spatial variation in isotopic compositions to greater amount of crustal assimilation northwards, as the crust thickened, in a deep crustal zone of Mixing, Assimilation, Storage and Homogenization (MASH, Fig. 3). The south-to-north isotopic changes are similar in magnitude to the temporal changes observed between the early Miocene and Pliocene at 34°S (Fig. 7), and the arguments against increased crustal assimilation as the crust thickens northward in producing these spatial isotopic changes are similar to those against producing the temporal changes as the crust thickened through time below this area. First and foremost is that the spatial isotopic changes are observed in olivine-bearing mafic mantle-derived samples. Primitive olivine-bearing (Fo76–84) basaltic andesites (MgO = 4.5 to 5.6 wt%; Mg# >60) erupted from both the <150 ka Maipo stratovolcano and Casimiro parasitic cone at 34°S, below which the crust is ~50 km thick, have $^{87}Sr/^{86}Sr \geq 0.7045$ and $^{143}Nd/^{144}Nd \leq 0.51260$ ($\varepsilon_{Nd} < -1$; Fig. 7; Futa and Stern, 1988; Wieser et al., 2019) compared to $^{87}Sr/^{86}Sr \leq 0.7039$ and $^{143}Nd/^{144}Nd \geq 0.51288$ ($\varepsilon_{Nd} \geq +5$; Hickey-Vargas et al., 2016) for basalts erupted from CSVZ volcanoes south of 39°S, below which the crust is only ~35 km thick (Tassara

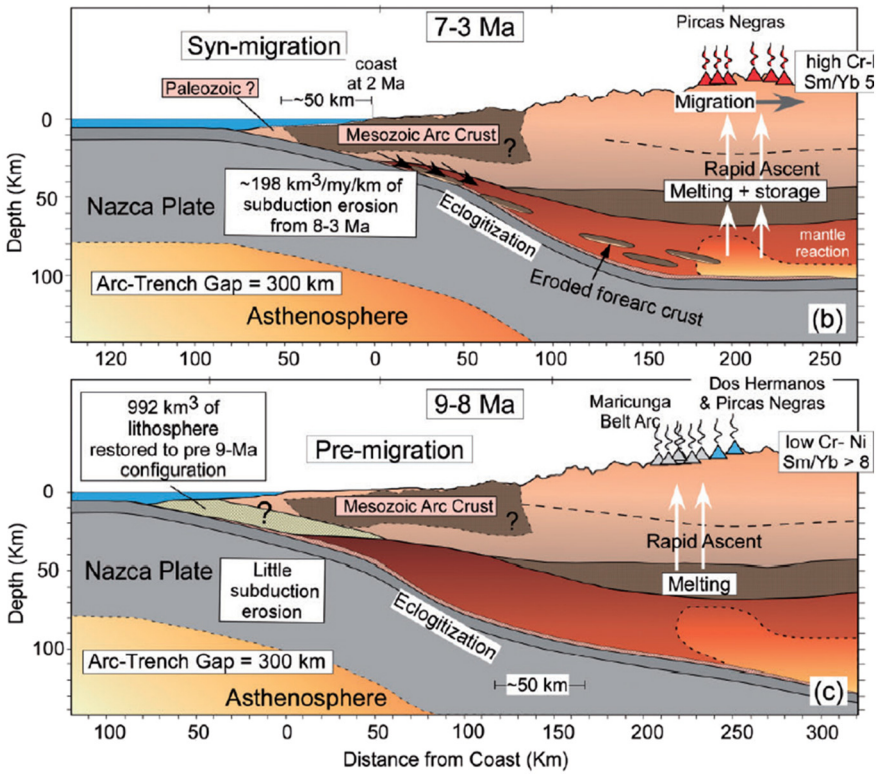

Fig. 12. Schematic near-trench to back-arc cross-sections at about 28.5–27°S from Goss et al. (2013), showing major tectonomagmatic features and processes before and during late Miocene to Pliocene arc front migration. Sections assume a nearly constant 300 km arc-trench gap. Volcanic centers in each period are shown schematically by triangles. The lower panel shows the Maricunga Belt within the restored pre-arc migration cross section at 9–7 Ma, with the paleo-coastline and trench located some 50 km to the west of the modern arc front. The wedge near the coast shows the 992 km^3 of material needed to restore the forearc to its position before removal by fore-arc subduction erosion between 8 and 3 Ma at a rate of ~198 km^3/km/my. The upper panel shows the 7–3 Ma tectonic setting during arc migration, with the horizontal arrow indicating the ~50 km of frontal arc migration to the ≤3 Ma CVZ arc front. Slivers of forearc material composed of 80–90% mafic Mesozoic crust and 10–20% Paleozoic crust are shown being removed from the base of the overriding crust at the time of arc migration. The removed forearc crust is then transported into the subarc mantle wedge, where flux melting and reaction with mantle peridotite generates the 7–3 Ma syn-migration high-Mg adakite-like Pircas Negras andesites.

and Echaurren, 2012). Also, intra-crustal assimilation models require an unacceptably large amount (≥40 wt%; Figs. 7 and 11) of assimilation of late Paleozoic to Triassic Choiyoi Group granite crust by a typical central SVZ basalt to produce the isotopic composition of the mafic olivine-bearing basaltic andesites erupted at the northern end of the SVZ (Stern, 1991; Kay et al., 2005; Stern et al., 2011a, 2019).

Furthermore, although the increasing crustal character of the rocks erupted northwards in the SVZ would require increasing amount of assimilation according to the MASH model, the volume of these rocks progressively decreases northwards, with an average of ≥10 km^3/km/my erupted from the active centers in the CSVZ south of 39°S compared to ≤4 km^3/km/my of erupted from the NSVZ volcanoes north of 34°S (Völker et al., 2011). This northward decrease in extrusive volumes is consistent with an increase in La/Yb ratios from ≤5 for basalts erupted south of 39°S to ≥12 for the basaltic andesites erupted in the NSVZ at 34°S (Hickey-Vargas et al., 2016). Both these northward trends imply a northward decrease in the degrees of mantle partial melting (Tormey et al., 1991; Jacques et al., 2013, 2014), and therefore less available heat for crustal melting and intra-crustal assimilation, opposite to what is required to explain the observed isotopic changes.

Wieser et al. (2019) also suggest that the trace element and isotopic characteristics of the most mafic samples in the NSVZ cannot result from intra-crustal assimilation, as no known regional or global basement lithologies contain all of the necessary incompatible trace elements in the correct proportions. Following Turner et al. (2017), they propose a model in which a substantial, but nearly uniform contribution of melts from subducting sediment and altered oceanic crust are required at all latitudes of the Andean SVZ, and that the distinctive isotopic characteristics of NSVZ relative to CSVZ mafic magmas are derived from an ambient mantle component similar to EM1-type ocean island basalts, superimposed on a northward decline in melt extent. They suggest that this EM1-type enriched (relative to N-MORB) mantle component is derived from the recycling of metasomatized subcontinental lithospheric mantle stored for long periods east of the Andean volcanic arc before it is returned to the asthenosphere by delamination or erosion driven by mantle corner flow above the subducted slab. In support of the presence of such lithosphere they note the presence of geographically separated suites of isotopically enriched (relative to MORB) rocks across South America, interpreted as direct melts of metasomatized subcontinental lithosphere, including Carboniferous granitoids from the Santo Domingo Complex of the Coastal Cordillera in central Chile (Pzg in Fig. 6; Parada et al., 1999).

For the uniform contribution from the subducted slab to all SVZ volcanoes, Turner et al. (2017) and Wieser et al. (2019) invoke a melt of altered oceanic crust and subducted Nazca plate pelagic sediment, without any contribution from tectonically eroded crust, despite the strong evidence for subduction erosion occurring west of the NSVZ, where the Paleozoic accretionary belts of metamorphic rocks and granites disappear (Fig. 6; Rutland, 1971; Kay et al., 2005; Stern, 2011) and the subduction of the Juan Fernández Ridge has generated the unique and prominent deep-water forearc Valparaiso Basin in central Chile (Laursen et al., 2002; Kukowski and Oncken, 2006). They correctly conclude that such a model slab contribution produces a mantle which trends towards relatively high $^{87}Sr/^{86}Sr$ at the observed $^{143}Nd/^{144}Nd$ of the NSVZ mafic volcanic rocks. However, if tectonically eroded crust, specifically crust derived from the Santo Domingo Complex Paleozoic coastal granitoids, which outcrop on the coast west of the NSVZ (Parada et al., 1999), is included in the slab-derived contribution, the

isotopic composition of the NSVZ mafic samples can be approximated with the addition of 6 wt% of this crust to a depleted subarc mantle (Figs. 7 and 11).

Turner et al. (2017) and Wieser et al. (2019) do not address the fact that the isotopic compositions of the mafic magmas erupted from recent volcanoes in the NSVZ reflect progressive temporal changes from the early Miocene to the present in the increasing crustal character and hydration of the mantle source at this latitude as reviewed above. They conclude that the northward increase observed in the crustal isotopic character of the SVZ volcanic rocks has nothing what-so-ever to do with the northward increase in either crustal thickness or the rates of subduction erosion. They suggest instead that it only reflects a northward decrease in the extent of dilution of the enriched EM1-type mantle source component they invoke due to the influx of upwelling depleted Pacific mantle through a tear in the subducted Nazca plate at 39°S, fortuitously located just at the latitude where crustal thickness and subduction erosion rates begin to increase northward. However, Jacques et al. (2013, 2014) demonstrate that the Sr-, Nd- and Pb-isotopic compositions of SVZ volcanoes, specifically those at 39°S, as well as northwards to 34.5°S, are sourced from South Atlantic Mid Ocean-Ridge Basalt (MORB) source type mantle modified by the input of slab-derived components, and not from Pacific MORB source type mantle. The ubiquitous presence of South Atlantic MORB source type mantle below the SVZ arc is consistent with the mantle flow model proposed by Husson et al. (2012), which suggests that the Andes owe their existence to basal drag beneath South America caused by a cylindrical convection cell under the South Atlantic operating since the breakup of Gondwanaland (Fig. 13).

Alternatively, a number of other recent studies support the suggestion, originally made by Stern (1989, 1990, 1991a, 1991b), that the increase in the radiogenic character of magmas erupted from volcanoes towards the northern end of the Andean SVZ reflect increased proportion of subducted continental crust into the mantle source region of these volcanoes as subduction erosion rates increase north of 39°S (Fig. 4). Stern and Skewes (1995), Kay et al. (2005) and Stern et al. (2011a, 2019) all conclude that the temporal trends in magmatic chemistry observed at the northern end of the SVZ between the early Miocene and Pliocene, as described in the previous section, are similar to the well-documented south-to-north trends in magmas erupted from the Pleistocene to Holocene volcanic centers of the SVZ, and both can be linked to the same events. As shown by isotopic data, these magmatic changes require differences in magma source regions which can be explained by small but increased amounts of Paleozoic Coastal Cordillera continental crust entering the subarc mantle due to a northward increase in the rates of subduction erosion (Figs. 7 and 11).

Holm et al. (2014), based on elemental and Sr-, Nd- and Pb-isotopic data, also conclude that primitive mafic basaltic-andesite volcanic rocks from the Andean SVZ exhibit a northward increase in their mantle source of upper continental crustal components, distinctly different than Chile trench sediments. They suggest that progressively greater amounts of granitic rocks, increasing from 2 wt% south of 35°S to 5 wt % at 34°S, entered the source mantle below the NSVZ by means of subduction erosion. In a subsequent study of primitive back-arc olivine-phyric alkali basalts in the northern Payenia volcanic province to the east behind the NSVZ, which have typical subduction zone type incompatible element enrichment (Søager et al., 2013, 2015a, 2015b; Holm et al., 2016), they concluded that both Ba–Th–Sm variations in these basalts, their low Eu/Eu* and Sr/Nd ratios and their isotopic compositions all indicate evidence for a crustal components having been added into their mantle source. They argue that the low Zr/Sm and Hf/Sm ratios of these basalts, together with their relatively high Th/U ratios, indicate that these components were derived by partial melting of subducted continental crust that had residual zircon, and that the contribution of Chile trench marine sediments to the magmas seems insignificant. They characterize the unmodified mantle source as being depleted mantle similar to the source of South Atlantic N-MORB, as does Jacques et al. (2013, 2014).

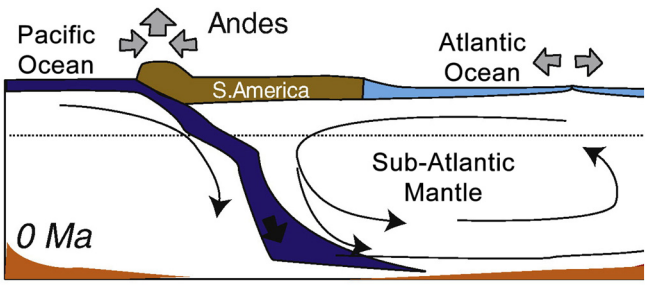

Fig. 13. Model of mantle flow below the south Atlantic and southern South American continent from Husson et al. (2012), illustrating the dominant presence of Atlantic Ocean MORB source type mantle below the Andean cordillera and volcanic arc.

In summary, models of a northward increase in mantle source region contamination by small proportions (1 to 6 wt%) of continental components introduced into the mantle by subduction erosion of the Paleozoic Coastal Cordillera, not terrigenous sediment subduction since the trench terrigenous sediments west of the NSVZ lack the isotopic leverage to sufficiently affect the mantle source, can account for the along strike south-to-north variations in the isotopic compositions of the mafic magmas erupted towards the northern end of the Andean SVZ (Figs. 7 and 11), where subduction erosion rates increase significantly due to the subduction of the Juan Fernández Ridge (Fig. 4). The crust also thickens northwards in this region, but intra-crustal assimilation models fail to explain the isotopic changes observed in mafic mantle-derived magmas. Models involving a northward increase in the involvement of enriched subcontinental lithospheric materials introduced into the source of arc magmas by corner flow in the subarc mantle wedge require an ad hoc southward dilution of this component by the introduction of depleted Pacific MORB source type mantle below the central SVZ, a suggestion that contradicts substantial isotopic evidence for South Atlantic MORB source type mantle below this part of the Andean arc. The enriched EM1-type mantle model also invokes, as a uniform contribution from the subducted slab to all SVZ volcanoes, a melt of altered oceanic crust and subducted Nazca plate sediment, without any contribution from tectonically eroded crust. Given the strong evidence for subduction erosion along the western South American continental margin, if this were the case the question would be: How did the fluid-soluable and low-melting components of the subducted continental crust avoid becoming involved in magma genesis? As reviewed in the following sections, geochemical studies from other convergent plate boundary arcs, where subduction erosion rates are often much lower that west of the Andean NSVZ, show clear evidence of the addition of tectonically eroded and subducted crust into the mantle source of the magmas erupted from the overlying volcanoes.

3. Other convergent plate boundary arcs

3.1. The Aleutian Islands arc

The Aleutian Islands intra-oceanic volcanic arc, along the northern edge of the Pacific/Bering sea plate boundary, extends for ~3500 km from SW Alaska to near the Kamchatka Peninsula (Fig. 14). The tectonic regime of the Aleutian arc changes markedly along strike. The convergence angle of the Pacific plate varies from nearly orthogonal to the trench in the eastern part of the arc along the Alaska Peninsula to oblique/strike-slip in the western Aleutians. Orthogonal convergence rates are ~6.8 to 6.5 cm/year in the eastern and central Aleutians, but decreases to ~4.5 cm/year in the far western Aleutians (Syracuse and Abers, 2006; Scholl and von Huene, 2007). The slab dip is steeper in the central and western Aleutians (54–56°) compared to the eastern Aleutians (46°). These tectonic characteristics, along with variations in the amount and composition of the sediment and arc crust being subducted, are

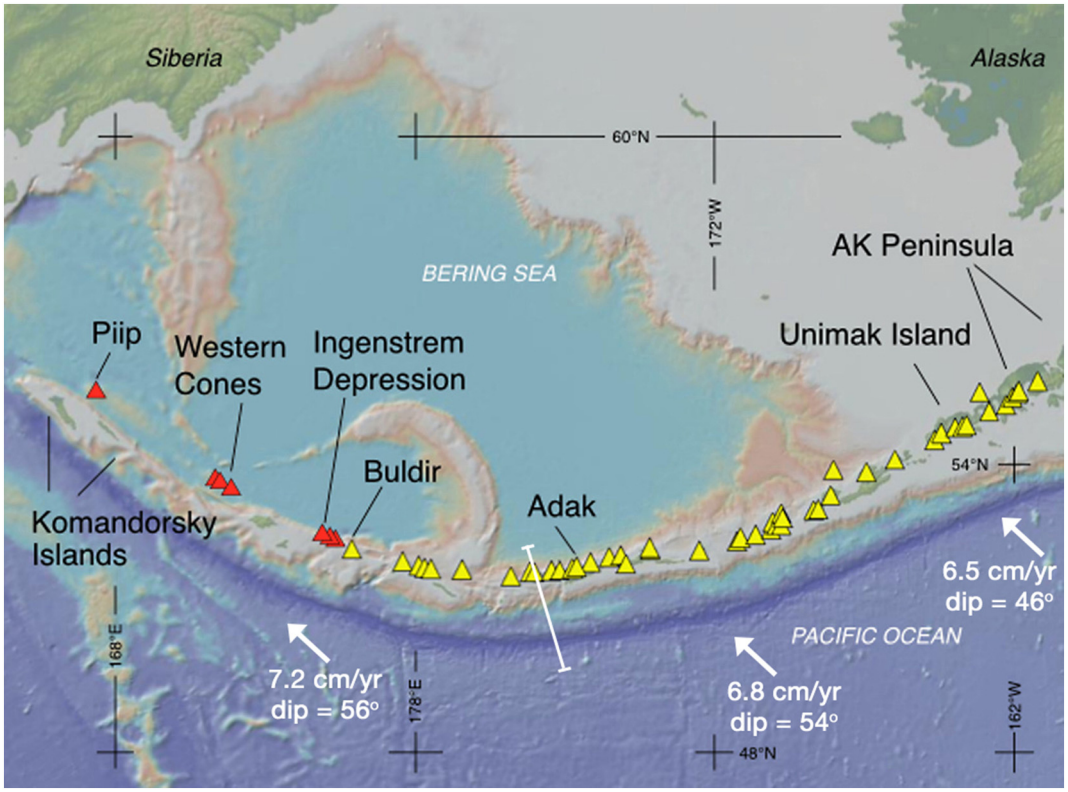

Fig. 14. Map of the north Pacific Ocean, Bering Sea, and Aleutian Island arc from Yogodzinski et al. (2015, 2017). Yellow triangles mark the locations of emergent volcanoes on Aleutian islands and red triangles indicate the locations of western Aleutian seafloor volcanoes. White arrows show the Pacific–North America plate convergence direction. White line just west of Adak Island indicates the position of the cross-section illustrated in Fig. 15.

thought to explain systematic variations in Quaternary lava chemistry along strike (Kelemen et al., 2003; Jicha et al., 2004; Singer et al., 2007; Yogodzinski et al., 2010, 2015, 2017; Jicha and Kay, 2018).

The timing of the onset of Aleutian arc volcanism is constrained to have occurred sometime before the oldest reliably dated Aleutian arc volcanic rock at 46 Ma (Jicha et al., 2006). The central part of the Aleutian islands arc (Fig. 15) was apparently built to near its current size during a period of peak volcanism from 38 to 29 Ma, and has since experienced several episodes of magmatism from 16 to 11 Ma, from 7 to 5 Ma, and again after 3 Ma. As summarized by Jicha and Kay (2018) for this part of the arc, the oldest arc rocks are located in the south and the volcanic front of the arc has migrated north with time in association with each of these episodes of magmatism (Fig. 15).

Jicha and Kay (2018) suggest that a change in slab dip is unlikely to explain the northward migration of central Aleutian arc front magmatism with time, because it requires an extreme subduction zone configuration in the past for which there is no observable evidence. They propose instead that a viable mechanism for central Aleutian arc migration is forearc subduction erosion (Fig. 15). Thus, although the Aleutian arc is commonly classified as an accreting margin, because it has accumulated a young <5 Ma old frontal prism of accreted.

sediment supplied by enhanced input of Quaternary glacial sediments (von Huene and Scholl, 1991; Clift and Vannucchi, 2004; Clift et al., 2009), it can also be considered to be a erosional convergent plate boundary over the long-term (Scholl and von Huene, 2007, 2009; Jicha and Kay, 2018). Long-term average arc front migration rates in the central Aleutians range between 1 and 2 km/my, but are greatest, ranging up to 5 km/my over the last six million years, as the arc migrated from the 7–5 Ma volcanic front to its current location. Jicha and Kay (2018) note that the Kula Ridge was subducted below the central Aleutians around 6 Ma (Fig. 16), and that this topographic anomaly, although not as large as the Juan Fernández Ridge on the Nazca plate west of central Chile, nevertheless rises several hundred meters above the adjacent seafloor, and its subduction may be partly responsible for the relatively rapid northward migration from the 5–7 Ma to the modern arc location, but not for the previous episodes of migration. Since seafloor reconstructions indicate that no other aseismic ridges or seamount chains have been subducted below the central Aleutians, the previous episodes of arc migration and forearc subduction erosion can be considered as long-term aspects of the Aleutian arc convergent plate boundary.

Jicha and Kay (2018) estimate long-term subduction erosion rates of ~27 km^3/km/my in the Adak region of the central Aleutians (Fig. 14), and higher rates of ~40 km^3/km/my since ~14 Ma, facilitated by the subduction of the Kula Ridge around 6 Ma. Near the Delarof Islands in the western part of the central Aleutians (Fig. 15) these rates are at least 50% higher, or ~ 60 km^3/km/my since 14 Ma, because the arc has migrated almost twice as far to the north as in the region of Adak Island. They suggest that forearc subduction erosion would affect the entire thickness of the remnant Kula oceanic crust embedded in the middle of the Aleutian crust. In support of this model they note that there is a concentration of large earthquakes between 13 and 20 km at the interface between the slab and the overriding plate, which is the approximate depth of the former Kula Plate within the Aleutian crust. Wang et al. (2010) have suggested that significant basal erosion of the hanging wall in a subduction zone occurs during large earthquakes as the overlying wedge weakens. Thus, subduction erosion is likely introducing Aleutian crystalline forearc material from the mid-crust into the down-going plate.

Forearc subduction erosion of the Kula oceanic crust embedded in the middle of the Aleutian crust would allow partial melts of this removed and subsequently metamorphosed oceanic crust to produce an eclogite melt component with elevated La/Yb and Sr/Yb that Jicha and Kay (2018) observe in central Aleutian magmas. The suggestion that such a melt component, which is similar in composition to the original adakites described from Adak Island (Kay, 1978), has been added to

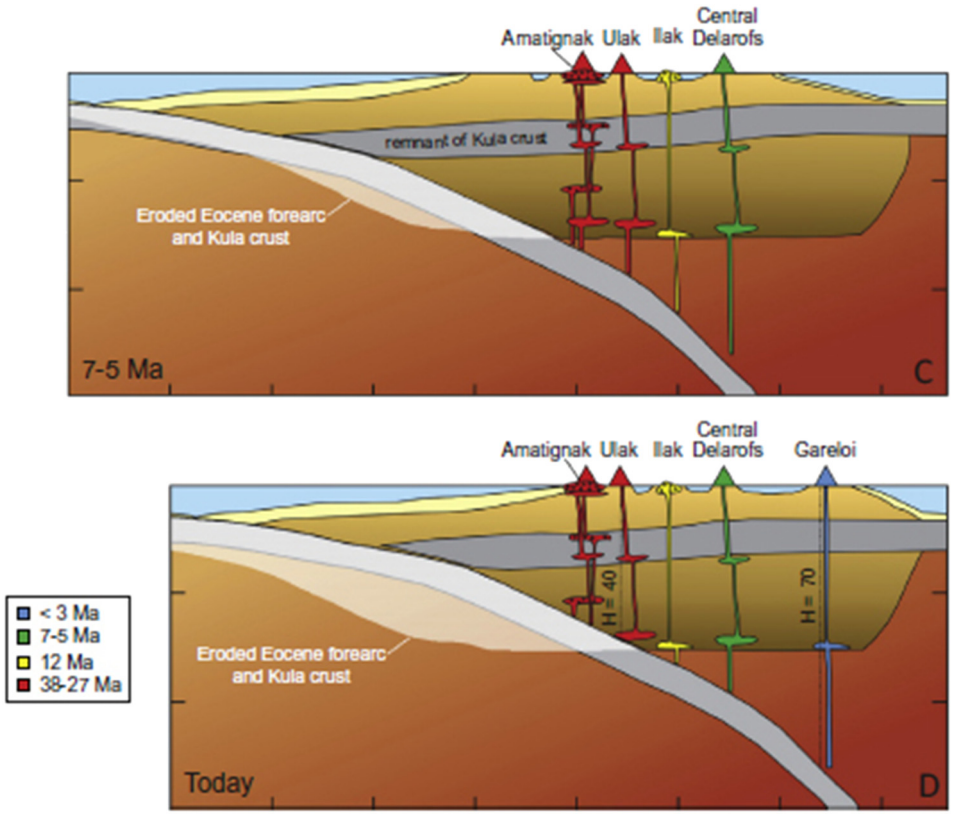

Fig. 15. Schematic near-trench to behind the arc cross-section, modified from Jicha and Kay (2018), in the Delarof region of the central Aleutian arc as indicated in Fig. 15, showing the structure of the arc with the prominent volcanic and plutonic units through time. Sections assume a nearly constant 160 km arc-trench gap, and also H (depth to slab) = 70 km for all units at the time of their formation. Volcanic centers in each period are shown by triangles and plutons as lenses with crosses. (C) The 7–5 Ma arc, already 40 km east of the 35–31 Ma volcanic and plutons on Amatignak and Ulak. This is the approximate time during which the Kula Ridge was subducted (Lonsdale, 1988). (D) The modern arc. The H (depth to slab) for Amatignak and Ulak is currently ≤40 km, which suggests that significant forearc subduction erosion has taken place since their formation. The faint white area represents the amount of arc crust, including a significant portion of the remnant Kula Plate oceanic crust in the mid crust that has been subducted via forearc subduction erosion.

the mantle source of central Aleutians magmatic rocks is reinforced by the observation that their Sr- and Nd-isotopic compositions are encompassed by mixing between subducted Aleutian sediment, depleted MORB mantle and a hydrous eclogite melt formed by 5–10% melting of subducted oceanic crust as modeled by Yogodzinski et al. (2015, 2017) for western Aleutian arc magmas. In the case of the central Aleutian arc, distinguishing the source of the eclogite melt signature between melts of the down-going oceanic slab and the tectonically eroded Kula oceanic crust embedded in the forearc is difficult based solely on isotopic evidence, as both can be isotopically similar. However, Jicha and Kay (2018) conclude that given that significant subduction erosion of the forearc, which includes the former Kula plate, is the most likely mechanisms for arc migration, than partial melting of the tectonically eroded and subducted Kula oceanic crust is also the most plausible explanation for both the geochemical and isotopic signature of the eclogite melt component observed in central Aleutian magmas.

In summary, Jicha and Kay (2018) suggest that the genesis of central Aleutain arc magmas involves a component derived from small degrees (5–10%) of partial melting of Kula plate basaltic oceanic crust tectonically eroded out of the forearc, subducted and metamorphosed to eclogite. Following the models of Kelemen et al. (2003) and Yogodzinski et al. (2015, 2017), interaction of this hydrous eclogite melt, along with a small contribution from subducted Aleutian sediment, with mantle peridotite in the subarc mantle wedge produces buoyant diapirs of pyroxenite metasomatites which melt to produce central Aleutian arc magmas. As in the case of the Andes, although the eroded and subducted forearc crust makes an important contribution to central Aleutian arc magmas, a significant proportion of this crust must also be subducted deeper into the mantle.

3.2. The South Sandwich Islands arc

The South Sandwich Islands intra-oceanic volcanic arc comprise a 400 km long arcuate array of eleven main islands and two seamounts situated on the Sandwich plate (Fig. 17). The islands consist largely of basalt and andesite lavas of late Tertiary and Quaternary age. The small Sandwich plate is bound on the east by the South Sandwich Trench, into which the South America plate is being subducted at a rate of 67–79 mm/yr (Thomas et al., 2003). The Sandwich plate consists of oceanic crust generated at the eastern flank of the East Scotia Ridge (ESR), and magnetic anomalies indicate that most of the arc is built on oceanic crust formed within the last 10 Ma (Barker, 1995; Barker and Hill, 1981; Larter et al., 2003). All sediment arriving at the trench is subducted, as there is virtually no accretionary prism within the trench. These geological and geophysical data have led to the interpretation that the South Sandwich margin is dominated by subduction erosion, with an average rate of removal of forearc lithosphere near 40 km^3/km/my (Larter et al., 2003; Vanneste and Larter, 2002).

Tonarini et al. (2011) determined boron isotopic ($\delta^{11}B$) compositions which range from 12 to 18‰ for representative lavas from along the arc (Fig. 18). They determined that the samples have high boron abundances (3 to 25 ppm) and variable fluid-mobile/fluid-immobile element ratios, with high enrichments of B/Nb (2.7 to 55) and B/Zr (0.12 to 0.57). The fact that B-enrichment is decoupled from fluid immobile elements (Ti, Zr, Nb), but parallels that of fluid-mobile elements implies dominant transfer of the latter elements into arc magma sources via aqueous fluids rather than silicate melts (Leeman, 1996; Noll et al., 1996). $\delta^{11}B$ values are among the highest so far reported for mantle-derived lavas (Fig. 18). The $\delta^{11}B$ values are roughly positively correlated

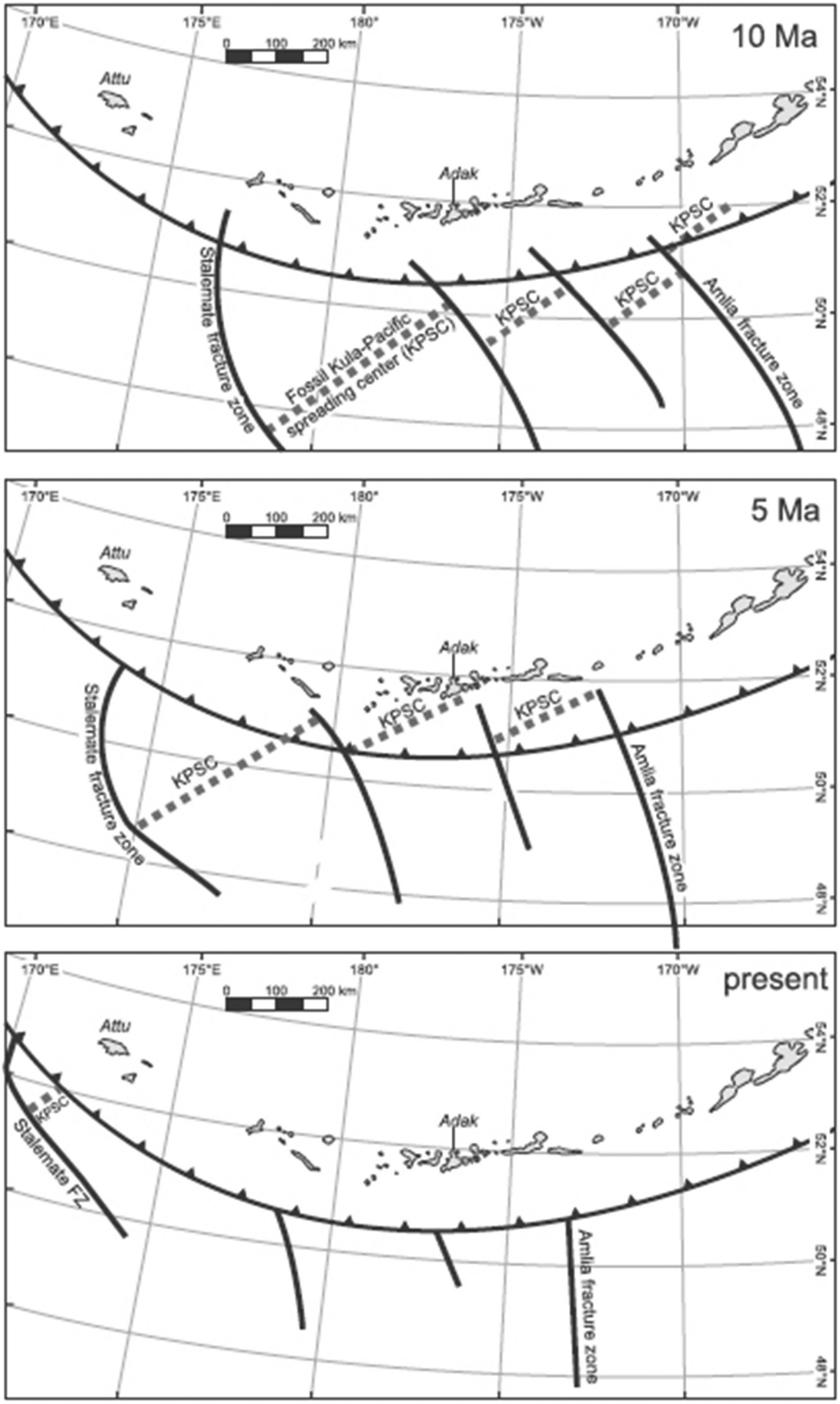
10 Ma
170°E
175°E
180°
175°W
170°W
0 100 200 km
Attu
Adak
KPSC
Stalemate fracture zone
Fossil Kula-Pacific spreading center (KPSC)
Amlia fracture zone
5 Ma
present
Stalemate FZ

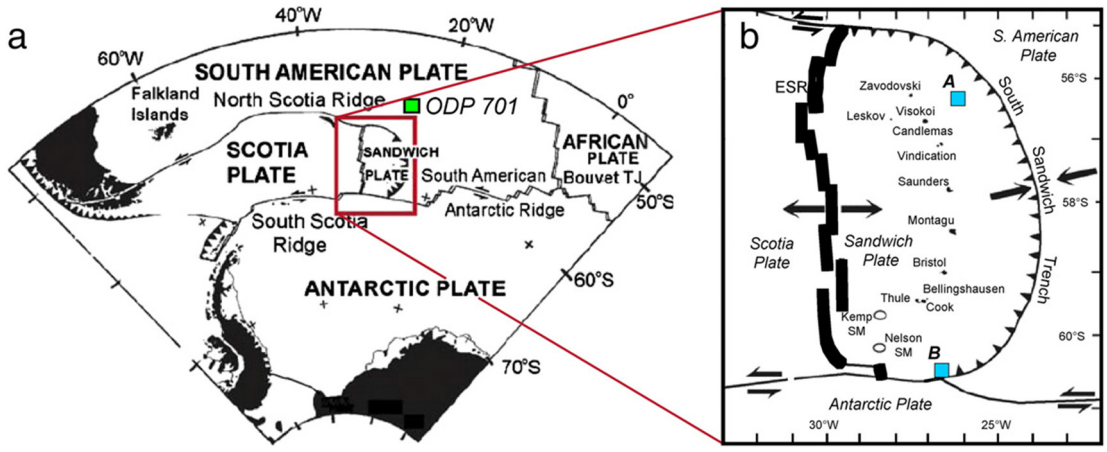

Fig. 17. (a) Geological sketch map of the South Sandwich Island (SSI) arc–East Scotia Ridge (ESR) region after Leat et al. (2004). The ESR is generated by east–west divergence of the Scotia and Sandwich plates. Filled square shows location of ODP Site 701. Filled triangles, present-day subduction zone. (b) Detailed locations of the eleven islands, from Zavodovski in the north to Thule in the south, and the two Kemp and Nelson seamounts (SM) southwest of Thule, that form the SSI,. Shaded boxes indicate locations where peridotites were dredged ('A': forearc 671 sites DR52–DR54 and 'B': trench-fracture zone intersection site DR110).

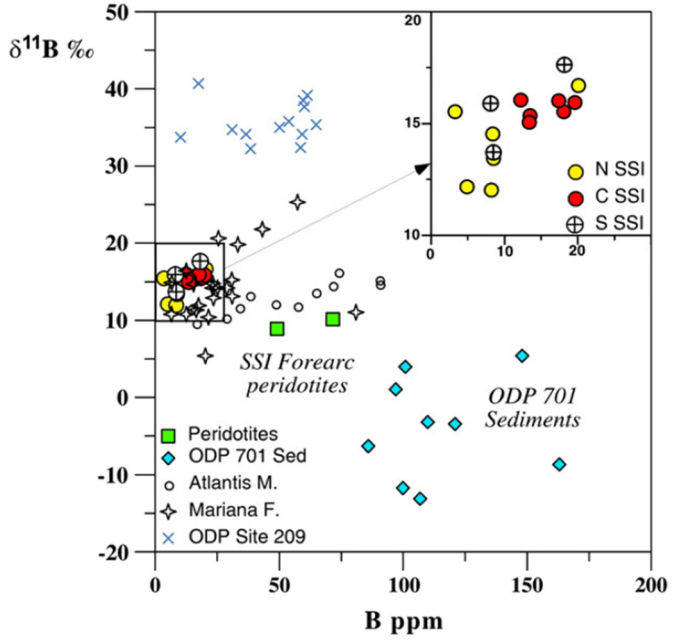

Fig. 18. Plot from Tonarini et al. (2011) showing $\delta^{11}B$ vs. B relations for north (N SSI; yellow circles), central (C SSI; red circles) and southern (S SSI; + within the circles) South Sandwich Island lavas, two representative forearc peridotites, and proximal marine sediments (ODP 701 site; Fig. 17). These parameters are roughly correlated in the lavas, such that $\delta^{11}B$ increases with overall B-enrichment (bold arrow). This trend is inconsistent with incorporation of materials similar to either the peridotites or the sediments into the arc magma source or as assimilants in the magmas themselves. Mariana forearc (Benton et al., 2001), Atlantis Massif (Boschi et al., 2008), and ODP leg 209 (Vils et al., 2009) serpentinites are plotted for comparison.

with B concentrations and with $^{87}Sr/^{86}Sr$ ratios. Peridotites dredged from the forearc trench also have high $\delta^{11}B$ (+10‰) and elevated B contents (38–140 ppm). Incoming pelagic sediments sampled at ODP Site 701 display a wide range in $\delta^{11}B$ (+5 to −13‰; average = −4.1‰), with negative values most common.

The unusually high $\delta^{11}B$ values inferred for the South Sandwich mantle wedge source of mafic arc volcanic rocks cannot be attributed to direct incorporation of subducting slab materials, specifically the pelagic sediments, or from fluids derived directly therefrom (Tonarini et al., 2011). Rather, the heavy $\delta^{11}B$ isotopic signatures of the magma sources are more plausibly explained by ingress into the subarc mantle of fluids derived from subduction erosion of altered frontal arc mantle wedge materials similar to those in the Marianas forearc (Fig. 18). Tonarini et al. (2011) propose that multi-stage recycling of high-$\delta^{11}B$ and high-B serpentinite (possibly embellished by arc crust and volcaniclastic sediments) can produce extremely ^{11}B-rich fluids at slab depths beneath the volcanic arc, and that infiltration of such fluids into the mantle wedge likely accounts for the unusual magma sources inferred for the South Sandwich intra-oceanic volcanic arc.

3.3. The Central American arc

Miocene to Holocene calc-alkaline arc volcanism along the Central American margin (Fig. 19), which results from the subduction of the Cocos and Nazca plates beneath the Caribbean plate (Carr, 1984; de Boer et al., 1991), began with initiation of the Costa Rican volcanic arc at 23 Ma (Seyfried et al., 1991). The NW-SE trending active volcanic arc stretches 1200 km from western Guatemala to central Panama. Subarc crustal thicknesses decrease from 48 km in western Guatemala to <30 km under Panama (Mickus, 2003). Fast 8.8 cm/yr nearly orthogonal subduction of the Cocos plate under Costa Rica contrasts with slower 3.7 cm/yr oblique convergence of the Nazca plate under western Panama (Fig. 19). The Wadati-Benioff zone shows a progressive change in subduction angle from 60° beneath Guatemala to <30° under central Costa Rica and possibly follows a subhorizontal 10° path under the base of the Caribbean plate below Panama. Uplift of the Cordillera de Talamanca and progressive slab shallowing have been attributed to the subduction of the aseismic Cocos Ridge that collided with southern Costa Rica at <5 Ma (Kolarsky et al., 1995). Contemporaneous with ridge collision, the onset of low-angle subduction is thought to have caused 40 to 50 km of northeastward arc migration in central Costa Rica (Alvarado et al., 1993; Marshall et al., 2003).

The Costa Rican forearc is dominantly composed of the 60–100 Ma Nicoya Complex belt of ophiolites that extends from the northernmost Santa Elena Peninsula to the Burica Peninsula in the south, and farther south ophiolites are also exposed on the peninsulas along the

Fig. 16. Reconstructions, modified from Ryan et al. (2012) and Jicha and Kay (2018), of the Pacific Plate and central Aleutian arc at 10 Ma, 5 Ma and the present day configuration, based on Lonsdale (1988). The location of the fossil Kula-Pacific spreading center (KPSC) is shown as a thick gray dotted line. The change in orientation of the fracture zones from 10 to 5 Ma is the result of a clockwise rotation of the Pacific Plate that occurred sometime between 10 and 5 Ma (Stotz et al., 2017). Subduction of the Kula-Pacific spreading center occurred in the Adak region around 6–5 Ma (Lonsdale, 1988) causing an increase in the rate of subduction erosion at this time. A tiny sliver of the Kula plate is still subducting today SW of Attu Island.

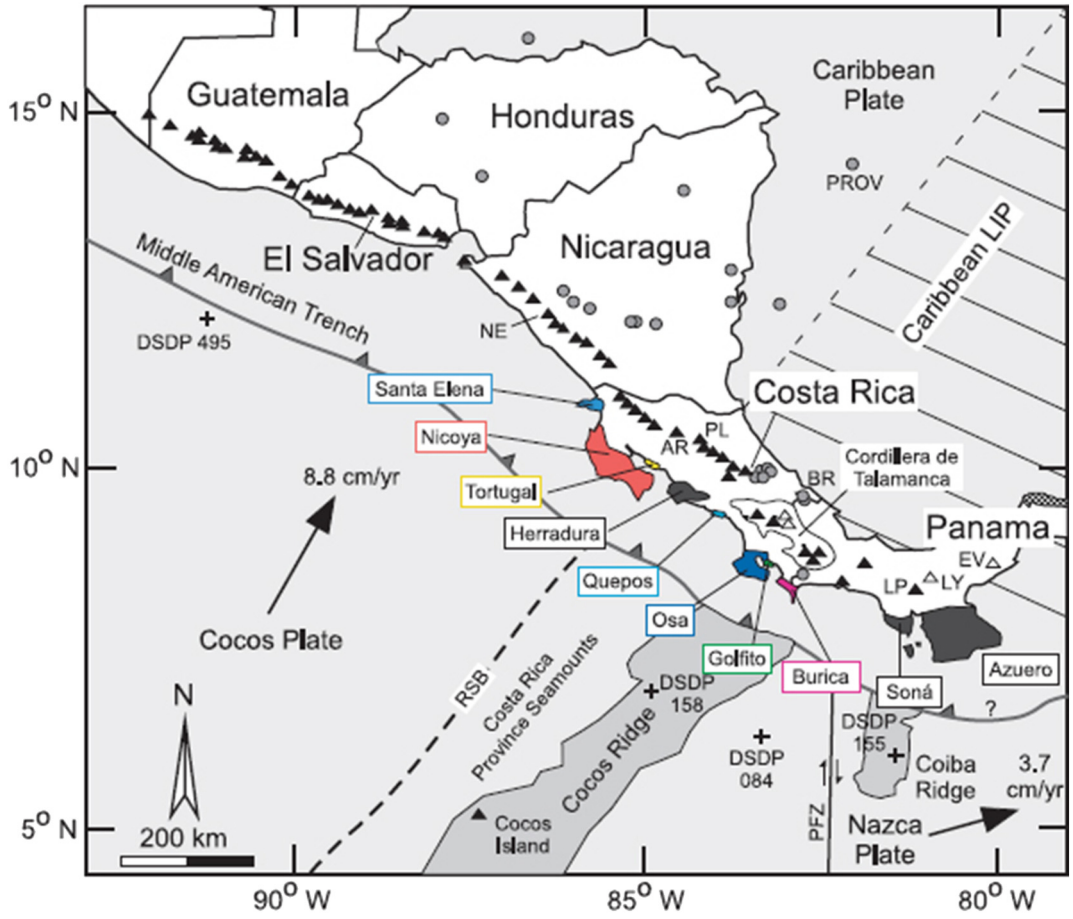

Fig. 19. Map of Central America showing major tectonic features from Goss and Kay (2006). Black triangles show positions of frontal arc volcanoes including Nejapa (NE), Arenal (AR), Platanar (PL), with open triangles marking locations of adakitic magmatism including Laguna del Pato Frontal Cone (LP), La Yeguada (LY), El Valle (EV) (de Boer et al., 1991; Defant et al., 1991a, 1991b; Feigenson et al., 2004). Gray circles show sites of pre-Quaternary backarc lavas including Providencia backarc lavas (PROV), and Bribri backarc lavas (BR). (Abratis and Wörner, 2001; Feigenson et al., 2004). Deep Sea Drilling Program (DSDP) sites are marked with plus signs (495, Cocos Plate sediments; 158, Cocos Ridge; 084, Cocos Plate; 155, Coiba Ridge). Shaded colored regions identify outcrop locations of Cretaceous/Tertiary forearc mafic igneous complexes. Stippled region shows the regional extent of the Cordillera de Talamanca. Panama Fracture Zone = PFZ. Convergence rates and directions are from De Mets (2001).

southwestern Panamanian coast, with the most voluminous outcrops on the Azuero and Soná Peninsulas (Fig. 19). Hauff et al. (2000a, 2000b) and Hoernle et al. (2002) have shown that the basalts and gabbros in these forearc ophiolites have chemical characteristics similar to the Caribbean Large Igneous Province (CLIP) that forms the basement of the southern Caribbean Sea and interpret them as obducted and accreted segments of CLIP crust.

Subduction erosion is considered to be a major process in shaping the nonaccretionary Central American margin (von Huene and Scholl, 1991; Ranero and von Huene, 2000; Clift et al., 2005; Vannucchi et al., 2001, 2016), although alternative opinions have recently been published (Gardner et al., 2013; Edwards et al., 2018; Morell et al., 2019; Buchs and Oemering, 2020). For northern Costa Rica, Vannucchi et al. (2016) estimated subduction erosion rates of 80 km^3/km/my during the Miocene and Pliocene. Accelerated subduction erosion along the Costa Rican margin during the last ≤6 Ma is supported by sediment drilling records that indicate a dramatic landward shift in the coastline coincident with a 40 to 50 km NE migration of the arc volcanic front (Alvarado et al., 1993; Meschede et al., 1999a, 1999b). These data indicate a subduction erosion rate of >140 km^3/km/my over the last ≤2 m.y. (Vannucchi et al., 2003, 2016), similar to subduction erosion rates associated with the subduction of the Juan Fernández Ridge below the Andes of central Chile (Fig. 4). However, in southern Costa Rica, where the Cocos Ridge is currently being subducted, rates may be significantly higher (Vannucchi et al., 2016). The observed uplift of the innermost Costa Rican forearc units (Gardner et al., 1992; Marshall and Anderson, 1995; Fisher et al., 1998) is consistent with models of margins affected by subduction erosion and likely reflects the topographic effects of subducted seamounts, serpentinization, and/or sediment underplating (Lallemand, 1995; Meschede et al., 1999a, 1999b). Clift and Vannucchi (2004) calculated that in the last ≤6 m.y. tectonically eroded forearc composed ~86% of the subducted material below Costa Rica, only the other 14% being incoming sediments. In Central Panama, ~120 km of apparent arc migration since the Eocene has also been attributes to subduction erosion (Lissinna et al., 2002). Since the collapsing Central American forearc basement is likely composed of the late Cretaceous Nicoya Complex belt of ophiolites and their seaward extension, these mafic CLIP rocks dominate the subducted material (Meschede et al., 1999a, 1999b).

Chemical data also provide additional evidence for subduction erosion along the southern Central American margin. Morris and Tera (1989, 2000) and Morris et al. (2002b) suggested that lower concentrations of ^{10}Be in Costa Rican compared to Nicaraguan lavas require dilution of the subducted marine sediment component in the mantle wedge by eroded forearc basement. Evidence for the incorporation of forearc crust into the mantle wedge by subduction erosion also comes from Pb-isotopic and trace element characteristics of magmas erupted along the Central American arc (Goss and Kay, 2006). Pb-isotopic data for lavas along the entire arc show that a distinctive enriched mantle source component is present in arc lavas from central Costa Rica and Panama (Abratis and Wörner, 2001; Feigenson et al., 2004). These lavas have $^{206}Pb/^{204}Pb$ and

$^{208}Pb/^{204}Pb$ ratios >18.7 and 38.3, respectively, whereas volcanic front lavas north of central Costa Rica have $^{206}Pb/^{204}Pb$ < 18.7 and $^{208}Pb/^{204}Pb$ < 38.3. A distinct temporal change to a similar enriched source is seen in the Cordillera de Talamanca (Fig. 20) where older Miocene volcanic rocks have lower $^{206}Pb/^{204}Pb$ and $^{208}Pb/^{204}Pb$ ratios (<18.7 and <38.6) than <4 Ma adakitic lavas (>19.0 and >38.7). Abratis and Wörner (2001) show that the $^{206}Pb/^{204}Pb$ ratios of adakitic lavas within the Cordillera de Talamanca are too high to be explained by melting of subducted MORB crust of the Cocos plate. Feigenson et al. (2004) used Sr- and Nd-, as well as and Pb-isotopic data to show that the majority of Central American volcanic front lavas, including those with elevated $^{206}Pb/^{204}Pb$ ratios, show little contamination from passage through the crust. On the basis of the nonradiogenic character of the Pb in pelagic sediments, they also ruled out subducted marine sediments as the source of the high $^{206}Pb/^{204}Pb$ ratios in the arc lavas.

Goss and Kay (2006) conclude that the measured $^{206}Pb/^{204}Pb$ and $^{208}Pb/^{204}Pb$ ratios in recently erupted lavas along the southern Central American arc have a striking similarity to those of the Costa Rican and Panamanian Nicoya, Tortugal, and Herradura forearc ophiolites (Fig. 20). They present mixing models which illustrate that the enriched Pb isotopes in the recent Costa Rican lavas cannot be explained by mixing of enriched mantle and subducted sediments alone, but must also include a source enriched in both ^{206}Pb and ^{208}Pb like the forearc ophiolites and/or mafic CLIP basement that likely underlies the volcanic arc, and they attribute the Pb signatures in the arc front lavas to addition of mafic forearc crust into the mantle wedge by subduction erosion (Fig. 21). They calculate that over half (61–65%) of the mass of crustal Pb delivered to the subarc mantle wedge could be from forearc subduction erosion.

Goss and Kay (2006) show that arc volcanic rocks in the Cordillera de Talamanca and in west-central Panama with ages of <4 Ma (Fig. 17) are chemically distinct from lavas to the north in having steeper REE patterns (La/Yb = 20–90) and Sr/Yb ratios >700. These adakitic signatures became dominant after 2.5 Ma and are absent in the older Miocene volcanic rocks from the same region (Defant et al., 1991a, 1991b; de Boer et al., 1995). To generate the characteristic steep REE patterns of adakitic lavas, heavy REE (Yb) need to preferentially partition into garnet in a high-pressure feldspar-poor residual mineral assemblage, leaving the magma depleted in these elements and enriched in Sr. These adakitic signatures can be explained in areas of thick continental crust by the stability of garnet at crustal depths >50 km (Hildreth and Moorbath, 1988). However, in the absence of a thick crust below southern Central America, Goss and Kay (2006) suggest that the spatial and temporal pattern of erupted adakites with enriched Pb-isotopes substantiates a model of subduction erosion, metamorphism to eclogite and high-pressure melting of forearc mafic ophiolitic crust. They argue that the MORB-like oxygen-isotopic data for <4 Ma Panamanian adakites ($\delta^{18}O$olivine = 5.08–5.8‰; $\delta^{18}O$parental melts = 6.36–6.9‰; Bindeman et al., 2005) can also be explained in terms of forearc subduction erosion of the obducted Panamanian forearc ophiolite complexes if these have an oxygen isotope profile like Samail ophiolites (Gregory and Taylor, 1981; Bosch et al., 2004), for which $\delta^{18}O$ values range from 7.5 to 12‰ for the top 1 km of hydrothermally altered upper crust to as low as 4‰ for the gabbroic lower crustal section, yielding a depth integrated average similar to MORB ($\delta^{18}O = 5.7 \pm 0.2$‰). In this case melting of eroded upper and lower segments of forearc mafic complexes could explain the MORB-like $\delta^{18}O$ character of the Panamanian adakites.

Based on these geochemical considerations, Goss and Kay (2006) present a model similar to that for the central Aleutian arc described in the previous section, incorporating after ~4 Ma increased amounts of forearc mafic crust by subduction erosion into the mantle source below Central America (Fig. 21). The tectonically eroded forearc mafic crust, when transported to mantle depths, is subjected to eclogite-facies metamorphism, thus stabilizing garnet. This forearc material will partially melt as it enters the subarc asthenosphere, contaminating the mantle source below Central America with adakitic-like melts. The so-modified subarc mantle source would produce the adakitic lavas that reached the surface along the arc during the period of increase subduction erosion rates over the last <4 Ma along the Central American margin. Although a high proportion of the Pb in the <4 Ma Central American adakites may be derived from the subducted forearc mafic crust, the overall contribution from this partially melted subducted material is small, and as in the cases of the Andes and the Aleutians described above, most of the tectonically eroded crust returns to the deeper mantle.

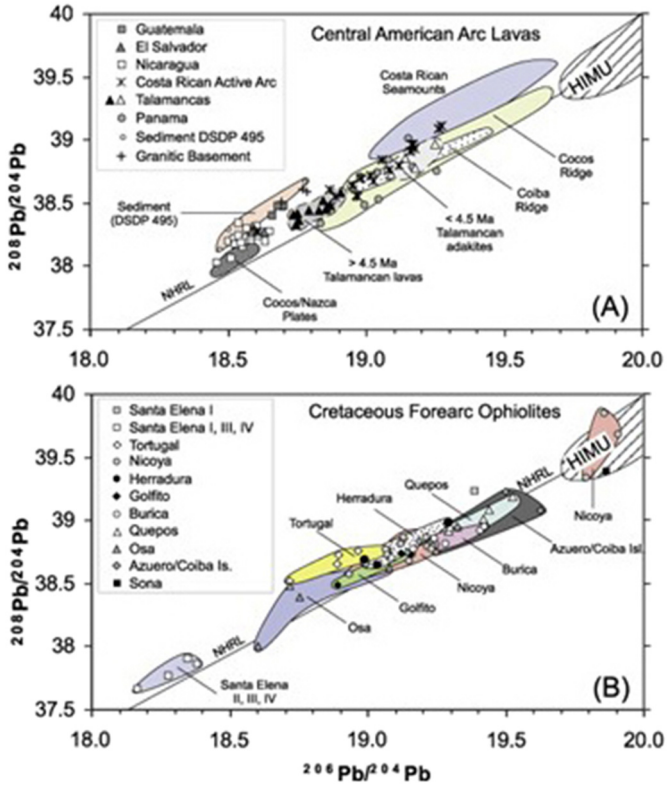

Fig. 20. Graphs from Goss and Kay (2006) of $^{206}Pb/^{204}Pb$ versus $^{208}Pb/^{204}Pb$ for (a) Central American volcanic front lavas and (b) Cretaceous/Tertiary forearc mafic complexes. Shaded triangles mark >4 Ma Talamancan lavas, while open triangles show data from <4 Ma Talamancan adakites.

3.4. The Trans-Mexican Volcanic Belt

The active Pliocene-Quaternary central Trans-Mexican Volcanic Belt (TMVB) is related to the subduction of the Cocos plates along the Middle American Trench (Fig. 22; Gómez-Tuena et al., 2007, 2018; Straub et al., 2015). The trench runs oblique to the arc volcanic front because the slab dip decreases eastward and the arc-trench gap widens. In the central TMVB, the slab subducts horizontally beneath the forearc at a nearly constant depth of ~40 km for nearly 300 km inboard before plunging into the mantle at a ~75° angle, just a few km before the appearance of arc front volcanoes, and the arc-trench gap measures ~360 km (Pardo and Suarez, 1995; Pérez-Campos et al., 2008). There is strong evidence for long-term crustal erosion along the Mexican Trench as indicated by trench retreat and fore-arc uplift (Clift and Vannucchi, 2004), the location of the trench at <30 km from the shoreline, and by large volumes of missing Mesozoic and Cenozoic crust along the coast (Schaaf et al., 1995; Morán-Zenteno et al., 1996, 2018; Keppie et al., 2012; Ducea and Chapman, 2018), with an estimated long-term subduction erosion rate of 60–90 km^3/km/my (Fig. 22; Straub et al., 2015, 2020). Thermochronology studies have also estimated that at least 90% of the subaerial sediment produced by unroofing of the plutonic

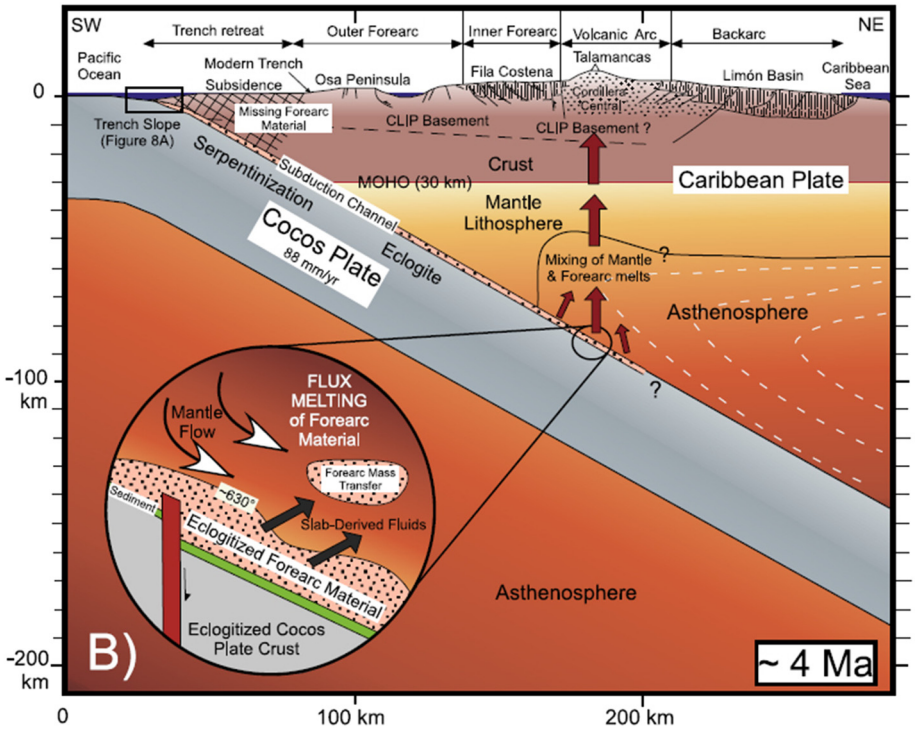

Fig. 21. Cartoon from Goss and Kay (2006) showing a transect across the Central American arc through the Osa Peninsula and Cordillera de Talamanca during the Pliocene (≤4 Ma). Cocos plate subduction geometry is based on seismic imaging of the Wadati-Benioff zone (Protti et al., 1995) and forearc (<50 km depth) (Sallarés et al., 2001). Subduction velocity is from De Mets (2001), and Cocos plate lithospheric thickness (35 km depth at 1300 °C isotherm) obtained from half-space cooling of 10 Ma slab. Slab-surface temperatures given from Peacock et al. (2005) using an isoviscous mantle wedge rheology model. Subduction channel model adapted from Cloos and Shreve (1988a, 1988b). The hatched forearc area represents the calculated amount of forearc eroded in the last 6 Ma with ~50 km arc retreat (Alvarado et al., 1993; Meschede et al., 1999a, 1999b; Vannucchi et al., 2003). Inset schematic of forearc material transported into hotter overriding asthenospheric mantle wedge modified from von Huene et al. (2004).

and metamorphic forearc has also been subducted (Ducea et al., 2004a, 2004b). As such, the crustal inputs entering the subduction channel are by far dominated by a combination of tectonically eroded and ablated forearc debris with seafloor pelagic sediments playing a volumetrically negligible role (Parolari et al., 2018; Straub et al., 2015, 2020).

The central TMVB is constructed on thick continental basement and consequently many studies proposes that andesites and dacites evolve from primary basaltic mantle melt by crustal processing (fractional crystallization, crustal assimilation; Marquez et al., 1999; Verma, 1999; Schaaf et al., 2005; Agustín-Flores et al., 2011). However, in recent years evidence has accumulated from several comprehensive petrologic and geochemical studies that the entire range of central TMVB basaltic to andesitic, and even dacitic and ryolitic magmas, are near-primary melts from a subduction-modified mantle that pass through the crustal basement nearly unchanged (Blatter and Carmichael, 1998; Carmichael, 2002; Gómez-Tuena et al., 2007, 2008, 2018; Straub et al., 2008, 2011, 2013, 2015; Parolari et al., 2018). For instance, Straub et al. (2015), in a comprehensive geochemical study, compared Sr–Nd–Pb–Hf and trace element data of subducted crustal input to the subarc mantle, including both pelagic marine and terrigenous trench sediment, altered oceanic crust and tectonically eroded coastal forearc Eocene Acapulco granodiorites and offshore biotite gneiss and granodioritic crust recovered from DSDP Leg 66 drill sites (Sites 489 and 493, respectively; Fig. 22), to Sr–Nd–Pb–Hf–He–O isotope chemistry of a series of olivine-phyric, high-Mg# basalts to dacites erupted from both monogenetic cones in the Sierra Chichinautzin Volcanic Field and the Popocatépetl and Toluca stratvolcanoes located in the central TMVB just south of Mexico City (Fig. 22). The basaltic to andesitic magmas crystallize high-Ni olivines that have high mantle-like $^{3}He/^{4}He = 7–8\ R_a$ and high crustal $d^{18}Omelt = +6.3–8.5‰$, implying that their host magmas are near-primary melts from a mantle infiltrated by slab-derived crustal components. Although some lavas erupted from some TMVB stratovolcanoes such as Popcatéperl and Citlaltépetl contain quartzite and granitoid xenoliths (Schaaf and Carrasco-Núñez, 2010), there is no evidence of significant intra-crustal crustal contamination of these magmas in the olivine crystallization stage (Straub et al., 2015). Rather, the olivines crystallize from basaltic to andesitic mantle melts that contain a crustal component from the subducted slab. Their Hf-Nd isotope and Nd/Hf trace element systematics (Fig. 23) rule out both the pelagic marine and terrigenous trench sediments as the recycled crust end member, and imply instead that coastal Acapulco and offshore granodiorites, tectonically removed by forearc subduction erosion, are the dominant recycled crust component. The combined Sr–Nd–Pb–Hf isotope modeling (Straub et al., 2015, 2020) shows that these tectonically eroded and subducted crustal components control the highly to moderately incompatible elements in the calc-alkaline central TMVS arc magmas, together with lesser additions of Pb- and Sr-rich fluids from subducted mid-oceanic ridge basalt (MORB)-type altered oceanic crust (AOC).

The Nd-Hf mass balance suggests that the rate of subduction ersoion of the coastal and offshore forearc granodiorite exceeds the flux of the trench sediment by at least an order of magnitude. Assuming the subducted granodiorite component to be 10 times thicker than trench sediment (=170 m thick), Straub et al. (2015) suggest a thickness of 1500–1700 m for the granodiorite in the subduction channel, and that this low density crustal material may buoyantly rise as a bulk 'slab diapir' into the mantle melt region (Fig. 24). Such slab diapirs would be a highly efficient way to transfer large amounts of slab material into the mantle and impose their trace element signature on the prevalent calc-alkaline central TMCB arc magmas.

The presence of high-Ni olivines, with up to 5400 ppm Ni, in both basaltic and andesitic magmas that have high $^{3}He/^{4}He$ ratios, which confirms that they originated in the upper mantle, suggests that these magmas are partial melts of secondary olivine-free pyroxenite segregations in the mantle wedge (Straub et al., 2011). Such pyroxenite segregations could form following the infiltration of silicic components from the subducted slab or rising slab diapirs (Fig. 25). They would melt

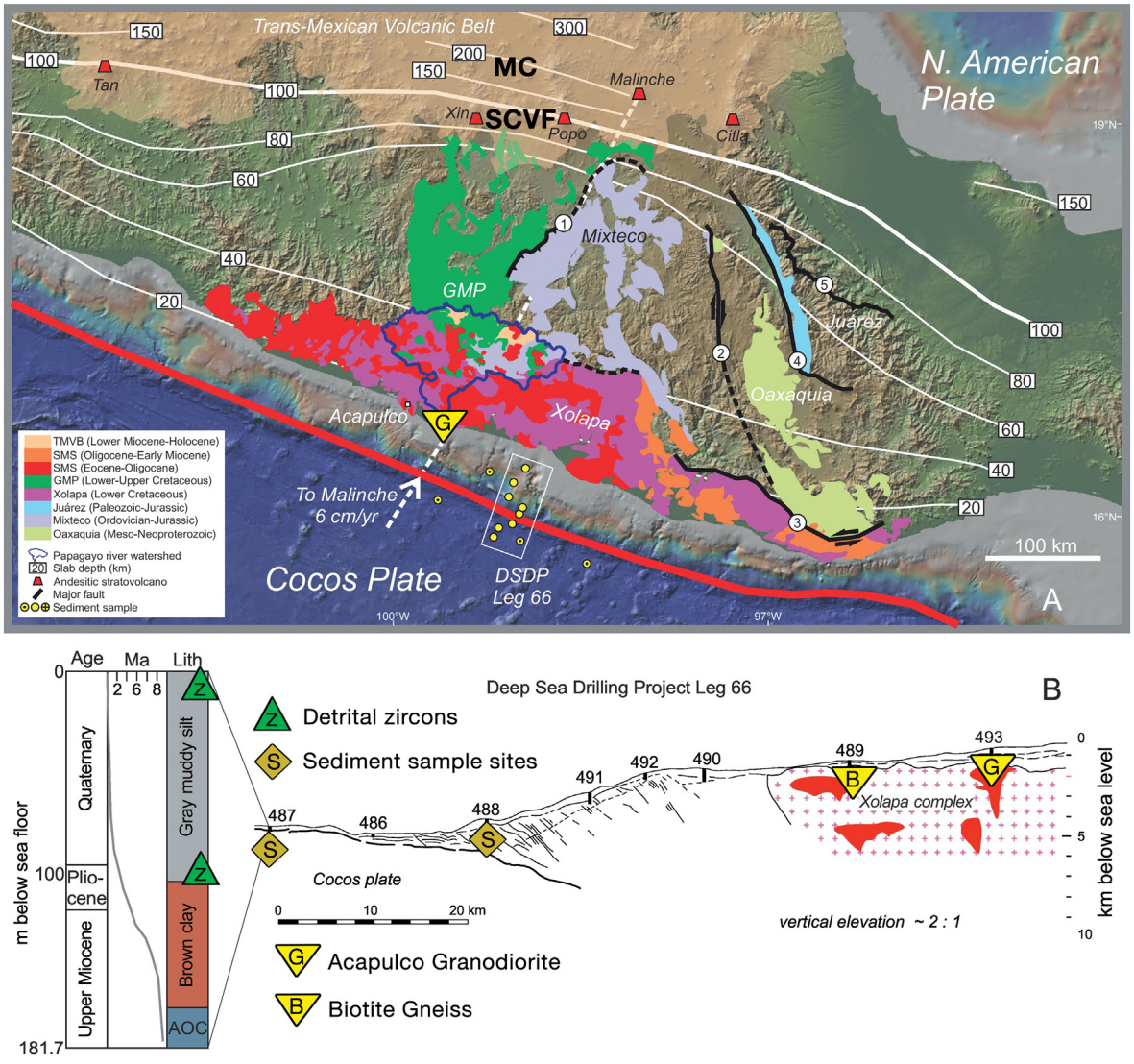

Fig. 22. Plate tectonic setting of the central Trans-Mexican Volcanic Belt (TMVB) modified from Gómez-Tuena et al. (2018). (A) Simplified geologic map of the Mexican subduction zone. Slab depth contours (km) as outlined by Ferrari et al. (2012). Configuration of basement terranes in southern Mexico are from Ortega-Gutiérrez et al. (2018). MC = Mexico City. GMP = Guerrero-Morelos platform. Forearc geology simplified according to Morán-Zenteno et al. (2018) and Ortega-Gutiérrez et al. (2014). Terrane-bounding regional faults include Papalutla (1), Caltepec (2), Chacalapa (3), Oaxaca (4), Vista Hermosa (5). Quaternary andesitic stratovolcanoes of the TMVB: include Citláltépetl (Citla), Malinche, Popocatépetl (Popo), Xinantécatl or Nevado de Toluca (Xin), Tancítaro (Tan). Small monogenetic cones occur within the Sierra Chichinautzin Volcanic Field (SCVF) between the Popo and Xin volcanoes (Straub et al., 2015). Also shown are the sampling locations of Papagayo river watershed (crossed yellow circle), the Deep Sea Drilling Project Expedition 66 (DSDP, clean yellow circles) and of the Vemaand Robert Conrad piston corers of the Lamont-Doherty (LDEO, dotted yellow circles) core repository. Segmented line connecting the trench to Malinche volcano is a circle projection from the Cocos-North America rotational pole (28.1°N, 123.1°W; De Mets, 2001). (B) Cross section of the Mexican continental slope drilled during DSDP Expedition 66 and the schematic sedimentary column of the extensively studied Site 487 (Straub et al., 2015). Altered Oceanic Crust (AOC). Samples of Acapulco granodiorite (G within yellow triangles) were obtained from southeast of Acapulco and Site 493, and biotite gneiss (B within yellow triangle) from Site 489.

preferentially relative to the surrounding peridotite in an upwelling mantle and could produce a broad range of primary basaltic to dacitic melts that mix variably during ascent to form andesites (Straub et al., 2008, 2013, 2015; Parolari et al., 2018). This 'pyroxenite model' requires a minimum of 15–18% or more of a silicic slab component in the source in order to convert peridotite to olivine-free pyroxenite (Straub et al., 2008, 2011, 2015). There is thus a confluence of evidence for strong slab contributions to the mantle source that may contribute up to several tens of percent of the erupted magmas in the central TMVB (Gómez-Tuena et al., 2007, 2018, 2014; Straub et al., 2011, 2013, 2015; Castro et al., 2013), and the slab components therefore control the highly incompatible trace element budgets and isotopic compositions of the central TMVB olivine-bearing mafic and intermediate magmas. Straub et al. (2015) estimated the total percentage of slab-derived Sr, Pb, Nd and Hf in the calc-alkaline TMVZ arc magmas as 69 to 89%, significantly higher than required to produce the isotopic variations in Andean, Aleutian and South Sandwich Island arc magmas. This suggests that the TMVB arc grows by recycling of tectonically eroded and subducted continental crust rather than by formation of new continental crust.

Parolari et al. (2018), based on isotopic mixing models between an altered oceanic crust melt and bulk forearc crust and sediment, estimate that at least half of the magma mass of the volumetrically dominant andesitic volcanoes of Colima, Sangangüey and Tequila in the western TMVB must come from reworking of subducted lithologies in the form of altered ocean crust, both marine and terrigenous trench sediments, and, most importantly, crystalline crustal rocks cannibalized by subduction erosion from the base of the forearc wedge and incorporated into the mantle as a subduction mélanges (Fig. 25). Such subduction mélanges have positive buoyancies in the upper mantle and can rise as "thermo-chemical plumes" into the hot core of the mantle wedge, where temperatures of >1000 °C (Gerya et al., 2004; Behn et al., 2011;

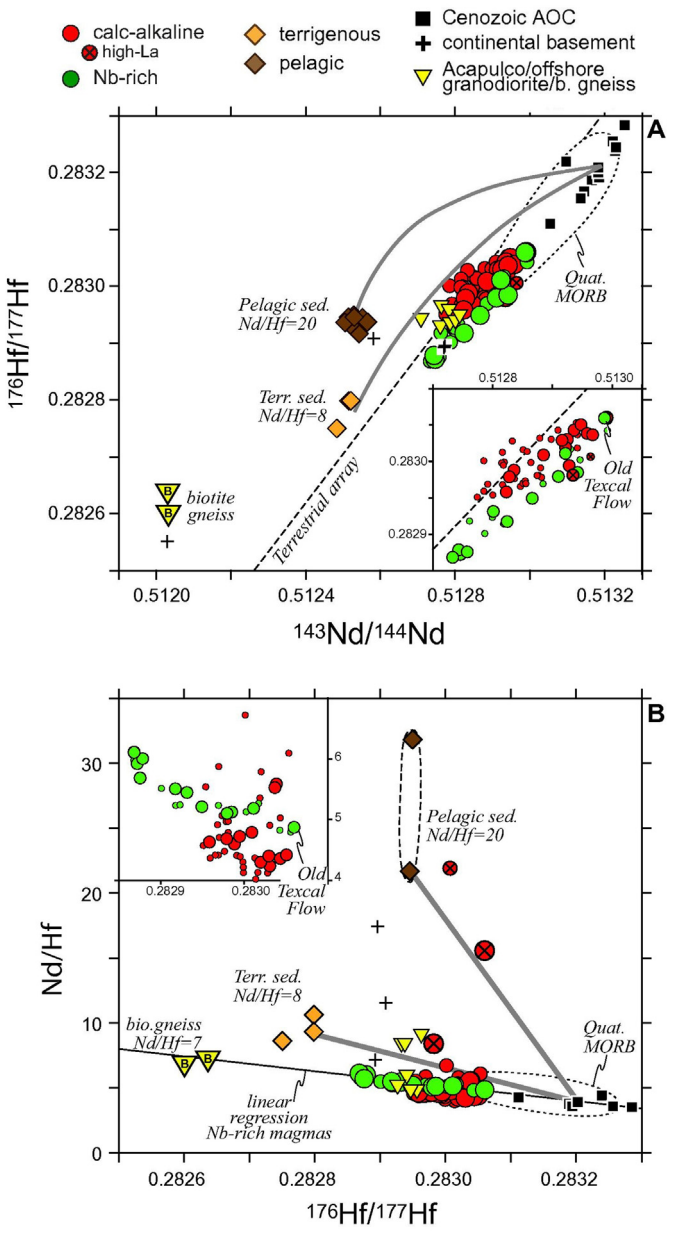

Fig. 23. (a) $^{143}Nd/^{144}Nd$ vs $^{176}Hf/^{177}Hf$, and (b) $^{176}Hf/^{177}Hf$ vs Nd/Hf of central TMVB magmas and crustal materials (MORB, pelagic and terrigenous trench sediment, continental basement) from Straub et al. (2015). Thick gray lines are simple mixing curves between AOC and trench sediment. Mixing models must match arc data in both diagrams to be valid. The trench sediment fails as as a crustal end member, while the offshore/Acapulco granodiorite within the forearc wedge lie in line with the AOC and arc rock compositions.

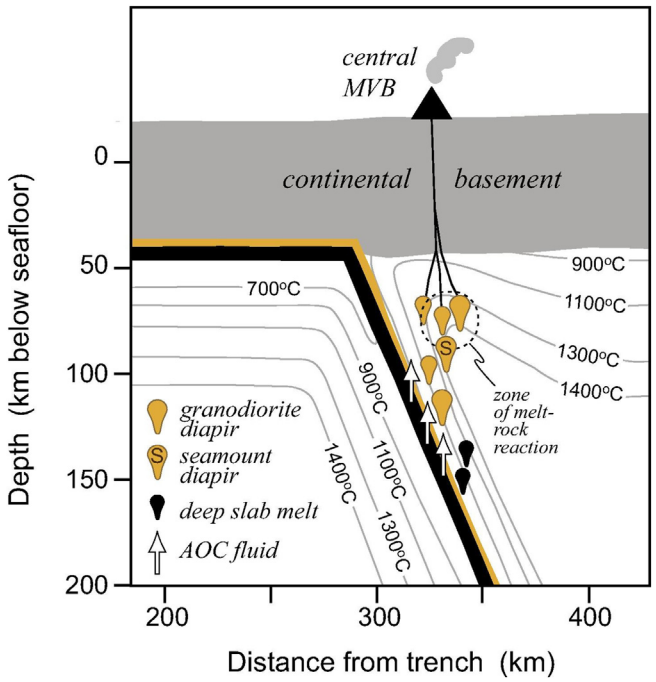

Fig. 24. Cartoon model from Straub et al. (2015) of the diapiric uprise of tectonically eroded and subducted coastal and offshore granodiorite below the central TMVB. Thermal structure model assumes mantle potential temperature of 1450 °C within the mantle wedge and temperatures of ~700 to 800 °C along the slab-mantle interface at about 110 km beneath the central TMVB arc front. Although slab surface temperatures remains below sediment solidus (~1050 °C, Behn et al., 2011), they are conducive to the formation of thermochemical instabilities, allowing the formation of low density slab diapirs, consisting of subducted coastal and offshore granodiorites, which transfer large amounts of slab material into the mantle, forming pyroxenite segregations. These pyroxenite segregations melt preferentially relative to the surrounding peridotite, generating the range of magmas, from basaltic to dacitic, erupted in the TMVB.

Marschall and Schumacher, 2012) are sufficient to extensively, or completely if enough free fluids are available from the breakdown of hydrous phases, melt the quartzo-feldspathic constituents of the subduction mélange to form andesites (Gómez-Tuena et al., 2018). A mantle origin for the western TMVB andesites is also consistent with the existence of amphibole-bearing peridotite enclaves in other TMVC andesites (Blatter and Carmichael, 1998), and with phase equilibria studies indicating that andesitic magmas in Mexico are extracted as true liquids from sub-MOHO depths (Carmichael, 2002).

In a more recent study of the large andesitic Malinche volcano located in the eastern sector of the TMVB (Fig. 22), Gómez-Tuena et al. (2018) use U-Pb zircon geochronology and whole-rock geochemical data of arc and forearc lithologies from the Mexican convergent margin to show that subducted trench sediments and tectonically eroded forearc debris are being tectonically transported and magmatically reworked into the mantle source of this typical andesitic continental arc volcano. They document a remarkable variety of inherited zircons carried by the Malinche magmas, with ages ranging from the Early Miocene (~16 Ma) to the Paleoproterozoic (~1.8 Ga), and argue that this large variety of inherited zircons is not consistent with contamination from a single type of Mexican basement terrane. Specifically, assimilation of basement rocks from the Mixteco terrane, on which the Malinche volcano is located, would not be able to provide zircon crystals younger than Jurassic, whereas some of the most abundant zircons found in Malinche are Cretaceous and Paleogene and therefore could not have been acquired during ascent of Malinche magmas through the upper plate crust. They suggest instead that these zircons were incorporated into a subduction mélange constituted by a heterogeneous mixture of tectonically eroded forearc lithologies and subducted terrigenous sediments, hydrous mantle and altered ocean floor basalts, and that partial melting of this subduction mélanges, either as uprising diapirs (Fig. 25) or after being relaminated below the continental crust (Fig. 26), generate the andesitic magmas erupted from the Malinche volcano, without the intervention of parental basalts or intra-crustal assimilation.

These findings imply a fast and efficient connectivity between subduction inputs and magmatic outputs and indicate that a significant proportion of the subducted continental crust, either terrigenous sediments or subduction eroded crystalline forearc wedge, is being recycled back into continents by arc magmatism. This suggestion is also supported by the results of a number of other recent U-Pb studies of detrital zircons in both arc and continental basalts, as well as mantle xenoliths. Rojas-Agramonte et al. (2016) use zircons to

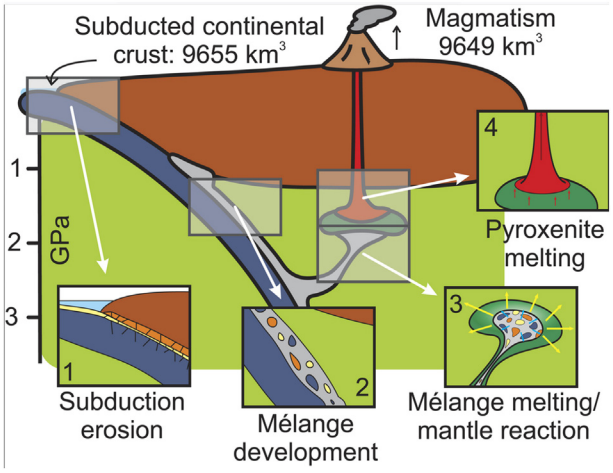

Fig. 25. Model from Parolari et al. (2018) for the origin of andesitic volcanoes as melts of buoyant subduction mélanges made of mixtures of hydrous mantle, altered oceanic crust (AOC), sediments, and fore-arc crustal fragments that, upon melting, react with the peridotitic mantle to form secondary pyroxenites segregations which may melt during diapiric uprise or after being relaminated to the base of the continental lithosphere.

track crustal recycling in mantle-derived rocks of the intra-oceanic volcanic arc of Cuba, which was active from ~135 to 47 Ma during the formation of the present-day Caribbean region. Their findings suggest transport of continental detritus through the mantle wedge above subduction zones in magmas that otherwise do not show strong evidence for crustal input and imply that crustal recycling rates in some arcs may be higher than hitherto realized. Proenza et al. (2017) also document zircons grains, within chromites hosted in the mantle section of the early Cretaceous age supra-subduction Mayarí-Baracoa Ophiolitic Belt in eastern Cuba, that have U-Pb ages ranging from Cretaceous (99 Ma) to Neoarchean (2750 Ma). Most analyzed zircon grains are older than the ophiolite body, show negative $\varepsilon_{Hf}(t)$ (−26 to −0.6) and occasional inclusions of quartz, K-feldspar, biotite, and apatite that indicate derivation from a granitic

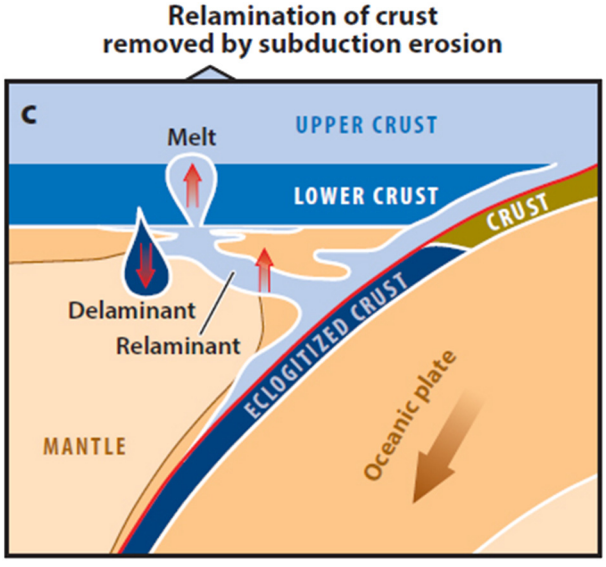

Fig. 26. Schematic diagram from Hacker et al. (2015) of the evolution of the lower crust by the addition of recycled felsic crustal material removed from the upper plate by subduction erosion, incorporated in buoyant low density subduction mélanges, which rise as diapirs through the mantle wedge and are then relaminated to the base of the crust. There may also be melting of these diapirs that produces a liquid that ascends well above the relaminating layer, and there may be mafic residues that are negatively buoyant with respect to the adjacent mantle. These denser mafic material transform to eclogite and sinks within upper mantle.

continental crust. They interpret the chromitite zircon grains as sedimentary-derived xenocrystic grains that were delivered into the mantle wedge beneath the Greater Antilles intra-oceanic volcanic arc during subduction processes, and conclude that continental crust recycling by subduction could explain all populations of old xenocrystic zircon in the Cretaceous mantle-hosted chromitites from eastern Cuba ophiolite. Xu et al. (2018) present zircon U-Pb ages and geochemical evidence that indicates that detrital zircons were carried by terrigenous sediments into a subcontinental subduction zone, where the zircon were transferred into the mantle source of Cenozoic continental basalts in eastern China. They suggest that the occurrence of relict zircons in continental basalts indicates that this refractory mineral can survive extreme temperature-pressure conditions in the asthenospheric mantle, allowing for detrital zircons to survive during partial melting of subarc mantle modified by the addition of subduction mélange. Liu et al. (2010) document continental crust-derived Precambrian zircons in garnet/spinel pyroxenite veins within mantle xenoliths carried by the Neogene Hannuoba basalt in the central zone of the North China Craton, and suggest that these Precambrian zircons were xenocrysts that survived melting of recycled continental crustal rocks and were then injected with silicate melt into the host peridotite.

4. Discussion

4.1. Arc magma genesis

Intra-crustal assimilation (Bowen, 1928), assimilation combined with fractional crystallization (DePaolo, 1981), and the more recently proposed MASH (Fig. 3; Mixing, Storage, Assimilation and Homogenization; Hildreth and Moorbath, 1988) scenario all might play a role in the production of specific individual masses of igneous rocks. However, no combination of these processes can have influenced the generation of the spatial and temporal isotopic and trace-element variations observed in primitive mantle-derived basalts erupted in various convergent plate boundary arcs as reviewed above. Such differences require variations in the chemistry of the mantle source itself. For the MASH model in particular, originally proposed by Hildreth and Moorbath (1988) to explain the correlation between increasing crustal thickness and increasing evidence for crustal components in recently active volcanoes towards the northern end of the Andean Southern Volcanic Zone (NSVZ; Fig. 6), geochemical studies of mafic magmas erupted in the NSVZ rule out the significant amounts of intra-crustal assimilation required to explain their isotopic compositions (Figs. 7 and 11; Stern, 1989, 1990, 1991a, 1991b; Kay et al., 2005). Wieser et al. (2019) also argue that there are no known crustal lithologies capable of providing the full range of both trace-element and isotopic variations observed in the NSVZ. The increased amount of northward crustal assimilation proposed by the MASH model is also contradictory to the decreased magma production rates in this region (Völker et al., 2011) and thus the available heat for crustal assimilation northwards in the SVZ (Kay et al., 2005).

The advent of plate tectonics and the recognition of that both trench sediment subduction and subduction erosion of the forearc crystalline wedge (Fig. 1) are important processes along all convergent plate boundaries provides a powerful alternatives to intra-crustal assimilation for introducing continental crust into the mantle source region of volcanic arc magmas. Over the last 30 years, an increasing number of geochemical studies in different arcs, as reviewed in detail above, have documented the role of subduction erosion and mantle source region contamination with tectonically eroded and subducted forearc wedge crystalline crustal components in the generation of some primitive mantle-derived arc basalts, as well as in the generation of more silica-rich rocks such as basaltic andesites and andesites, often considered to be derivative from basaltic magmas, which have isotopic compositions distinct from the marine or terrigenous trench sediments also being subducted below these arcs. The geochemical data and U-Pb studies of

zircons reviewed above provide strong support for the suggestion that eroded forearc crystalline lithologies are being tectonically transported and magmatically reworked into the mantle source of both some basalts as well as andesites erupted from continental arc volcanos.

The transfer of small proportions of tectonically eroded and subducted forearc crystalline wedge crustal components into the mantle source of arc basalts, such as had been suggested for the generation of Andean mafic magmas at the northern end of the Andean SVZ (Stern, 1989, 1990, 1991; Stern and Skewes, 1995; Kay et al., 2005; Stern et al., 2011a, 2019), and also in both the Aleutian (Jicha and Kay, 2018) and Central American arcs (Goss and Kay, 2006), may result from dehydration and/or partial melting of the subducted slab. On the other hand, larger amounts of subducted low density crustal materials may form diapirs of subducted crust (Fig. 24; Straub et al., 2015) or tectonic mélanges (Fig. 25; Nielsen and Marschall, 2017; Parolari et al., 2018; Gómez-Tuena et al., 2018) that produce silicic melts which interact and metasomatize the peridotite mantle to form pyroxenite metasomatites. These pyroxenite segregations may then melt to form a wide range of arc rocks, from basalts though andesites, which include a large proportion of recycled crustal materials. This scenario has important implications for the understanding of evolution of the continental crust, both in terms of its overall composition and also with respect to its growth and preservation.

4.2. Crustal evolution

Given the remarkable compositional similarities among andesites erupted from convergent plate boundary arc volcanoes and the bulk continental crust (Taylor and McLennan, 1985; Rudnick, 1995; Kelemen, 1995; Plank and Langmuir, 1998; Kelemen et al., 2003; Rudnick and Gao, 2003; Plank, 2004; Hacker et al., 2011, 2015), understanding how convergent plate boundary andesites form is a significant step in understanding how the continents have evolved. Some theories regard andesites as derivative liquids from basalts by crystal-liquid fractionation, intracrustal assimilation and mixing in so-called MASH (Fig. 3; Hildreth and Moorbath, 1988) or crustal hot zones (Annen et al., 2006), and assume a basaltic net flux from the mantle to arcs and continents (Gill, 1981). In order to maintain the overall composition of the crust as andesitic, the basalt-input model requires the elimination from the continents, by delamination into the underlying mantle (Fig. 26), of an unknown volume of ultramafic cumulates that form during the crystal-liquid fractionation processes that generate an andesite from a basalt (Arndt and Goldstein, 1989; Kay and Kay, 1993; Rudnick, 1995).

Alternatively, Taylor (1967) suggested that new andesitic continental crust is formed in convergent plate boundary arcs by the generation of primary andesitic magmas in and/or above subduction zones. Green and Ringwood (1968) argued that melting of subducted oceanic basalts transformed at high pressure into eclogites could partially melt to form andesites. The origin of adakitic andesites has been attributed to the partial melting of subducted oceanic basalts (Kay, 1978; Stern et al., 1984; Defant and Drummond, 1990; Stern and Kilian, 1996), but these are not volumetrically significant on a global scale.

Kelemen (1995) proposed that the net magmatic flux from the mantle into the crust might be high Mg# andesites, formed by reaction between ascending mafic or silicic slab melts and mantle peridotite. Hacker et al. (2011, 2015), Castro et al. (2013) and Kelemen and Behn (2016) have all elaborated on this idea, suggesting that although subducted mafic oceanic basalts become dense eclogites and may continue to descend into the mantle, more silica-rich rocks, derived by sediment subduction and subduction erosion, are transformed into felsic gneisses that are less dense than peridotite. These more felsic rocks may therefore rise buoyantly, undergo decompression melting and melt extraction, and be relaminated to the base of the crust (Fig. 26). As a result of this refining and differentiation process, such relatively felsic rocks could form much of the continental lower crust.

Blatter and Carmichael (2001) and Carmichael (2002) also concluded from phase equilibria studies that andesitic magmas erupted from large calc-alkaline andesitic volcanoes in Mexico are extracted as true liquids from sub-MOHO depths. Blatter and Carmichael (1998) described the existence of peridotite enclaves in Mexican andesites, consistent with a mantle origin for these andesites. The isotopic and U-Pb zircon age data reviewed above for andesites from the TMVB are interpreted to suggest that these formed by partial melting of pyroxenite metasomatites produced by hybridization of mantle peridotite with melts derived from uprising diapirs (Figs. 24 and 25; Straub et al., 2015, 2020; Nielsen and Marschall, 2017; Gómez-Tuena et al., 2018; Parolari et al., 2018) of buoyant low-density subduction mélanges constituted by a mixture of tectonically eroded forearc debris, oceanic sediments, subducted altered oceanic crust and hydrous mantle peridotite.

In contrast to previous models for adakitic (Kay, 1978; Stern et al., 1984; Defant and Drummond, 1990; Stern and Kilian, 1996) and high Mg# andesite (Kelemen, 1995) genesis, tectonically eroded crust plays an important role in these more recent models of andesite genesis and crustal evolution. This is not a theoretical role, but one supported by the isotopic and U-Pb zircon age data which imply an efficient connectivity between subduction inputs and magmatic outputs. Given the evidence that subduction erosion occurs along all convergent plate boundaries, and the isotopic and trace-element evidence from a number of arcs that tectonically eroded crust is incorporated into the source of both basaltic and andesitic magmas erupted from the volcanoes that form these arcs, subduction erosion must be considered as a key process in the recycling and regeneration of continental crust through the generation of andesitic magmas in the subarc mantle above subduction zones. The formation of lower continental crust by the addition of andesites derived from the melting of tectonically eroded and subducted crust, or from the relamination of subduction mélanges in which subducted crust is an important component, negates the necessity for extensive delamination of the lower crust to preserves the continental crust's overall andesitic composition (Hacker et al., 2011, 2015; Castro et al., 2013). Thus, delamination might be of lesser importance and subduction erosion of even greater importance in crustal recycling than previously estimated (Fig. 2).

The presence of zircon remnants derived from the subaerial and/or tectonic erosion of the forearc implies that a significant portion of the subducted continental crust is not lost at convergent margins, but reworked by the incorporation into melts of subducted material. Parolari et al. (2018) calculate that along the western Mexican subduction zone the volume of subducted continental crust has been effectively counterbalanced by contemporaneous magmatism, with no net crustal growth, at least over the past one million years. However, they estimate that only half of the magma mass of the volumetrically dominant andesitic volcanoes in the TMVB come from reworking of subducted lithologies in the form of altered ocean crust, sediments, and, most importantly, cannibalized forearc continental crust, incorporated into the mantle wedge as buoyant subduction mélanges (Fig. 25). Thus some significant portion of the tectonically eroded crust may be being transported deeper into the mantle. Coltice et al. (2000) also suggested, based on ^{40}K-^{40}Ar constraints on recycling of continental crust back into the mantle, that only 50 to 70% of subducted crustal materials are reincorporated back into the continental crust and that at least 30% of the modern mass of the continents has been subducted back into the mantle during Earth's history.

On a global scale, the total current rate of return of continental crust into the deeper mantle, the most important process for which is subduction erosion, is equal to or greater than the estimates of the rate at which the crust is being replaced by arc and plume magmatic activity (Fig. 2; Stern, 2011). This implies that currently the continental crust is probably slowly shrinking and that overall some significant proportion of subducted crust and sediment is transported deeper into the mantle and neither underplated below the forearc wedge nor incorporated in

arc magmas. This has important implications for the evolution of the Earth's mantle.

4.3. Mantle evolution

Sr–Nd–Pb-Hf isotope data from ocean island basalts (OIB) demonstrate ubiquitous heterogeneity in the Earth's mantle, with a number of distinctive mantle reservoirs identified, such as depleted mantle (DM), HIMU (high μ = high U/Pb), and enriched mantle (EM; White and Hofmann, 1982; White, 1985; Zindler and Hart, 1986; Hart et al., 1986, 1992; Hart, 1988; Farley et al., 1992; Hanan and Graham, 1996; Stracke et al., 2005; Chauvel et al., 2009, Chauvel et al., 2008, 2009). Willbold and Stracke (2010) suggest that all the EM-type OIB mantle sources share a common heritage from the continental crust. They propose that the recycling of both upper and lower continental crust and oceanic lithosphere at convergent plate margins, and their subsequent incorporation into the mantle sources of OIB, can account for the entire range of chemical and isotopic signatures in EM-type oceanic basalts, and that the compositional heterogeneity in the Earth's mantle is induced by, and intrinsic to the processes involved in the recycling of continental crust. Although subduction of terrigenous sediments may provide some portion of upper crustal components to the mantle, processes other than sediment subduction, such as subduction erosion or crustal delamination (Fig. 26), are required to provide a source for the transport of lower crustal components into the mantle, since large exposed areas of lower continental crust are exceedingly rare (Rudnick and Fountain, 1995; Rudnick and Gao, 2003). Given that subduction erosion is estimated to return more crust into the mantle than either subduction of sediment or delamination (Fig. 2), it is likely that this process plays a significant role in generating the enriched mantle sources that produce EM-type OIB (Fig. 27).

In fact, Willbold and Stracke (2010) advocate subduction erosion as a more important process than delamination for lower crust recycling into the deep mantle, because it accounts for fluxes of both upper and lower continental crust into the mantle as concurrent events resulting from the same principal geodynamic process. They note that delamination of lower continental crust requires concomitant delamination of subcontinental lithospheric mantle, which is characterized by subchondritic $^{187}Os/^{186}Os$ ratios (Walker et al., 1989; Pearson et al., 2004) unlike the supra-chondritic $^{187}Os/^{186}Os$ ratios in some EM-type basalts (Eisele et al., 2002; Escrig et al., 2004). Willbold and Stracke (2006, 2010) therefore question the role of delaminated and foundered of continental lithosphere as a way to incorporate lower continental crust into the source of EM basalts. This is consistent with the andesite-input model of crustal growth discussed in the previous section, which negates the need for delamination as a significant process in crustal evolution (Hacker et al., 2011, 2015; Castro et al., 2013).

It appears evident that some portions of the relatively thin continental materials within subduction channels may be subducted deeper mantle beyond the depth of arc magma generation (Fig. 27). The common occurrence of ultrahigh-pressure (UHP) metamorphic rocks in collisional orogenic belts also suggests that subduction of even thick sections of continental crust may reach depths of ~300 km (Ye et al., 2000; Liou et al., 2002; Liu et al., 2007). The transformations of plagioclase to jadeite (3.34 g/cm^3) + grossular (3.6 g/cm^3) + quartz (2.65) and quartz to stishovite (4.29 g/cm^3) at ~9 GPa, cause the zero-pressure density of model continental crust to jump dramatically to 3.96 g/cm^3 (Komabayashi et al., 2009), thus allowing felsic crust to be subducted well below the MOHO. Maruyama and Safonova (2019) suggest that through time the eroded and subduction crustal materials may accumulate in the mantle transition zone (MTZ; 410–660 km depth; Fig. 28A), and that the volume of this "2nd continent" in the MTZ may even exceed that of the surface continents.

Kawai et al. (2009) conclude that the zero-pressure density of felsic granitoids does not exceed that of pyrolite in the lower mantle and therefore subducted crustal material will remain above the mantle transition zone and not sink deeper into the lower mantle. In contrast, Komabayashi et al. (2009) suggest that at 22 GPa (660 km depth), the reaction of jadeite to a Na-Al phase (NAL; 3.92 g/cm^3) + more stishovite (4.29 g/cm^3) could lead to another zero-pressure density jump of subducted continental crust from 3.96 to 4.21 g/cm^3. They therefore suggest that together with MORB, subducted continental crust could descend into the lower mantle and accumulated in the D″ layer on the bottom of mantle (Fig. 28). They consider that the D″ layer is a chemically distinct region, the "anti-crust" or what Maruyama and Safonova (2019) call the "3rd continent", composed of subducted continental crust, MORB and the mantle portion of past oceanic lithosphere.

Because subducted continental crust is enriched in K, U and Th, this processes replenishes the deep mantle with radioactive elements and may play a critical role in the initiation of plumes and/or superplumes related to the origin of the superplume–supercontinent cycle (Fig. 28; Senshu et al., 2009). Subduction erosion is thus a key process in maintaining global tectonic activity (Stern, 2011).

5. Conclusions

1) Isotopic and trace-element data indicate that tectonically eroded and subducted continental crust is being incorporated into the mantle source of mafic magmas erupted from volcanoes along several different convergent plate boundaries, including the Andes, Aleutian and South Sandwich Islands, and the Central American and Trans-Mexican Volcanic Belts.

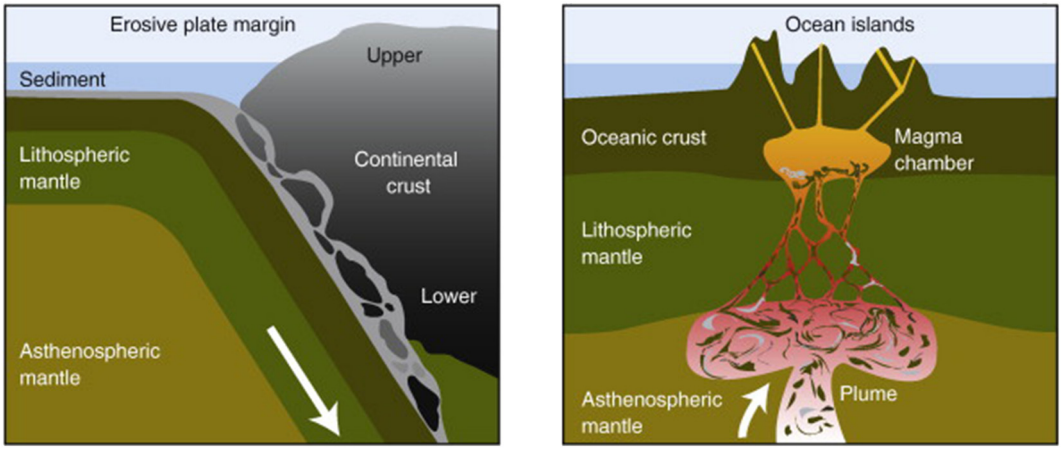

Fig. 27. Schematic sketch, from Willbold and Stracke (2010), depicting possible transfer of continental crustal material into the mantle plume source of EM-type oceanic island basalts by sediment subduction and subduction erosion.

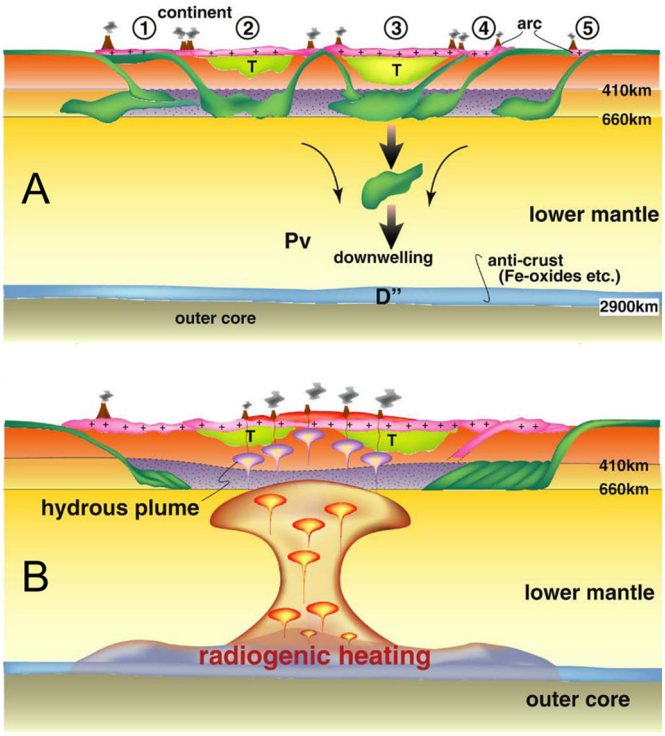

Fig. 28. A schematic cartoon, from de Wit and Hart (1993) and Senshu et al. (2009), showing (A) arc and sediment subduction, and the possible accumulation of subducted slabs, including crust, on to the core-mantle boundary; and (B) model of plume formation caused by selective accumulation of TTG crust in the slab graveyard in the D″ layer. Radiogenic heating from the subducted TTG crust in the D″ layer plays a major role for the birth of the superplume which later breaks up the supercontinent.

2) U-Pb ages for zircons within andesites from the Trans-Mexican Volcanic Belt suggest that these are xenocrysts inherited from subducted trench sediments and tectonically eroded forearc crystalline basement magmatically reworked into the mantle source of these typical continental arc andesites.
3) The data suggest that andesites may form within the mantle by partial melting of pyroxenite metasomatites produced by hybridization of mantle peridotite with melts derived from uprising diapirs of buoyant low-density subducted crust and/or subduction mélanges constituted by a mixture of tectonically eroded forearc debris, oceanic sediments, subducted altered oceanic crust and hydrous mantle peridotite.
4) The formation of lower continental crust by the addition of andesites derived from the melting of tectonically eroded and subducted crust in the mantle, or from the relamination of subduction mélanges in which subducted crust is an important component, negates the necessity for extensive delamination of the lower crust to preserves the continental crust's overall andesitic composition.
5) Subduction erosion is thus a more important process than delamination for lower crust recycling into the deep mantle, and it can account for fluxes of both upper and lower continental crust into the mantle as concurrent events resulting from the same principal geodynamic process.
6) The recycling by subduction erosion of both upper and lower continental crust at convergent plate margins, and their subsequent incorporation into the mantle sources of oceanic island basalts, can account for the entire range of chemical and isotopic signatures in EM-type OIB, and these compositional heterogeneity in the Earth's mantle are thus induced by the processes involved in the recycling of continental crust.
7) The evidence has grown substantially over the last 20 years in support of subduction erosion and mantle source region contamination with crustal components as a powerful alternative to intra-crustal assimilation in the generation of intermediate magmas at convergent plate boundaries, and its role in the evolution of the continental crust and mantle cannot be ignored and should not be underestimated.

Declaration of competing interest

The authors declare that they have no known competing financial interests or personal relationships that could have appeared to influence the work reported in this paper.

Acknowledgments

I wish to thank T. Horscroft and M. Santosh for inviting me to prepare this review. Peter Schaaf, Stephen Turner, Jorge Muñoz and Richard Goldfarb provided reviews with many constructive suggestions that helped me improve the final manuscript.

References

Abratis, M., Wörner, G., 2001. Ridge collision, slab-window formation, and the flux of Pacific asthenosphere into the Caribbean realm. Geology 29, 127–130.
Agustín-Flores, J., Siebe, C., Guilbaud, M.N., 2011. Geology and geochemistry of Pelagatos, Cerro del Agua, and Dos Cerros monogenetic volcanoes in the Sierra Chichinautzin Volcanic Field, south of México City. J. Volcanol. Geotherm. Res. 201, 143–162. https://doi.org/10.1016/j.jvolgeores.2010.08.010.
Alvarado, G.E., Kussmaul, S., Chiesa, S., Gillot, P.Y., Appel, H., Wörner, G., Rundle, C., 1993. Resumen cronoestratigrafico de las rocas igneas de Costa Rica basado en dataciones radiometricas. J. S. Am. Earth Sci. 6, 151–168.
Annen, C., Blundy, J.D., Sparks, R.S.J., 2006. The genesis of intermediate and silica magmas in deep crustal hot zones. J. Petrol. 47, 505–539.
Armstrong, R.L., 1981. Radiogenic isotopes: the case for crustal recycling on a near-steady-state no-continental growth Earth. Royal Society of London Philosophical Transactions 301, 443–472.
Armstrong, R.L., 1991. The persistent myth of crustal growth. Aust. J. Earth Sci. 38, 613–630.
Arndt, N.T., Goldstein, S.L., 1989. An open boundary between lower continental crust and mantle; its role in crust formation and crustal recycling. Tectonophysics 161, 201–212.
Barazangi, M., Isacks, B.L., 1976. Spatial distribution of earthquakes and subduction of the Nazca plate beneath South America. Geology 4, 686–692.
Barcley, J., Carmichael, I.S.E., 2004. A hornblende basalt from Western Mexico: water-saturated phase relations constrain a pressure-temperature window of eruptibility. J. Petrol. 45, 485–506.
Barker, P.F., 1995. Tectonic framework of the East Scotia Sea. In: Taylor, B. (Ed.), Backarc Basins: Tectonics and Magmatism. Plenum Press, New York, pp. 281–314.
Barker, P.F., Hill, I.A., 1981. Back-arc extension in the Scotia Sea. Philos. Trans. R. Soc. Lond. Ser. A 300, 249–262.
Barreiro, B.A., 1984. Lead isotopes and Andean magmagenesis. In: Harmon, R.S., Barreiro, B.A. (Eds.), Andean Magmatism; Chemical and Isotopic Constrains. Shiva Geology Series. Shiva Publishing Limited, Natwich, UK, pp. 21–30.
Behn, M.D., Kelemen, P.B., Hirth, G., Hacker, B.R., Massonne, H.-J., 2011. Diapirs as the source of the sediment signature in arc lavas. Nat. Geosci. 4, 641–646. https://doi.org/10.1038/ngeo1214.
Benton, L.D., Ryan, J.G., Tera, F., 2001. Boron isotope systematics of slab fluids as inferred from serpentinite seamount, Mariana forearc. Earth Planet. Sci. Lett. 187, 273–282.
Bevis, M., Isacks, B., 1984. Hypocentral trend surface analysis: probing the geometry of Benioff zones. J. Geophys. Res. 89, 6153–6170.
Bindeman, I.N., Eiler, J.M., Yogodzinski, G.M., Tatsumi, Y., Stern, C.R., Grove, T., Portnyagin, M., Hoernle, K., Danyushevsky, L.V., 2005. Oxygen isotope evidence for slab melting in modern and ancient subduction zones. Earth Planet. Sci. Lett. 235, 480–496.
Blatter, D.K., Carmichael, I.S.E., 1998. Hornblende peridotite xenoliths from central Mexico reveal the highly oxidized nature of subarc upper mantle. Geology 26, 1035–1038.
Blatter, D.K., Carmichael, I.S.E., 2001. Hydrous phase equilibria of a Mexican high-silica andesite: a candidate for mantle origin? Geochim. Cosmochim. Acta 65, 4043–4065.
Bosch, D., Jamais, M., Boudier, F., Nicolas, A., Dautria, J.M., Agrinier, P., 2004. Deep and high-temperature hydrothermal circulation in the Oman ophiolite: petrological and isotopic evidence. J. Petrol. 45, 1181–1208.
Boschi, C., Dini, A., Früh-Green, L., Kelley, D.S., 2008. Isotopic and element exchange during serpentinization and metasomatism at the Atlantis massif (MAR 30°N): insights from B and Sr isotope data. Geochim. Cosmochim. Acta 72, 1801–1823.
Bowen, N.L., 1928. The Evolution of the Igneous Rocks. Princeton University Press, Princeton.
Buchs, D.M., Oemering, S.A., 2020. Long-term non-erosive nature of the south Costa Rican margin supported by arc-derived sediments accreted in the Osa Mélange. Earth Planet. Sci. Lett. 531, 115968.
Carmichael, I.S.E., 2002. The andesite aqueduct: perspectives in the evolution of intermediate magmas in west-central Mexico. Contrib. Mineral. Petrol. 143, 641–663.
Carr, M.J., 1984. Symmetrical and segmented variation of physical and geochemical characteristics of the Central American Volcanic Front. J. Volcanol. Geotherm. Res. 20, 231–252.

Castro, A., Vogt, K., Gerya, T., 2013. Generation of new continental crust by sublithospheric silicic-magma relamination in arcs: a test of Taylor's andesite model. Gondwana Res. 23, 1554–1566. https://doi.org/10.1016/j.gr.2012.07.004.
Charrier, R., Munizaga, F., 1979. Edades K Ar de vulcanitas cenozoicas del sector cordillerano del río Cachapoal (34°15′). Rev. Geol. Chile 7, 41–51.
Charrier, R., Baeza, O., Elgueta, S., Flynn, J.J., Gans, P., Kay, S.M., Muñoz, N., Wyss, A.R., Zurita, E., 2002. Evidence for Cenozoic extensional basin development and tectonic inversion south of the flat-slab segment, southern Central Andes, Chile (33°–36°S). J. S. Am. Earth Sci. 15, 117–139.
Chauvel, C., Lewin, E., Carpentier, M., Arndt, N.T., Marini, J.C., 2008. Role of recycled oceanic basalt and sediment in generating the Hf–Nd mantle array. Nat. Geosci. 1. https://doi.org/10.1038/ngeo.2007.1051.
Chauvel, C., Marini, J.C., Plank, T., Ludden, J.N., 2009. Hf-Nd input flux in the Izu-Mariana subduction zone and recycling of subducted material in the mantle. Geochem. Geophys. Geosyst. 10. https://doi.org/10.1029/2008GC002101.
Chen, L., Zhao, Z.-F., 2017. Origin of continental arc andesites: the composition of source rocks is the key. J. Asian Earth Sci. 145, 217–232.
Chen, L., Zhao, Z.-F., Zheng, Y.-F., 2014. Origin of andesitic rocks: geochemical constraints from Mesozoic volcanics in the Luzong basin, South China. Lithos 190, 220–239.
Chen, L., Zheng, Y.-F., Zhao, Z.-F., 2016. Geochemical constraints on the origin of Late Mesozoic andesites from the Ningwu basin in the Middle–Lower Yangtze Valley, South China. Lithos 254, 94–117.
Clift, P.D., Vannucchi, P., 2004. Controls on tectonic accretion versus erosion in subduction zones; implications for the origin and recycling of the continental crust. Rev. Geophys. 42, RG2001. https://doi.org/10.1029/2003RG000127.
Clift, P.D., Chan, L.-H., Blusztajn, J., Layne, G.D., Kastner, M., Kelly, R.K., 2005. Pulsed subduction accretion and tectonic erosion reconstructed since 2.5 Ma from the tephra record offshore Costa Rica. Geochem. Geophys. Geosyst. 6. https://doi.org/10.1029/2005GC000963.
Clift, P.D., Vannucchi, P., Morgan, J.P., 2009. Crustal redistribution, crust–mantle recycling and Phanerozoic evolution of the continental crust. Earth Sci. Rev. 97, 80–104.
Cloos, M., Shreve, R.L., 1988a. Subduction-channel model of prism accretion, mélange formation, sediment subduction, and subduction erosion at convergent plate margins, 1: background and description. Pure Appl. Geophys. 128, 456–500.
Cloos, M., Shreve, R.L., 1988b. Subduction-channel model of prism accretion, mélange formation, sediment subduction, and subduction erosion at convergent plate margins, 2: implications and discussion. Pure Appl. Geophys. 128, 501–545. https://doi.org/10.1007/BF00874549.
Coltice, N., Albarède, F., Gillet, P., 2000. ^{40}K-^{40}Ar constraints on recycling continental crust into the mantle. Science 288, 845–847. https://doi.org/10.1126/science.288.5467.845.
Cuadra, P., 1986. Geocronología K-Ar del yacimiento El Teniente y áreas adyacentes. Rev. Geol. Chile 27, 3–26.
De Boer, J.Z., Defant, M.J., Stewart, R.H., Bellon, H., 1991. Evidence for active subduction below western Panama. Geology 19, 649–652.
De Boer, J., Drummond, M.S., Bordelon, M.J., Defant, M.J., Bellon, H., Maury, R.C., 1995. Cenozoic magmatic phases of the Costa Rican island arc (Cordillera de Talamanca). In: Mann, P. (Ed.), Geologic and Tectonic Development of the Caribbean Plate Boundary in Southern Central America, Geologic Society of America, Special Paper 295, 35–55.
De Mets, C., 2001. A new estimate for present-day Cocos-Caribbean Plate motion: implications for slip along the Central American volcanic arc. Geophys. Res. Lett. 28, 4043–4046.
De Wit, M.J., Hart, R.A., 1993. Earth's earliest continental lithosphere, hydrothermal flux and crustal recycling. Lithos 30, 309–335.
Deckart, K., Godoy, E., Bertens, A., Saeed, A., Jeréz, D., 2010. Barren Miocene granitoids in the central Andean metallogenic belt, Chile: geochemistry and Nd-Hf and U-Pb isotope systematics: Andean. Geology 37, 1–31.
Defant, M.J., Drummond, M.S., 1990. Derivation of some modern arc magmas by melting of young subducted lithosphere. Nature 347, 662–665.
Defant, M.J., Richerson, P.M., de Boer, J.Z., Stewart, R.H., Maury, R.C., Bellon, H., Drummond, M.S., Feigenson, M.D., Jackson, T.E., 1991a. Dacite genesis via both slab melting and differentiation: petrogenesis of La Yeguada volcanic complex, Panama. J. Petrol. 32, 1101–1142.
Defant, M.J., Clark, L.F., Stewart, R.H., Drummond, M.S., de Boer, J.Z., Maury, R.C., Bellon, H., Jackson, T.E., Restrepo, J.F., 1991b. Andesite and dacite genesis via contrasting processes: the geology and geochemistry of El Valle Volcano, Panama. Contrib. Mineral. Petrol. 106, 309–324.
DePaolo, D.J., 1981. Trace element and isotopic effects of combined wallrock assimilation and fractional crystallization. Earth Planet. Sci. Lett. 53, 189–202.
Ducea, M.N., Chapman, A.D., 2018. Sub-magmatic arc underplating by trench and forearc materials in shallow subduction systems; a geologic perspective and implications. Earth Sci. Rev. 185, 763–779. https://doi.org/10.1016/j.earscirev.2018. 08.001.
Ducea, M.N., Gehrels, G.E., Shoemaker, S., Ruiz, J., Valencia, V.A., 2004a. Geologic evolution of the Xolapa complex, southern Mexico: evidence from U-Pb zircon geochronology. Geol. Soc. Am. Bull. 116, 1016–1025. https://doi.org/10.1130/B25467.1.
Ducea, M.N., Valencia, V.A., Shoemaker, S., Reiners, P.W., Decelles, P.G., Campa, M.F., Morán-Zenteno, D., Ruiz, J., 2004b. Rates of sediment recycling beneath the Acapulco trench: constraints from (U-Th)/He thermochronology. J. Geophys. Res. 109, B09404. https://doi.org/10.1029/2004JB003112.
Edwards, J.H., Kluesner, J.W., Silver, E.A., Bangs, N.L., 2018. Pleistocene vertical motions of the Costa Rican outer forearc from subducting topography and a migrating fracture zone triple junction. Geosphere 14 (2), 510–534.
Eisele, J., Sharma, M., Galer, S.J.G., Blichert-Toft, J., Devey, C.W., Hofmann, A.W., 2002. The role of sediment recycling in EM-1 inferred from Os, Pb, Hf, Nd, Sr isotope and trace element systematics of the Pitcairn hotspot. Earth Planet. Sci. Lett. 196, 197–212.
Escrig, S., Campas, F., Dupré, B., Allègre, C.J., 2004. Osmium isotopic constraints on the nature of the DUPAL anomaly from Indian mid-ocean-ridge basalts. Nature 431, 59–63.
Farley, K.A., Natland, J.H., Craig, H., 1992. Binary mixing of enriched and undegassed (primitive?) mantle components (He, Sr, Nd, Pb) in Samoan lavas. Earth Planet. Sci. Lett. 111, 183–199.
Feigenson, M.D., Carr, M.J., Maharaj, S.V., Juliano, S., Bolge, L.L., 2004. Lead isotope composition of Central American volcanoes: influence of the Galapagos plume. Geochem. Geophys. Geosyst. 5, Q06001. https://doi.org/10.1029/2003GC000621.
Ferrari, L., Orozco-Esquivel, T., Manea, V., Manea, M., 2012. The dynamic history of the Trans-Mexican Volcanic Belt and the Mexico subduction zone. Tectonophysics 522–523, 122–149. https://doi.org/10.1016/j.tecto.2011.09.018.
Fisher, D.M., Gardner, T.W., Marshall, J.S., Sak, P.B., Protti, M., 1998. Effect of subducting sea-floor roughness on fore-arc kinematics, Pacific Coast, Costa Rica. Geology 26, 467–470.
Futa, K., Stern, C.R., 1988. Sr and Nd isotopic and trace element compositions of Quaternary volcanic centers of the Southern Andes. Earth Planet. Sci. Lett. 88, 253–262.
Gardner, T.W., Verdonck, D., Pinter, N.M., Slingerland, R.L., Furlong, K.P., Bullard, T.E., Wells, S.G., 1992. Quaternary uplift astride the aseismic Cocos Ridge, Pacific Coast, Costa Rica. Geol. Soc. Am. Bull. 104, 219–232.
Gardner, T.W., Fisher, D.M., Morell, K.D., Cupper, M.L., 2013. Upper-plate deformation in response to flat slab subduction inboard of the aseismic Cocos Ridge, Osa Peninsula, Costa Rica. Lithosphere 5 (3), 247–264.
Gerya, T.V., Yuen, D.A., Sevre, E.O.D., 2004. Dynamical causes for incipient magma chambers above slabs. Geology 32, 89–92. https://doi.org/10.1130/G20018.1.
Giambiagi, L., Tassare, A.S., Mescua, J., Tunik, M., Alvarez, P.P., Godoy, E., Hoke, G., Pinto, L., Spanotto, S., Porras, H., Tapia, F., Jara, P., Bechis, F., Gaercía, V.H., Suriano, J., Moreiras, S.M., Pagano, S.D., 2015. Evolution of shallow and deep structures along the Maipo–Tunuyán transect (33°40'S): from the Pacific coast to the Andean foreland. In: Sepúlveda, S.A., Giambiagi, L.B., Moreiras, S.M., Pinto, L., Tunik, M., Hoke, G.D., Farías, M. (Eds.), Geodynamic Processes in the Andes of Central Chile and Argentina. 399, pp. 63–82 Geological Society, London, Special Publications.
Gill, J., 1981. Orogenic Andesites and Plate Tectonics. Springer-Verlag, Berlin.
Gómez-Tuena, A., Langmuir, C.H., Goldstein, S.L., Straub, S., Ortega-Gutiérrez, F., 2007. Geochemical evidence for slab melting in the Trans-Mexican Volcanic Belt. J. Petrol. 48, 537–562.
Gómez-Tuena, A., Mori, L., Rincón-Herrera, N.E., Ortega-Gutiérrez, F., Solé, J., Iriondo, A., 2008. The origin of a primitive trondhjemite from the Trans-Mexican Volcanic Belt and its implications for the construction of a modern continental arc. Geology 36, 471–474. https://doi.org/10.1130/G24687A.1.
Gomez-Tuena, A., Straub, S.M., Zellmer, G.F., 2014. An introduction to orogenic andesites and crustal growth. In: Gomez-Tuena, A., Straub, S.M., Zellmer, G.F. (Eds.), Orogenic Andesites and Crustal Growth. Geological Society of London, London, pp. 1–13 https://doi.org/10.1144/SP1385.16.
Gómez-Tuena, A., Cavazos-Tovar, J.G., Parolari, M., Straub, S.M., Espinasa-Pereña, R., 2018. Geochronological and geochemical evidence of continental crust 'relamination' in the origin of intermediate arc magmas. Lithos 322, 52–66.
Goss, A.R., Kay, S.M., 2006. Steep REE patterns and enriched Pb isotopes in southern Central American arc magmas; evidence for forearc subduction erosion. Geochem. Geophys. Geosyst. 7. https://doi.org/10.1029/2005GC00116.
Goss, A.R., Mahlburg Kay, S., Mpodozis, C., 2013. Andean adakite-like high-Mg andesites on the Northern margin of the Chilean-Pampean flat-slab (27–28.5°S) associated with frontal arc migration and fore-arc subduction erosion. J. Petrol. 54, 2193–2234. https://doi.org/10.1093/petrology/egt2044.
Green, T.H., Ringwood, A.E., 1968. Genesis of the calc-alkaline igneous rock suite. Contrib. Mineral. Petrol. 18, 105–162.
Gregory, R.T., Taylor, H.P., 1981. An oxygen isotope profile in a section of Cretaceous oceanic-crust, Samail Ophiolite, Oman: Evidence for $d^{18}O$ buffering of the oceans by deep (less than 5 km) seawater-hydrothermal circulation at mid-ocean ridges. J. Geophys. Res. 86, 2737–2755.
Grove, T.L., Till, C.B., Krawczynski, M.J., 2012. The role of H_2O in subduction zone magmatism. Annu. Rev. Earth Planet. Sci. 40, 413–439.
Hacker, B.R., Kelemen, P.B., Behn, M.D., 2011. Differentiation of the continental crust by relamination. Earth Planet. Sci. Lett. 307, 501–516. https://doi.org/10.1016/j.epsl.2011.05.024.
Hacker, B.R., Keleman, P.B., Behns, M.D., 2015. Continental lower crust. Annu. Rev. Earth Planet. Sci. 43, 167–205. https://doi.org/10.1146/annurev-earth-050212-124117.
Hanan, B.B., Graham, D.W., 1996. Lead and helium isotope evidence from oceanic basalts for a common deep source of mantle plumes. Science 272, 991–995.
Hart, S., 1988. Heterogeneous mantle domains: signatures, genesis and mixing chronologies. Earth Planet. Sci. Lett. 90, 273–296.
Hart, S.R., Gerlach, D.C., White, W.M., 1986. A possible new Sr–Nd–Pb mantle array and consequences for mantle mixing. Geochim. Cosmochim. Acta 50, 1551–1557.
Hart, S.R., Hauri, E.H., Oschmann, L.A., Whitehead, J.A., 1992. Mantle plumes and entrainment: isotopic evidence. Science 256, 517–520.
Hauff, F., Hoernle, K., Tilton, G., Graham, D.W., Kerr, A.C., 2000a. Large volume recycling of oceanic lithosphere over short time scales: geochemical constraints from the Caribbean Large Igneous Province. Earth Planet. Sci. Lett. 174, 247–263.
Hauff, F., Hoernle, K., van den Bogaard, P., Alvarado, G., Garbe-Schönberg, D., 2000b. Age and geochemistry of basaltic complexes in western Costa Rica: contributions to the geotectonic evolution of Central America. Geochem. Geophys. Geosyst. 1(5), doi: https://doi.org/10.1029/1999GC000020.
Hickey, R., Frey, F., Gerlach, D., López-Escobar, L., 1986. Multiple sources for basaltic arc rocks from the Southern Volcanic Zone of the Andes (34°-41°S): trace element and isotopic evidence for contributions from subducted oceanic crust, mantle and continental crust. J. Geophys. Res. 91, 5963–5983.
Hickey-Vargas, R., 1991. Peeled or MASHed? Nature 350, 381–382.
Hickey-Vargas, R., Moreno, H., López-Escobar, L., Frey, F., 1989. Geochemical variations in Andean basaltic and silicic lavas from the Villarrica-Lanín volcanic chain (39.5°S): an

evaluation of source heterogeneity, fractional crystallization and crustal assimilation. Contrib. Mineral. Petrol. 103, 361–386.
Hickey-Vargas, R., Sun, M., López-Escobar, L., Moreno, H., Reagan, M.K., Morris, J.D., Ryan, J.G., 2002. Multiple subduction components in the mantle wedge: evidence from eruptive centers in the Central Southern volcanic zone, Chile. Geology 30, 199–202.
Hickey-Vargas, R., Holbik, S., Torney, S., Grey, F.A., Moreno-Roa, H., 2016. Basaltic rocks from the Andean Southern Volcanic Zone: insights from the comparison of along-strike and small-scale geochemical variations and their sources. Lithos 258, 115–132.
Hildreth, W., Moorbath, S., 1988. Crustal contributions to arc magmatism in the Andes of central Chile. Contrib. Mineral. Petrol. 103, 361–386.
Hoernle, K., van den Bogaard, P., Werner, R., Lissinna, B., Hauff, F., Alvarado, G., 2002. Missing history (16–71 Ma) of the Galapagos hotspot: implications for the tectonic and biological evolution of the Americas. Geology 30, 795–798.
Holm, P.M., Søager, N., Dyhr, C.T., Nielsen, M.R., 2014. Enrichments of the mantle sources beneath the Southern Volcanic Zone (Andes) by fluids and melts derived from abraded upper continental crust. Contrib. Mineral. Petrol. 167 (5), 1004. https://doi.org/10.1007/s00410-014-1004-8.
Holm, P.M., Søager, N., Alfastsen, M., Bertotto, G.W., 2016. Subduction zone mantle enrichment by fluids and Zr–Hf depleted crustal melts as indicated by backarc basalts of the Southern Volcanic Zone, Argentina. Lithos 262, 145–152.
Husson, L., Conrad, C.P., Husson, C.F., 2012. Plate motions, Andean orogeny, and volcanism above the South Atlantic convection cell. Earth and Planetary Science Letters 317–318, 126–135.
Jacques, G., Hoernle, K., Gill, J., Hauff, F., Wehrmann, H., Garbe-Schönberg, D., van den Bogaard, P., Bindeman, I., Lara, L.E., 2013. Across-arc geochemical variations in the Southern Volcanic Zone, Chile (34.5–38.0°S): constraints on mantle wedge and slab input compositions. Geochim. Cosmochim. Acta 123, 218–243.
Jacques, G., Hoernle, K., Gill, J., Wehrmann, H., Bindeman, I., Lara, L.E., 2014. Geochemical variations in the Central–Southern volcanic zone, Chile (38–43 degrees S); the role of fluids in generating arc magmas. Chem. Geol. 371, 27–45.
Jicha, B.R., Kay, S.M., 2018. Quantifying arc migration and the role of forearc subduction erosion in the central Aleutians. J. Volcanol. Geotherm. Res. 360, 84–99.
Jicha, B.R., Singer, B.S., Brophy, J.G., Fournelle, J.H., Johnson, C.M., Beard, B.L., Lapen, T.J., Mahlen, N.J., 2004. Variable impact of the subducted slab on Aleutian Island arc magma sources: evidence from Sr, Nd, Pb, and Hf isotopes and trace element abundances. J. Petrol. 45, 1845–1875.
Jicha, B.R., Scholl, D.W., Singer, B.S., Yogodzinski, G.M., Kay, S.M., 2006. Revised age of Aleutian Island arc formation implies high rate of magma production. Geology 34, 661–664.
Kawai, K., Tsuchiya, T., Tsuchiya, J., Maruyama, S., 2009. Lost primordial continents. Gondwana Res. 16, 581–586.
Kay, R.W., 1978. Aleution magnesian andesites: melts from subducted Pacific Oceanic crust. J. Volcanol. Geotherm. Res. 4, 117–132.
Kay, R.W., 1980. Volcanic arc magmas: implications of a melting mixing model for element recycling in the crust-upper mantle system. J. Geol. 88, 497–522.
Kay, S.M., Coira, B.L., 2009. Shallowing and steepening subduction zones, continental lithospheric loss, magmatism, and crustal flow under the Central Andean Altiplano-Puna Plateau. In: Kay, S.M., Ramos, V.A., Dickenson, W.D. (Eds.), Backbone of the Americas: Shallow Subduction. 204, pp. 229–259. https://doi.org/10.1130/2009.1204(11) Plateau Uplift, and Ridge and Terrane Collision, Geological Society of America Memoirs.
Kay, R.W., Kay, S.M., 1993. Delamination and delamination magmatism. Tectonophysics 219, 177–189.
Kay, S.M., Mpodozis, C., 2002. Magmatism as a probe to the Neogene shallowing of the Nazca plate beneath the modern Chilean flat-slab. J. S. Am. Earth Sci. 15, 39–57.
Kay, R.W., Sun, S.S., Lee-Hu, C.N., 1978. Pb and Sr isotopes in volcanic rocks from the Aleutian Islands and Pribilof Islands, Alaska. Geochim. Cosmochim. Acta 42, 263–273.
Kay, S.M., Godoy, E., Kurtz, A., 2005. Episodic arc migration, crustal thickening, subduction erosion, and magmatism in the south-central-Andes. Geol. Soc. Am. Bull. 117, 67–88.
Kay, S.M., Mpodozis, C., Gardeweg, M., 2013. Magma sources and tectonic setting of Central Andean forearc subduction erosion and delamination andesites (25.5–28°S) related to crustal thickening. Geol. Soc. Lond. Spec. Publ. 385 Doi:org/10.1144/SP385.11.
Kelemen, P.B., 1995. Genesis of high-Mg andesites and the continental crust. Contrib. Mineral. Petrol. 120, 1–19.
Kelemen, P.B., Behn, M.D., 2016. Formation of lower continental crust by relamination of buoyant arc lavas and plutons. Nat. Geosci. 9, 197–205. https://doi.org/10.1038/ngeo2662.
Kelemen, P.B., Yogodzinski, G.M., Scholl, D.W., 2003. Along-strike variation in the Aleutian island arc: genesis of high Mg# andesite and implications for continental crust. Inside the Subduction Factory. AGU Geophysical Monograph Series vol. 138, pp. 223–276.
Kelemen, P.B., Hanghøj, K., Greene, A., 2014. One view of the geochemistry of subduction-related magmatic arcs, with an emphasis on primitive andesite and lower crust. In: Holland, H.D., Turekian, K.K. (Eds.), Treatise on Geochemistry, vol. 4: The Crust. Oxford, UK: Elsevier-Pergamon. 2nd ed., pp. 749–806
Keppie, D.F., Hynes, A.J., Lee, J.K.W., Norman, M., 2012. Oligocene-Miocene back-thrusting in southern Mexico linked to the rapid subduction erosion of a large forearc block. Tectonics 31. https://doi.org/10.1029/2011TC002976.
Kolarsky, R.A., Mann, T., Montero, E., 1995. Island arc response to shallow subduction of the Cocos Ridge, Costa Rica. In: Mann, P. (Ed.), Geologic and Tectonic Development of the Caribbean Plate Boundary in Southern Central America. 295, pp. 235–262 Geological Society of America, Special Paper.
Komabayashi, T., Maruyama, S., Rino, S., 2009. Structure of D″ layer; anti-crust grown through 4.6 Ga subduction history of the earth. Gondwana Res. 15, 342–353.
Kukowski, N., Oncken, O., 2006. Subduction erosion – the "normal" mode of fore-arc material transfer along the Chilean Margin. In: Oncken, O., Chong, G., Frantz, G., Giese, P., Gotze, H.J., Ramos, V.A., Strecker, M., Wigger, P. (Eds.), The Andes: Active Subduction Orogeny. 10, pp. 217–236 Springer, Chapter.
Kulm, L.D., Schweller, W.J., Masias, A., 1977. A preliminary analysis of the geotectonic processesof the Andean continental margin, 6° to 45°S. In: Talwani, M., Pitman III, W.C. (Eds.), Island Arcs, Deep Sea Trenches and Back-arc Basins. American Geophysical Union, Maurice Ewing Symposium. 1, pp. 285–301.
Kurtz, A.C., Kay, S.M., Charrier, R., Farrar, E., 1997. Geochronology of Miocene plutons and exhumation history of the El Teniente region, Central Chile (34–35°S). Rev. Geol. Chile 16, 145–162.
Lallemand, S., 1995. High rates of arc consumption by subduction processes: some consequences. Geology 23, 551–554.
Lamb, S., Davis, P., 2003. Cenozoic climate change as a possible cause for the rise of the Andes. Nature 425, 792–797.
Larter, R.D., Vanneste, L.E., Morris, P., Smyth, D.K., 2003. Tectonic evolution and structure of the South Sandwich arc. In: Larter, R.D., Leat, P.T. (Eds.), Intra-Oceanic Subduction Systems: Tectonic and Magmatic Processes: Ge6ologic Society of London. 219, pp. 255–284 Special Publication.
Laursen, J., Scholl, D.W., von Huene, R., 2002. Neotectonic deformation of the central Chile margin: deepwater forearc basin formation in response to hot spot ridge and seamount subduction. Tectonics 21. https://doi.org/10.1029/2001TC901023.
Leat, P.T., Pearce, J.A., Barker, P.F., Millar, I.L., Barry, T.L., Larter, R.D., 2004. Magma genesis and mantle flow at a subducting slab edge: the South Sandwich arc-basin system. Earth Planet. Sci. Lett. 227, 17–35.
Leeman, W.P., 1996. Boron and other fluid-mobile elements in volcanic arc lavas: implications for subduction processes. In: Bebout, G.E., Scholl, D., Kirby, S., Platt, J.P. (Eds.), Subduction Top to Bottom. 96. AGU Monograph, pp. 269–276.
Liou, J.G., Zhang, R.Y., Katayama, I., Maruyama, S., 2002. Global distribution and petrotectonic characterizations of UHPM terranes. In: Parkinson, C.D., Katayama, I., Liou, J.G., Maruyama, S. (Eds.), The Diamond-bearing Kokchetav Massif. Kazakhstan. Universal Academy Press, Inc, pp. 15–35.
Lissinna, B., Hoernle, K., van den Bogaard, P., Werner, R., 2002. Northern migration of arc volcanism in western Panama: evidence for subduction erosion, Eos Transactions of the American Geophysical Union 83(47), Fall Meeting, Abstract V11A-1368.
Liu, L., Zhang, J.F., Green II, H.W., Jin, Z.M., Bozhilov, K.N., 2007. Evidence of former stishovite in metamorphosed sediments, implying subduction to ~350 km. Earth Planet. Sci. Lett. 263, 180–191.
Liu, Y.-S., Gao, S., Hu, Z., Gao, C., Zong, K., Wang, D., 2010. Continental and oceanic crust recycling-induced melt–peridotite interactions in the Trans-North China Orogen: U–Pb dating, Hf isotopes and trace elements in zircons from mantle xenoliths. J. Petrol. 51, 537–571.
Lonsdale, P., 1988. Paleogene history of the Kula plate: offshore evidence and onshore implications. Geol. Soc. Am. Bull. 100, 733–754.
Macfarlane, A.W., 1999. Isotopic studies of northern Andean crustal evolution and ore metal sources. In: Skinner, B. (Ed.), Geology and Ore Deposits of the Central Andes. Society of Economic Geologists, Special Publication. 7, pp. 195–217.
Maksaev, V., Munizaga, F., McWilliams, M., Fanning, M., Marther, R., Ruiz, J., Zentilli, M., 2004. Chronology for El Teniente, Chilean Andes, from U-Pb, $^{40}Ar/^{39}Ar$, Re-Os, and fission track dating: implications for the formation of a supergiant porphyry Cu-Mo deposit. In: Sillitoe, R.H., Perelló, J., Vidal, C.E. (Eds.), Andean Metallogeny: New Discoveries, Concepts and Updates. 2004. Society of Economic Geologists, Littleton, CO, USA, pp. 15–54.
Marquez, A., Oyarzun, R., Doblas, M., Verma, S.P., 1999. Alkalic (ocean-island basalt type) and calc-alkalic volcanism in the Mexican Volcanic Belt: a case for plume-related and propagating rifting in an active margin. Geochim. Cosmochim. Acta 27, 51–54.
Marschall, H.R., Schumacher, J.C., 2012. Arcmagmas sourced frommelange diapirs in subduction zones. Nat. Geosci. 5, 862–867. https://doi.org/10.1038/ngeo1634.
Marshall, J.S., Anderson, R.S., 1995. Quaternary uplift and seismic cycle deformation, Peninsula de Nicoya, Costa Rica. Geol. Soc. Am. Bull. 107, 463–473.
Marshall, J.S., Idleman, B.F., Gardner, T.W., Fisher, D.M., 2003. Landscape evolution within a retreating volcanic arc, Costa Rica, Central America. Geology 31, 419–422.
Maruyama, S., Safonova, I., 2019. Orogeny and Mantle Dynamics: Role of Tectonic Erosion and Second Continent in the Mantle Transition Zone. Novosibirsk State University, Novosibirsk (208 p).
McGlashan, N., Brown, L.D., Kay, S.M., 2008. Crustal thickness in the central Andes from teleseismically recorded depth phase precursors. Geophys. J. Int. 175, 1013–1022.
Meschede, M., Zweigel, P., Kiefer, E., 1999a. Subsidence and extension at a convergent plate margin: Evidence for tectonic erosion off Costa Rica. Terra Nova 11, 112–117.
Meschede, M., Zweigel, P., Frisch, W., Voelker, D., 1999b. Mélange formation by subduction erosion: the case of the Osa mélange in southern Costa Rica. Terra Nova 11, 141–148.
Mickus, K., 2003. Gravity constraints on the crustal structure of Central America. AAPG Mem. 79, 638–655.
Moore, G.M., Carmichael, I.S.E., 1998. The hydrous phase equilibra (to 3kbar) of an andesite and basaltic andesite from Western Mexico: constraints on water content and conditions of phenocrysts growth. Contrib. Mineral. Petrol. 130, 304–319.
Morán-Zenteno, D.J., Corona-Chavez, P., Tolson, G., 1996. Uplift and subduction erosion in southwestern Mexico since the Oligocene: pluton geobarometry constraints. Earth Planet. Sci. Lett. 141, 51–65. https://doi.org/10.1016/0012-1821X(96)00067-2.
Morán-Zenteno, D.J., Martiny, B.M., Solari, L., Mori, L., Luna-González, L., González-Torres, E.A., 2018. Cenozoic magmatism of the Sierra Madre del Sur and tectonic truncation of the Pacific margin of southern Mexico. Earth-Science Reviews, Tectonic Systems of Mexico 183, 85–114. https://doi.org/10.1016/j.earscirev.2017.01.010.
Morell, K.D., Fisher, D.M., Bangs, N., 2019. Plio-Quaternary outer forearc deformation and mass balance of the southern Costa Rica convergent margin. J. Geophys. Res. Solid Earth 124 (9), 9795–9815.
Morris, J.D., Tera, F., 1989. ^{10}Be and ^{9}Be in mineral separates and whole rocks from volcanic arcs: implications for sediment subduction. Geochim. Cosmochim. Acta 53, 3197–3206.

Morris, J.D., Tera, F., 2000. Beryllium isotope systematics of volcanic arc cross-chains. Goldschmidt 2000. Journal of Conference Abstracts 5, 720.
Morris, J.D., Leeman, W.P., Tera, F., 1990. The subducted component in island arc lavas constraints from Be isotopes and B-Be systematics. Nature 344, 31–36.
Morris, J.D., Gosse, J., Brachfeld, S., Tera, F., 2002a. Cosmogenic ^{10}Be and the solid earth. In: Grew, E. (Ed.), Reviews in Mineralogy. Mineralogical Society of America, Washington, DC, USA, pp. 207–270.
Morris, J.D., Valentine, R., Harrison, T., 2002b. ^{10}Be imaging of sediment accretion and subduction along the northeast Japan and Costa Rica convergent margins. Geology 30, 59–62.
Muñoz, M., Fuentes, F., Vergara, M., Aguirre, L., Nyström, J.O., 2006. Abanico East Formation: petrology and geochemistry of volcanic rocks behind the Cenozoic arc front in the Andean Cordillera, central Chile (33.5°S). Rev. Geol. Chile 33, 109–140.
Muñoz, M., Charrier, R., Fanning, C.M., Maksaev, V., Deckart, K., 2012. Zircon trace element and O-Hf isotope analyses of mineralized intrusions from El Teniente ore deposit, Chilean Andes: constraints on the source and magmatic evolution of porphyry Cu-Mo related magmas. J. Petrol. 53, 1091–1122. https://doi.org/10.1093/petrology/egs010.
Muñoz, M., Farías, M., Charrier, R., Fanning, C.M., Polvé, M., Deckart, K., 2013. Isotopic shifts in the Cenozoic Andean arc of central Chile: records of an evolving basement throughout cordilleran arc mountain building. Geology 41, 931–934.
Nielsen, S.G., Marschall, H.R., 2017. Geochemical evidence for mélange melting in global arcs. Sci. Adv. 3 (doi:1602410.1601126/sciadv.1602402.
Noll, P.D., Newsom, H., Leeman, W.P., Ryan, J.G., 1996. The role of hydrothermal fluids in the production of subduction zone magmas: evidence from siderophile and chalcophile trace elements and boron. Geochim. Cosmochim. Acta 60, 587–611.
Nyström, J., Vergara, M., Morata, D., Levi, B., 2003. Tertiary volcanism during extension in the Andean foothills of central Chile (33°15′-33°45′S). Geol. Soc. Am. Bull. 115, 1523–1537.
Ortega-Gutiérrez, F., Elías-Herrera, M., Morán-Zenteno, D.J., Solari, L., Luna-González, L., Schaaf, P., 2014. A review of batholiths and other plutonic intrusions of Mexico. Gondwana Res. 26, 834–868. https://doi.org/10.1016/j.gr.2014.05.002.
Ortega-Gutiérrez, F., Elías-Herrera, M., Morán-Zenteno, D.J., Solari, L., Weber, B., Luna-González, L., 2018. The pre-Mesozoic metamorphic basement of Mexico, 1.5 billion years of crustal evolution. Earth-Science Reviews Tectonic Systems of Mexico 183.
Parada, M.A., Nyström, J.O., Levi, B., 1999. Multiple sources for the Coastal Batholith of central Chile (31–34°S): geochemical and Sr–Nd isotopic evidence and tectonic implications. Lithos 46, 505–521.
Pardo, M., Suarez, G., 1995. Shape of the subducted Rivera and Cocos plate in southern Mexico: seismic and tectonic implications. J. Geophys. Res. 100, 12357–12373.
Parolari, M., Gómez-Tuena, A., Cavazos-Tovar, J.G., Hernández-Quevedo, G.T., 2018. A balancing act of crust creation and destruction along the western Mexican convergent margin. Geology 46, 455–458.
Peacock, S.M., van Keken, P.E., Holloway, S.F., Hacker, B.R., Abers, G.A., Fergason, R.L., 2005. Thermal structure of the Costa Rica–Nicaragua subduction zone. Phys. Earth Planet. Inter. 149, 187–200.
Pearson, D.G., Irvine, G.J., Ionov, D.A., Boyd, F.R., Dreibus, G.E., 2004. Re–Os isotope systematics and platinum group element fractionation duringmantlemelt extraction: a study of massif and xenolith peridotite suites. Chem. Geol. 208, 29–59.
Pérez-Campos, X., Kim, Y., Husker, A., Davis, P.M., Clayton, R.W., Iglesias, A., Pacheco, J.F., Singh, S.K., Manea, V.C., Gurnis, M., 2008. Horizontal subduction and truncation of the Cocos Plate beneath central Mexico. Geophys. Res. Lett. 35. https://doi.org/10.1029/2008GL035127.
Plank, T., 2004. Constraints from thorium/lanthanum on sediment recycling at subduction zones and the evolution of the continents. J. Petrol. 46, 921–944. https://doi.org/10.1093/petrology/egi005.
Plank, T., Langmuir, C.H., 1998. The geochemical composition of subducting sediment and its consequences for the crust and the mantle. Chem. Geol. 145, 325–394.
Proenza, J.A., González-Jiménez, J.M., Garcia-Casco, A., Belousova, E., Griffin, W.L., Talavera, C., Rojas-Agramonte, Y., Aiglsperger, T., Navarro-Ciurana, D., Pujol-Solà, N., Gervilla, F., O'Reilly, S.Y., Jacob, D.E., 2017. Cold plumes trigger contamination of oceanic mantle wedges with continental crust-derived sediments: evidence from chromitite zircon grains of eastern Cuban ophiolites. Geosci. Front. https://doi.org/10.1016/j.gsf.2017.12.005.
Protti, M., Guendel, F., McNally, K., 1995. Correlation between the age of the subducting Cocos Plate and the geometry of the Wadati-Benioff zone under Nicaragua and Costa Rica. In: Mann, P. (Ed.), Geologic and Tectonic Development of the Caribbean Plate Boundary in Southern Central America. Spec. Pap. Geol. Soc. Am. 295, pp. 309–326.
Puig, A., 1988. Geologic and metallogenic significance of the isotopic composition of lead in galenas of the Chilean Andes. Econ. Geol. 83, 843–858.
Ramos, V.A., 2010. The Grenville-age basement of the Andes. J. S. Am. Earth Sci. 29, 77–91. https://doi.org/10.1016/j.jsames.2009.09.004.
Ranero, C.R., von Huene, R., 2000. Subduction erosion along the Middle America convergent margin. Nature 404, 748–755.
Rech, J.A., Currie, B.S., Michalski, G., Cowan, A.M., 2006. Neogene climate change and uplift in the Atacama Desert, Chile. Geology 34, 761–764.
Risse, A., Trumbull, R.B., Kay, S.M., Coira, B., Romer, R.L., 2013. Multi-stage evolution of Late Neogene mantle-derived magmas from the Central Andes back-arc in the Southern Puna Plateau of Argentina. J. Petrol. 10, 1963–1995 (doi:1910.1093/petrology/egt1038).
Rogers, G., Hawkesworth, C.J., 1989. A geochemical transverse across the North Chilean Andes: evidence of crust generation from the mantle wedge. Earth Planet. Sci. Lett. 91, 271–285.
Rojas-Agramonte, Y., Garcia-Casco, A., Kempf, A., Krönera, A., Proenzah, J.A., Lázarod, C., Liua, D., 2016. Recycling and transport of continental material through the mantle wedge above subduction zones: a Caribbean example. Earth Planet. Sci. Lett. 436, 93–107.
Rudnick, R.L., 1995. Making continental crust. Nature 378, 571–578. https://doi.org/10.1038/378571a0.
Rudnick, R.L., Fountain, D.M., 1995. Nature and composition of the continental crust: a lower crustal perspective. Rev. Geophys. 33, 267–309.
Rudnick, R.L., Gao, S., 2003. Composition of the continental crust. In: Rudnick, R.L. (Ed.), Treatise on Geochemistry. Elsevier–Pergamon, Oxford, pp. 1–64.
Rutland, R.W.R., 1971. Andean orogeny and ocean floor spreading. Nature 233, 252–255.
Ryan, H.F., Draut, A.E., Karanen, K., Scholl, D.W., 2012. Influence of the Amlia fracture zone on the evolution of the Aleutian Terrace forearc basin, central Aleutian subduction zone. Geosphere 8, 1254–1273.
Sallarés, V., Danobeitia, J.J., Flueh, E.R., 2001. Lithospheric structure of the Costa Rican Isthmus: effects of subduction zone magmatism on an oceanic plateau. J. Geophys. Res. 106, 621–642.
Schaaf, P., Carrasco-Núñez, G., 2010. Geochemical and isotopic profile of Pico de Orizaba (Citlaltépetl) volcano, Mexico: insights for magma generation processes. J. Volcanol. Geotherm. Res. 197, 108–122.
Schaaf, P., Morales-Zenteno, D., del Sol Hernandez-Bernal, M., Solis-Pichardo, G., Tolson, G., Koehler, H., 1995. Paleogene continental margin truncation in southwestern Mexico: geochronological evidence. Tectonics 14, 1339–1350.
Schaaf, P., Stimac, J., Siebe, C., Macias, J.L., 2005. Geochemical evidence for mantle origin and crustal processes in volcanic rocks from Popocatepetl and surrounding monogenetic volcanoes, central Mexico. J. Petrol. 46, 1243–1282.
Scholl, D.W., von Huene, R., 2007. Crustal recycling at modern subduction zones applied to the past - issues of growth and preservation of continental basement crust, mantle geochemistry, and supercontinent reconstruction. In: Hatcher, J.R.D., Carlson, M.P., McBride, J.H., Catalán, J.R.M. (Eds.), 4-D Framework of Continental Crust. 200, pp. 9–32. https://doi.org/10.1130/2007.1200(02) Geological Society of America Memoir.
Scholl, D.W., von Huene, R., 2009. Implications of estimated magmatic additions and recycling losses at the subduction zones of accretionary (non-collisional) and collisional (suturing) orogens. In: Cawood, P., Kröner, A. (Eds.), Accretionary Orogens in Space and Time. 318, pp. 105–125 Geological Society of London, Special Publication.
Schweller, W.J., Kulm, L.D., 1978. Extensional rupture of oceanic crust in the Chile Trench. Mar. Geol. 28, 271–291.
Senshu, H., Maruyama, S., Rino, S., Santosh, M., 2009. Role of tonalite-trodhjemite-granite (TTG) crust subduction on the mechanism of supercontinent breakup. Gondwana Res. 15, 433–442.
Seyfried, H., Astorga, A., Amann, H., Calvo, C., Kolb, W., Schmidt, H., Winsemann, J., 1991. Anatomy of an evolving island arc; tectonic and eustatic control in the South Central American forearc area. In: Macdonald, D.I.M. (Ed.), Sea-level Changes at Active Plate Margins: Processes and Products. 12, pp. 217–240 International Association of Sedimentology, Special Publication.
Sigmarsson, O., Condomines, M., Morris, J.D., Harmon, R.S., 1990. Uranium and ^{10}Be enrichments by fluids in Andean arc magmas. Nature 346, 163–165.
Sigmarsson, O., Martin, H., Knowles, J., 1998. Melting of a subducting oceanic crust from U–Th disequilibria in Austral Andean lavas. Nature 394, 566–569.
Sigmarsson, O., Chmeleff, J., Morris, J., López-Escobar, L., 2002. Origin of ^{226}Ra-^{230Th} disequilibria in arc lavas from southern Chile and implications for magma transfer time. Earth Planet. Sci. Lett. 196, 189–196.
Singer, B.S., Jicha, B.R., Leeman, W.P., Rogers, N.W., Thirlwall, M.F., Ryan, J., Nicolaysen, K.E., 2007. Along-strike trace element and isotopic variation in Aleutian Island arc basalt: subduction melts sediments and dehydrates serpentine. J. Geophys. Res. 112, B06206. https://doi.org/10.1029/2006JB004897.
Skewes, M.A., Arevalo, A., Floody, R., Zuniga, P.H., Stern, C.R., 2002. The giant El Teniente breccia deposit: hypogene copper distribution and emplacement. In: Goldfarb, R.J., Nielsen, R.L. (Eds.), Integrated Methods for Discovery: Global Exploration in the Twenty-first Century. Society of Economic Geologists, Special Publication 9, pp. 299–332.
Søager, N., Holm, P.M., 2013. Melt–peridotite reactions in upwelling eclogite bod-ies: constraints from EM1-type alkaline basalts in Payenia, Argentina. Chem. Geol. 360, 204–219.
Søager, N., Holm, P.M., Llambías, E.J., 2013. Payenia volcanic province, southern Mendoza, Argentina: OIB mantle upwelling in a backarc environment. Chem. Geol. 349, 36–53.
Søager, N., Martin, P., Thirlwall, M.F., 2015a. Sr, Nd, Pb and Hf isotopic constraints on mantle sources and crustal contaminants in the Payenia volcanic province, Argentina. Lithos 212–215, 368–378.
Søager, N., Portnyagin, M., Hoernle, K., Holm, P.M., Hauff, F., Garbe-Schanberg, D., 2015b. Olivine major and trace element compositions in Southern Payenia Basalts, Argentina: evidencefor pyroxenite-peridotite melt mixing in a back-arc setting. J. Petrol. 56 (8), 1395–1518.
Stern, C.R., 1989. Pliocene to present migration of the volcanic front, Andean Southern Volcanic Front. Rev. Geol. Chile 16, 145–162.
Stern, C.R., 1990. Comment on "A geochemical traverse across the northern Chilean Andes: evidence for crust generation from the mantle" by G. Rogers and C. Hawkesworth. Earth Planet. Sci. Lett. 101, 129–133.
Stern, C.R., 1991a. Role of subduction erosion in the generation of the Andean magmas. Geology 19, 78–81.
Stern, C.R., 1991b. Comment on "Crustal contributions to arc magmatism in the Andes of central Chile" by W. Hildreth and S. Moorbath. Contrib. Mineral. Petrol. 108, 241–246.
Stern, C.R., 2004. Active Andean volcanism: its geologic and tectonic setting. Rev. Geol. Chile 31, 161–206.
Stern, C.R., 2011. Subduction erosion: rates, mechanisms, and its role in arc magmatism and the evolution of the continental crust and mantle. Gondwana Res. 20, 284–308. https://doi.org/10.1016/j.gr.2011.03.006.

Stern, C.R., Kilian, R., 1996. Role of the subducted slab, mantle wedge and continental crust in the generation of adakites from the Andean Austral Volcanic Zone. Contrib. Mineral. Petrol. 123, 263–281.
Stern, R.J., Scholl, D.W., 2010. Yin and yang of continental crust creation and destruction by plate tectonic processes. Int. Geol. Rev. 52, 1–31.
Stern, C.R., Skewes, M.A., 1995. Miocene to Present magmatic evolution at the northern end of the Andean Southern Volcanic Zone, Central Chile. Rev. Geol. Chile 22, 261–272.
Stern, C.R., Futa, K., Muehlenbachs, M., 1984. Isotope and trace element data for the orogenic andesites from the austral Andes. In: Harmon, R., Barreiro, B. (Eds.), Andean Magmatism: Chemical and Isotopic Constraints. Shiva Press, Ltd., Chesire, England, pp. 31–46.
Stern, C.R., Frey, F.A., Futa, K., Zartman, R.E., Peng, Z., Kyser, T.K., 1990. Trace element and Sr, Nd, Pb and O isotopic composition of Pliocene and Quaternary alkali basalts of the Patagonian Plateau Lavas of southernmost South America. Contrib. Mineral. Petrol. 104, 294–308.
Stern, C.R., Floody, R., Espiñeíra, D., 2011a. Olivine-hornblende-lamprophyre dikes from Quebrada los Sapos, El Teniente, Central Chile (34°S): implications for the temporal geochemical evolution of the Andean subarc mantle. Andean Geol. 38, 1–22.
Stern, C.R., Skewes, M.A., Arévalo, A., 2011b. Magmatic evolution of the giant El Teniente Cu-Mo deposit, central Chile. J. Petrol. 52, 1591–1617. https://doi.org/10.1093/petrology/egq029.
Stern, C.R., Pang, K., Lee, H., Skewes, M.A., Arévalo, A., 2019. Implications of Hf Isotopes for the evolution of the mantle source of magmas associated with the giant El Teniente Cu-Mo megabreccia deposit, Central Chile. Minerals 9 (9), 550. https://doi.org/10.3390/min9090550.
Stotz, I.L., Iaffaldano, G., Davies, D.R., 2017. Late Miocene Pacific plate kinematic change explained with coupled global models of mantle and lithosphere dynamics. Geophys. Res. Lett. 44. https://doi.org/10.1002/2017GL073920.
Stracke, A., Hofmann, A.W., Hart, S.R., 2005. FOZO, HIMU and the rest of the mantle zoo. Geochem. Geophys. Geosyst. 6 (Paper number 2004GC00824).
Straub, S.M., LaGatta, A.B., Martin-Del Pozzo, A.L., Langmuir, C.H., 2008. Evidence from high Ni olivines for a hybridized peridotite/pyroxenite source for orogenic andesites from the central Mexican Volcanic Belt. Geochem. Geophys. Geosyst. 9, Q03007. https://doi.org/10.1029/2007GC001583.
Straub, S.M., Gómez-Tuena, A., Stuart, F.M., Zellmer, G.F., Espinasa-Perena, R., Cai, M.Y., Iizuka, Y., 2011. Formation of hybrid arc andesites beneath thick continental crust. Earth Planet. Sci. Lett. 303, 337–347. https://doi.org/10.1016/j.epsl.2011.01.013.
Straub, S.M., Gómez-Tuena, A., Zellmer, G.F., Espinasa-Perena, R., Stuart, F.M., Cai, Y., Langmuir, C.H., Pozzo, A.L.M.-D., Mesko, G.T., 2013. The processes of melt differentiation in arc volcanic rocks: insights from OIB-type arc magmas in the central Mexican Volcanic Belt. J. Petrol. 54, 665–701. https://doi.org/10.1093/petrology/egs081.
Straub, S.M., Gómez-Tuena, A., Bindeman, I.N., Bolge, L.L., Brandl, P.A., Espinasa-Perena, R., Solari, L., Stuart, F.M., Vannucchi, P., Zellmer, G.F., 2015. Crustal recycling by subduction erosion in the central Mexican Volcanic Belt. Geochim. Cosmochim. Acta 166, 29–52. https://doi.org/10.1016/j.gca.2015.06.001.
Straub, S.M., Gómez-Tuena, A., Vannucchi, P., 2020. Subduction erosion and arc volcanism. Nature Reviews of Earth and Environmental Sciences (in press).
Syracuse, E.M., Abers, G.A., 2006. Global compilation of variations in slab depth beneath arc volcanoes and implications. Geochem. Geophys. Geosyst. 7, Q05017. https://doi.org/10.1029/2005GC001045.
Tassara, A., Echaurren, A., 2012. Anatomy of the Andean subduction zone: three-dimensional density model upgraded and compared against global-scale models. Geophys. J. Int. 189, 161–168.
Taylor, S.R., 1967. The origin and growth of continents. Tectonophysics 4, 17–34. https://doi.org/10.1016/0040-1951(67)90056-X.
Taylor, S.R., McLennan, S.M., 1985. The Continental Crust: Its Composition and Evolution. Blackwell, Melbourne.
Tera, F., Brown, l., Morris, J., Sacks, S.I., Klein, J., Middleton, R., 1986. Sediment incorporation in island-arc magmas: inferences from ^{10}Be. Geochim. Cosmochim. Acta 50, 535–550.
Thomas, C., Livermore, R.A., Pollitz, F.F., 2003. Motion of the Scotia Sea plates. Geophys. J. Int. 155, 789–804.
Thornburg, T., Kulm, L.D., 1987a. Sedimentation in the Chile Trench: depositional morphologies, lithofacies, and stratigraphy. Geol. Soc. Am. Bull. 98, 33–52.
Thornburg, T., Kulm, L.D., 1987b. Sedimentation in the Chile Trench: petrofacies and provenance. J. Sediment. Petrol. 57, 55–74.
Tonarini, S., Leeman, W.P., Leat, P.T., 2011. Subduction erosion of forearc mantle wedge implicated in the genesis of the South Sandwich Island (SSI) arc: evidence from boron isotope systematics. Earth Planet. Sci. Lett. 301, 275–284.
Tormey, D.R., Hickey-Vargas, R., Frey, F.A., López-Escobar, L., 1991. Recent lavas from the Andean volcanic front (33 to 42°S); interpretations of along-arc compositional variations. Geologic Society of America, Special Paper. 265, pp. 57–78.
Turner, S.J., Langmuir, C.H., Dungan, M.A., Escrig, S., 2017. The importance of mantle wedge heterogeneity to subduction zone magmatism and the origin of EM1. Earth Planet. Sci. Lett. 472, 216–228.
Vanneste, L.E., Larter, R.D., 2002. Sediment subduction, subduction erosion, and strain regime in the northern South Sandwich forearc. J. Geophys. Res. 107 (B7), 2149. https://doi.org/10.1029/2001JB000396.
Vannucchi, P., Scholl, D.W., Meschede, M., 2001. Tectonic erosion and consequent collapse of the Pacific margin of Costa Rica; combined implications from ODP Leg 170, seismic offshore data, and regional geology of the Nicoya Peninsula. Tectonics 20, 649–668.
Vannucchi, P., Ranero, C.R., Galeotti, S., Straub, S.M., McDougall-Ried, K., Scholl, D.W., 2003. Fast rates of subduction erosion along the Costa Rica Pacific margin: implications for nonsteady rates of crustal recycling at subduction zones. J. Geophys. Res. 108 (B11), 2511. https://doi.org/10.1029/2002JB002207.
Vannucchi, P., Morgan, J.P., Balestrieri, M.L., 2016. Subduction erosion, and the deconstruction of continental crust: the Central America case and its global implications. Gondwana Res. 40, 184–198 (doi:110.1016/j.gr.2016.1010.1001551).
Verma, S.P., 1999. Geochemistry of evolved magmas and their relationship to subduction-unrelated mafic volcanism at the volcanic front of the central Mexican Volcanic Belts. J. Volcanol. Geotherm. Res. 93, 151–171.
Vils, F., Tonarini, S., Kalt, A., Seitz, H.M., 2009. Boron, lithium and strontium isotopes as tracers of seawater-serpentine interaction at Mid-Atlantic ridge, ODP Leg 209. Earth Planet. Sci. Lett. 286, 414–425.
Vogt, K., Castro, A., Gerya, T., 2013. Numerical modeling of geochemical variations caused by crustal relamination. Geochem. Geophys. Geosyst. 14, 470–487.
Völker, D., Kutterolf, S., Wehrmann, H., 2011. Comparative mass balance of volcanic edifices in the southern volcanic zone of the Andes between 33°S and 46°S. J. Volcanol. Geotherm. Res. 205, 114–129.
von Huene, R., Scholl, D.W., 1991. Observations at convergent margins concerning sediment subduction, subduction erosion, and the growth of continental crust. Rev. Geophys. 29, 279–316.
von Huene, R., Ranero, C., Vannucchi, P., 2004. Generic model of subduction erosion. Geology 32, 913–916.
Walker, R.J., Carlson, R.W., Shirey, S.B., Boyd, F.R., 1989. Os, Sr, Nd, and Pb isotopic systematics of southern African peridotite xenoliths: implications for the chemical evolution of subcontinental mantle. Geochim. Cosmochim. Acta 53, 1583–1595.
Wang, K., Hu, Y., von Huene, R., Kukowski, N., 2010. Interplate earthquakes as a driver of shallow subduction erosion. Geology 38, 431–434.
White, W.M., 1985. Sources of oceanic basalts: radiogenic isotopic evidence. Geology 13, 115–118.
White, W.M., Hofmann, A.W., 1982. Sr and Nd isotope geochemistry of oceanic basalts and mantle evolution. Nature 296, 821–825.
Wieser, P.E., Turner, S.J., Mather, T.A., Pyle, D.M., Savov, I.P., Orozco, G., 2019. New constraints from Central Chile on the origins of enriched continental compositions in thick-crusted arc magmas. Geochim. Cosmochim. Acta 267, 51–74.
Willbold, M., Stracke, A., 2006. Trace element composition of mantle end-members: implications for recycling of oceanic and upper and lower continental crust. Geochem. Geophys. Geosyst. 7 (Paper number 2005GC001005).
Willbold, M., Stracke, A., 2010. Formation of enriched mantle components by recycling of upper and lower continental crust. Chem. Geol. 276, 188–197.
Xu, Z., Zheng, Y.-F., Zhao, Z.-F., 2018. Zircon evidence for incorporation of terrigenous sediments into the magma source of continental basalts. Sci. Rep. 8, 178. https://doi.org/10.1038/s41598-017-18549-7.
Yamamoto, S., Senshu, H., Rino, S., Omori, S., Maruyama, S., 2009. Granite subduction: arc subduction, tectonic erosion and sediment subduction. Gondwana Res. 15, 443–453.
Yáñez, G., Ranero, C., von Huene, R., Díaz, J., 2001. Magnetic anomaly interpretation across the southern Central Andes (32°-33.5°S): the role of the Juan Fernández ridge in the late Tertiary evolution of the margin. J. Geophys. Res. 106, 6325–6345.
Yáñez, G., Cembrano, J., Pardo, M., Ranero, C., Selles, D., 2002. The Challenger-Juan Fernández-Maipo major tectonic transition of the Nazca-Andean subduction system at 33–34°S: geodynamic evidence and implications. J. S. Am. Earth Sci. 15, 23–38.
Ye, K., Cong, B.L., Ye, D.N., 2000. The possible subduction of continental material to depths greater than 200 km. Nature 407, 734–736.
Yogodzinski, G.M., Vervoort, J.D., Brown, S.T., Gerseny, M., 2010. Subduction controls of Hf and Nd isotopes in lavas of the Aleutian island arc. Earth Planet. Sci. Lett. 300, 226–238. https://doi.org/10.1016/j.epsl.2010.09.035.
Yogodzinski, G.M., Brown, S.T., Kelemen, P.B., Vervoort, J.D., Portnyagin, M., Sims, K.W.W., Hoernle, K., Jicha, B.R., Werner, R., 2015. The role of subducted basalt in the source of island arc magmas: evidence from seafloor lavas of the Western Aleutians. J. Petrol. 56, 441–492. https://doi.org/10.1093/petrology/egv006.
Yogodzinski, G.M., Kelemen, P.B., Hoernle, K., Brown, S.T., Bindeman, I., Vervoort, J.D., Sims, K.W., Portnyagin, M., Werner, R., 2017. Sr and O isotopes in western Aleutian seafloor lavas: implications for the source of fluids and trace element character of arc volcanic rocks. Earth Planet. Sci. Lett. 475, 169–180.
Ziegler, A.M., Barret, S.F., Scotese, C.R., 1981. Paleoclimate, sedimentation and continental accretion. Royal Society of London Philosophical Transactions 301, 253–264.
Zindler, A., Hart, S., 1986. Chemical geodynamics. Annu. Rev. Earth Planet. Sci. 14, 493–571.

Charles R. Stern is Professor in the Department of Geological Sciences at the University of Colorado in Boulder, Colorado. He received his Ph.D. from the University of Chicago in 1973, and spent four years as a Research Associate at Lamont-Doherty Geological Observatory of Columbia University before arriving in Colorado in 1979. His research interests include igneous petrology, volcanology, economic geology, cosmochemistry and geoarchaeology. Much of his research work is focused on igneous rocks and recent volcanic activity in the Patagonian Andes of southernmost South America.